Carolina Isabel Paiva Coelho

Resposta de macrófagos murinos à fagocitose de *Cryptococcus neoformans*

Coimbra 2012

· U · C ·

UNIVERSIDADE DE COIMBRA

Resposta de macrófagos murinos à fagocitose de

Cryptococcus neoformans

The murine macrophage response to phagocytosis of *Cryptococcus neoformans*

Dissertação apresentada à Faculdade de Medicina da Universidade de Coimbra, para prestação de provas de doutoramento na área das Ciências da Saúde, especialidade Ciências Biomédicas.

Universidade de Coimbra 2012

Acknowledgements:

The work presented here and my mental sanity would have not been possible without the invaluable help of:

My supervisors, Teresa Gonçalves and Arturo Casadevall, who have allowed me all the freedom I requested, which is to say a whole lot of it. Despite that, they have never stopped teaching me. This is a very rare gift and I have no words to describe my gratitude.

My parents, Isabel and Acácio, and my siblings, Margarida and Acácio, who have gotten used to have a virtual daughter and sister for 11 months of the year and a real daughter for a very short, very busy month. For being my family.

Before I joined Arturo's lab it had been described to me as the best lab in the world. It is true.
In Teresa's lab I had the rare opportunity of becoming friends with Filipa, Marta and Vitor and Drª. Célia and D. Alzira, who warmingly adopted the northern girl.

To my labmates, present and past.
In particular, I would like to thank Julie Wolf, Radamés Cordero, Johanna Rivera, António Nakouzi, Anamélia Bocca, Lorena Derengowski, Luis Martinez, Monica Garcia-Solache, Jinghang Zhang, Lydia Tesfa, Carolyn Saylor, André Nicola and Patrícia Andrade for their infinite patience to teach me a small part of what they know and for holding my hand whenever I needed. Julie and Radamés have read this thesis several times, and I wish to say a thank you for every word I made them read. That's a lot.
Jinghang Zhang and Roy Noy have provided me with guidance and mentorship outside of the lab.

To Ana Sofia Rodrigues and Beatriz Lacerda de Sousa, who have been my sisters through all of moving abroad, science apprenticeship, thesis writing, late night troubleshooting and the process of becoming a grown-up.
To all of my BEB (...es, ...ados) for the best first year of PhD imaginable.
To all my friends and family, for contributing to my life and being a part of my happy life. Couldn't have done it without you all.

List of Publications

The experimental work presented has been carried out by the author, with the help of the following individuals, as described.

The work in Chapter 1 was written by Carolina Coelho. Parts of it will be used in a review manuscript which will be co-written by Carolina Coelho, Anamelia Bocca and Arturo Casadevall (Department of Microbiology and Immunology, Albert Einstein College of Medicine of Yeshiva University, Bronx, New York, USA).

In Chapter 2 ”Analysis of Cell Cycle and Replication of Mouse Macrophages after *In Vivo* and *In Vitro Cryptococcus neoformans* Infection Using Laser Scanning Cytometry”, animal infections were performed by Johanna Rivera (Department of Microbiology and Immunology, Albert Einstein College of Medicine of Yeshiva University, Bronx, New York, USA) and valuable technical advice regarding Laser Scanning Cytometry was given by Lydia Tesfa and Jinghang Zhang (Flow Cytometry Core Facility, Albert Einstein College of Medicine of Yeshiva University, Bronx, New York, USA).

In Chapter 3 “Mouse Macrophage mitochondria in response to *in vitro Cryptococcus neoformans* infection”, some of the Western blots were the work of Bo Wang (Albert Einstein College of Medicine of Yeshiva University, Bronx, New York, USA), under supervision by the author of the work. Anamelia Bocca provided unvaluable scientific discussions and helped with experimental setup.

All the work presented in this thesis was co-supervised by Teresa Gonçalves and Arturo Casadevall.

The following paper was published in peer-reviewed international scientific journals during the development of this thesis:

1.**Coelho, C.**, Tesfa, L., Zhang, J., Rivera, J., Gonçalves, T. & Casadevall, A. (2012). *Analysis of cell cycle and replication of mouse macrophages after* in vivo *and* in vitro Cryptococcus neoformans *infection using laser scanning cytometry.* Infection and immunity, 80(4), 1467–51478. doi:10.1128/IAI. 06332-11

The following papers are under various stages of preparation for submission in peer-reviewed international scientific journals, and data from them is included in this thesis:

2.**Coelho, C.**, Wang, B., Bocca, A., Gonçalves, T. & Casadevall, A. *The interaction of Cryptococcus neoformans with murine macrophages affects host mitochondrial function* (submitted)

3.**Coelho, C.,** Bocca, A. & Casadevall, A *The intracellular life of Cryptococcus neoformans* (manuscript accepted in Annual Reviews of Pathology)

The following papers are collaborations under various stages of submission in peer-reviewed international scientific journals:

4.Saylor, C.A.*, Nicola, A.*, **Coelho, C.***, Rusakova, V., Holemon, H., Yagita, H. & Casadevall, A. *Integrin beta 1 promotes the interaction of murine IgG3 with effector cells and thus functions as a non-classical Fc receptor*. (manuscript in preparation) * joint co-authorship

5.**Coelho, C.**, Bocca, A., Derengowski, L.S., Gonçalves, T. & Casadevall, A. *Gene expression analysis of macrophages exposed to* Cryptococcus neoformans*: insights into pathogenesis.* (manuscript in preparation)

6.Bocca, A., **Coelho, C.**, Saavedra, P., Prados-Rosales, R. & Casadevall, A. *Enhancement of macrophage antifungal activity against* Cryptococcus neoformans *by Dectin-1 stimulation* (manuscript in preparation)

Resumo

Os macrófagos têm a capacidade de rapidamente fagocitarem *Cryptococcus neoformans* (Cn). Estas células do sistema imunitário são cruciais na defesa, latência e reactivação da criptococose. Após fagocitose de Cn, foi descrito um aumento da proliferação dos macrófagos. No entanto, a interação do fungo com o hospedeiro resulta maioritariamente em dano para o macrófago, nomeadamente pela formação de um vacúolo gigante , o aumento de vacúolos citosólicos, uma alteração da morfologia, designada por "Hueco cell" e a permeabilização dos fagossomas. Para uma melhor compreensão da virulência de Cn, torna-se necessário elucidar a origem e a mecanística destes danos celulares, que culminam frequentemente na morte do macrófago. Nas células eucarióticas, tanto a morte como a proliferação são decisões celulares tomadas após integração de sinais da mitocôndria. Para além disso, apesar da mitocôndria ter sido implicada na resposta imune antimicrobiana, não existem ainda estudos no contexto das infecções fúngicas.

Este trabalho propôs-se a expandir o conhecimento existente da interacção entre macrófagos e Cn. Para tal, foi estudado o ciclo celular de macrófagos murinos após infecção prolongada com Cn e em seguida, foi caracterizado o tipo de morte que ocorre no macrófago. Dado que a mitocôndria está envolvida na morte celular, este trabalho prosseguiu no sentido de averiguar modificações da função mitocondrial após a fagocitose de Cn.

Para a concretização dos objetivos, desenvolveu-se um protocolo de microscopia automatizada ("Laser Scanning Microscopy") que facilitou as quantificações de eventos celulares observados por microscopia. Este protocolo mostrou que o macrófago, após uma resposta inicial de proliferação, sofreu um bloqueio no ciclo celular seguido por activação de vias metabólicas de morte. Foi igualmente observado que, mesmo em condições de bloqueio do ciclo celular causado por IFN-γ e LPS, a fagocitose de Cn é suficiente para reverter esse bloqueio. Foi possível observar a proliferação de macrófagos *in vivo,* o que demonstrou que macrófagos residentes nos alvéolos pulmonares são capazes de divisão celular, em condicões de homeostase ou de inflamação. O modelo experimental utilizado neste estudo não foi conclusivo acerca da existência de bloqueio de ciclo celular após infecção pulmonar por Cn. *In vitro,* a morte de macrófagos primários derivados de medula óssea ocorre pela ativação de caspase-1 e caspase-3 e AIF ("Apoptosis Inducing Factor"), o que sugere a activação simultânea de morte por apoptose e por necroptose. Em células J774.16, uma linha celular de macrófagos murinos, foi detectada necroptose mediada por RIP ("Receptor Interacting Protein"). Foi verificada, em ambos os tipos de células, uma redução no potencial mitocondrial, acompanhado por uma diminuição na concentração celular de ATP. Estes resultados foram reproducidos em macrófagos de origem

peritoneal. Foi igualmente demonstrada uma correlação entre a presença de cápsula fúngica e modulação de potencial mitocondrial na célula hospedeira.

Em resumo, os nossos resultados estabelecem a indução de respostas de estresse em resposta à fagocitose de Cn por macrófagos. Estas incluem o bloqueio do ciclo celular, a ativação de caspases e a diminuição do potencial mitocondrial, acompanhadas pela indução de moléculas efectoras de morte celular. Os resultados consolidam um papel activo da mitocôndria na fagocitose e na resposta imune. Estes mecanismos representam um passo importante na compreensão da patogénese de Cn. A longo prazo, estes resultados sugerem novos alvos terapêuticos, necessários ao incremento do prognóstico da infeção por Cn.

Abstract

Murine macrophages readily ingest *Cryptococcus neoformans* (Cn) and are known to play a crucial role in host defense, fungal latency and reactivation of infections. Phagocytosis of Cn by macrophages leads to increased macrophage proliferation, but mostly it causes macrophage damage, in the form of giant vacuole formation, cytosolic vacuoles in the form Hueco cell and phagosomal leakage. Understanding the cause of these injuries provides an insight into Cn virulence and disease. Decisions of cell death, survival or proliferation are frequently integrated by the mitochondria. Further, this organelle has been shown to participate in antimicrobial immunity, but thus far, no studies have been performed for fungal infections.

In this work, we proposed to expand current knowledge on the murine-macrophage-Cn interaction. Specifically, we studied macrophage cell cycle after prolonged Cn infection and then proceeded to characterize macrophage death modalities. Our evidence pointed to mitochondrial involvement in death and as such, we next investigated macrophage modulation, upon Cn ingestion.

To aid our studies, we developed a new protocol based on Laser Scanning Cytometry (LSC), which facilitated quantification of microscopic events. Using LSC, we showed that initial proliferation is a conserved response to phagocytosis, but at later time intervals there was cell cycle arrest and death. Furthermore, phagocytosis of Cn was sufficient to suppress IFN-γ and LPS cell cycle arrest. Macrophage proliferation *in vivo* was observed, demonstrating that resident alveolar macrophages are capable of cell division, both as part of tissue homeostasis and of the inflammatory process. However, the *in vivo* experimental model did not detect toxic effects of Cn in macrophage proliferation. Investigation of effector molecules of death detected activation of caspase-1, caspase-3 and AIF in primary bone marrow derived macrophages, suggesting the occurrence of apoptosis and Apoptosis inducing factor-mediated necroptosis. In an immortalized murine macrophage cell line, we showed Receptor Interacting Protein-mediated necroptosis. We verified a decrease in mitochondrial potential after phagocytosis of Cn, that was accompanied by a decrease in ATP content of the cells. These results were further reproduced in peritoneal macrophages. We also showed a correlation between presence of fungal capsule and mitochondrial modulation in the host.

In summary, this dissertation established induction of stress responses in macrophages after Cn infection. These included cell cycle arrest, caspase activation and decreased in mitochondrial potential, accompanied by induction of cell death effectors. Our results cement a role for mitochondria in phagocytosis and immunity. These mechanisms are a step towards better understanding of Cn pathogenesis. Ultimately, it would provide us with immunological targets, that are needed to improve poor prognosis of Cn infection.

Table of contents

Chapter 3   91

The interaction of Cryptococcus neoformans with murine macrophages results in mitochondrial damage

Chapter 4   117

Discussion and Future Directions

Index of figures and tables

Chapter 1

Introduction

Chapter 2

Analysis of Cell Cycle and Replication of Mouse Macrophages after In Vivo and In Vitro Cryptococcus neoformans Infection Using Laser Scanning Cytometry

Chapter 3

The interaction of Cryptococcus neoformans with murine macrophages results

in mitochondrial damage

We (meaning I) present observations on the scientific publishing process which (meaning that) are important and timely in that unless I have more published papers soon, I will never get another job. These observations are consistent with the theory that it is difficult to do good science, write good scientific papers, and have enough publications to get future jobs.

Schulman, R.E. (1996) *Annals of Improbable Research 2*(5)

Aims

The main aim of this dissertation was to investigate how phagocytosis of Cn by murine macrophages influences the macrophage metabolism and survival.

This objective encompasses the following specific aims:

- develop a high throughput assay of Cn phagocytosis, using Laser Scanning Cytometry.
- characterize how Cn phagocytosis influences cell cycle progression and replication of macrophages.
- characterize the pathways of macrophage death, and its effector molecules, after Cn phagocytosis *in vitro*.
- investigate mitochondrial function, upon Cn ingestion.

Chapter 1

_____

Introduction

***Cryptococcus neoformans* and cryptococcosis**

Cryptococcus neoformans (Cn) is a basidiomycetous fungus, whose teleomorph form is *Filobasidiella neoformans*. Cn was first described in 1894 by Otto Buse (1), but clinical cases were relatively rare until the 1980s, when the encapsulated yeast form jumped to notoriety as an AIDS-associated opportunistic pathogen. Up to one third of AIDS patients develops cryptococcosis and, even with access to medical care, it is fatal in 10-25% of the cases (2-6). Nowadays, AIDS prognosis has improved due to Highly Active Antiretroviral Therapy (HAART), which is reflected in a dramatic decrease in the incidence of cryptococcosis.

One of the distinguishing features of Cn is the presence of a polysaccharide capsule, of which serological reactivity serves for a widely accepted (but not definitive) classification of strains: serotype A corresponds to *C. neoformans* variety *grubii*; serotype D corresponds to *C. neoformans* var. *neoformans*; and serotype B and C strains correspond to *C. gattii* (7, 8). There is one additional serotype AD, very rarely isolated (8). Serotype A is the most commonly found in infected patients (9).
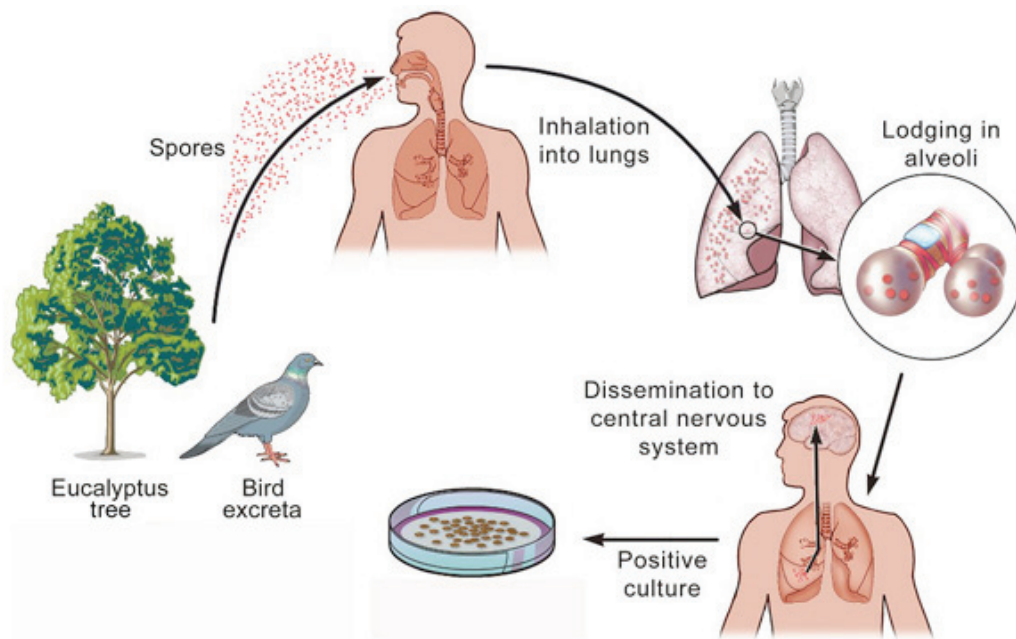
Figure 1. Cn life cycle.

Cn is a ubiquitous environmental yeast. It exists in trees and animals and it possibly has relevant interactions with free living amoeba. Primary infection of humans most likely occurs by ingestion of spores which deposits in the lungs. Infection is asymptomatic, but dormant cells persist in lungs and, possibly, in the

10

brain. If the host immune system is weakened, Cn might establish a life-threatening meningitis. Yeast cells can be identified by the characteristic capsule and production of melanin. *Taken from reference (245)*

Cn is distributed worldwide among trees, mammalians and birds and is actively excreted in pigeon feces (1, 10). Its widespread distribution might explain its wide prevalence, as illustrated by its life cycle in Figure 1. Based on serology from New York City children, it is believed that by the age of five up to 80% of individuals had been infected with Cn (11). Primary exposure most likely occurs by inhalation of a spore or a dried yeast from environmental sources. Primary infection is asymptomatic (11), however, infection is not cleared and the yeast persists in the lung (12). Although there is some evidence that latent Cn infection could lead to exacerbation of asthma (13, 14), it does not seem to affect host's health significantly and remains unnoticed.

Fungal infections are particularly dangerous for immunocompromised individuals (15). Cryptococcal disease is characterized by cryptococcal pneumonia and, due to a particular tropism for the brain, meningoenchepalitis. Once in the brain, in almost every case, the disease is fatal unless treated (16). How the yeast crosses the blood-brain barrier and why it has tropism for the brain is still a matter of discussion (17-19). Cryptococcal disease management is difficult and limited to fluconazole and amphotericin B. Neither caspofungin or nystatin are active against cryptococcal species. In patients with severe immune deficiencies, no drug therapy is curative and the best course of action is restoration of immune function (16, 20). Because most Cn infections occur in individuals with impaired cell-mediated immunity (CMI), such as AIDS patients, it is believed that cell mediated immunity is the main effector mechanism for the fungus. The search for alternative therapies has shown that antibodies can be protective in the context of a murine infection (reviewed in (21)). One capsular antibody has reached clinical trials as a candidate for treatment of cryptococcosis (22). The mechanism of antibody protection is not known, but it is believed to contribute to appropriate regulation of host immunity. Thus far, no vaccines have been licensed against Cn, or any other fungal pathogen. Therefore, better understanding of the mechanisms that control fungal infection in immunocompetent individuals are required for a more successful therapeutic approach.

The immune system

Humans function in close association with microbes. For most of the cases the interaction is a successful symbiosis, but a tight control is required to prevent microorganisms of causing harm to the host. This is the function of the immune system. However, immune function is significantly compromised in individuals undergoing treatments such as cancer chemotherapy or following organ transplantation, as well as in individuals infected by agents such as HIV. These individuals become susceptible to a new range of infectious diseases

where pathogenic/symbiotic duality does not apply. In response to this, the damage response framework (23, 24) was proposed, postulating that pathogenesis and virulence need to be understood as an emergent property between host and pathogen. If a delicate equilibrium is not achieved, with either insufficient or exaggerated inflammation, the host develops disease. This view has been widely accepted since it provides a working model that encompasses conditions from allergic pathologies to opportunistic infections and classical infectious diseases.

The immune system is divided into innate and adaptive immune system. The innate component is a primary defense, permanently in place and responsible for controlling the first 96 hours of infection. It involves highly phagocytic resident tissue cells, like macrophages and neutrophils, invariant NK cells, B1B cells and epithelial γδTcell. Secreted proteins like defensins, unspecific antibodies and the complement system are major components of the innate immune response (25). It takes 3-4 days for adaptive immunity to initiate a specific response, where specific means tailored to the pathogen in question. This assures that the response is effective for the pathogen encountered. The classic link between the innate and adaptive immune responses is the Dendritic cells (DC). DC will uptake the pathogen at the onset of innate immune response, travel to the lymph nodes and there, through a process called antigen presentation, will activate cells of the adaptive immune system. One of these subsets are cytotoxic CD8+ T cells, responsible for killing infected host cells. Other subsets of T cells activate and direct the immune system: CD4+ Th1 cells will activate macrophages and NK cells to kill intracellular pathogens and CD4+ Th2 cells will activate B cells to produce specific antibodies which will then activate eosinophils and kill extracellular pathogens. Through the phenomenon of immunological memory, the adaptive immune response is stronger and faster if the pathogen is encountered a second time. Ideally, innate and adaptive immunity cooperate in such a way that prevents the pathogen from causing significant long lasting host damage.

Innate immunity was for a long time considered not specific, meaning that it was not tailored to the pathogen in question. The discovery of Pathogen Associated Molecular Pattern (PAMP) has shown that the specificity of innate immunity begins at first contact (26, 27). PAMPs are characteristic microbial molecules that allow host cells to detect a foreign molecule. PAMP are recognized by Pattern Recognition Receptors (PRR) , which are grouped in 4 major families: Toll-like receptors (TLRs), nucleotide oligomerization domain (NOD)-like receptors (NLRs), C-type lectin receptors (CLRs) and retinoic acid-inducible gene I (RIG-I)-like receptors (RLRs). Simultaneously, the immune cells monitors molecules which reflect organelle and cellular injury to the host. These molecules, like purines and nucleic acids, are recognized through Danger Associated Molecular Receptors (DAMP), allowing the immune system to monitor excessive host damage. Through

DAMPS and PAMPs, immune cells possess very intricate sensors of their environments and are constantly fine tuning their response to the "inflammation" in question, balancing pathogen control and host damage (25).

Macrophages

Macrophages can be seen as the primary danger sensor of the body. From the a yolk sac or bone marrow progenitor, macrophages migrate to every tissue in the body where they become a resident population with critical homeostatic and immune functions (28, 29). As part of homeostasis, they remove apoptotic cells and remodel extracellular matrix. As part of immunity, they perform immunosurveillance, microbicidal killing, tissue healing, and scar formation. To better perform their functions they specifically adapt to the tissue where
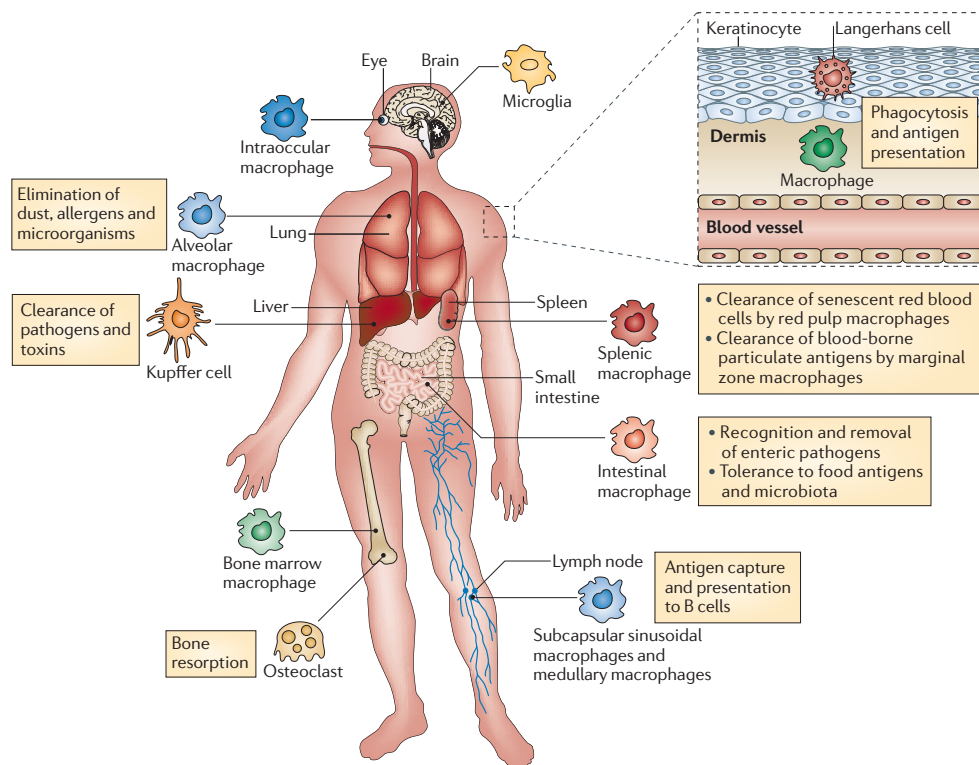
Figure 2. Macrophage heterogeneity in the body.
Bone marrow precursors originate cells of the mononuclear phagocyte lineage. They are released into the circulation as monocytes. A percentage of the population stays in the blood, while the others migrate into virtually all tissues of the body, where they differentiate into mature macrophages or dendritic cells. Resident macrophages adapt to the tissue in question, both in morphological markers, inflammatory status and specific functions. However all populations perform important immune surveillance activities and tissue remodeling activities. *Taken from reference (246)*

they are reside, as illustrated in Figure 2. For example, osteoclasts perform bone remodeling while thymic macrophages are important to remove apoptotic T cells during T cell selection (29). Macrophages are probably the cells that express the most complete set of PRR. Upon detection of pathogens or abnormal host cells by these receptors, macrophages start cytokine secretion, chemokine secretion and/or ingestion of the particle. An alveolar macrophage will have the widest array of PRR and scavenger receptors to defend against inhaled particles, but poor antigen presentation capabilities to avoids life-threatening pneumonitis (30). Microglial macrophages have low phagocytic abilities, while gut macrophages are highly phagocytic but secrete few inflammatory cytokines (29). Tissue specific adaptation confers heterogeneous morphologies and surface marker patterns to macrophages. But however heterogeneous, macrophages always play a central role in homeostasis and immunity of the tissue they reside in.

In order to accomplish such a wide array of functions, macrophages can further undergo differential activation. These activation states have been characterized *in vivo* and *in vitro*. A classically activated macrophage results from NK and T cell derived IFN-γ, together with bacterial LPS. These activate all of the macrophage microbicidal mechanisms, rendering the macrophage more effective in killing pathogens. Chitin stimulation of basophils and neutrophils causes Il-4 release, which in turn causes macrophages to become alternatively activated. They will upregulate chitinase-like molecules receptors (Ym1 and Ym2), which are related to renovation of extracellular matrix (31). Presence of apoptotic cells or immune complexes leads to the development of a third activation state: regulatory macrophages. This phenotype leads to macrophage production of Il-10, which is highly immunosuppressive (31, 32). A brief description of these states is shown in Figure 3. These different activation states allow macrophages to be involved in all steps of an immune response. Once infection is detected, macrophages ingest and degrade the pathogen, perform antigen presentation, and secrete appropriate cytokines to alert other immune cells. They can be activated by adaptive immunity to become a classically activated effector cell or, if alternatively activated, aid in granuloma formation. When infection is contained, macrophages switch their phenotype to help in the healing process and scar formation (31). It is interesting to note that while *in vitro* these phenotypes are clear cut *in vivo* activation states can overlap considerably (31). Intermediate phenotypes between these 3 states have been described, for example, in tumor macrophages (31). Thus it is believed that modulation of activation states has therapeutic potential. In short, macrophages are considered an extremely plastic cell, with a full spectrum of activation states, which are tightly and rapidly regulated by external cues (31).

Regardless of activation state, macrophage cells are professional phagocytic cells. Phagocytosis is defined as the ingestion of particles over 0.5 - 1 μm within a specialized dynamic compartment (33, 34), in order to

14
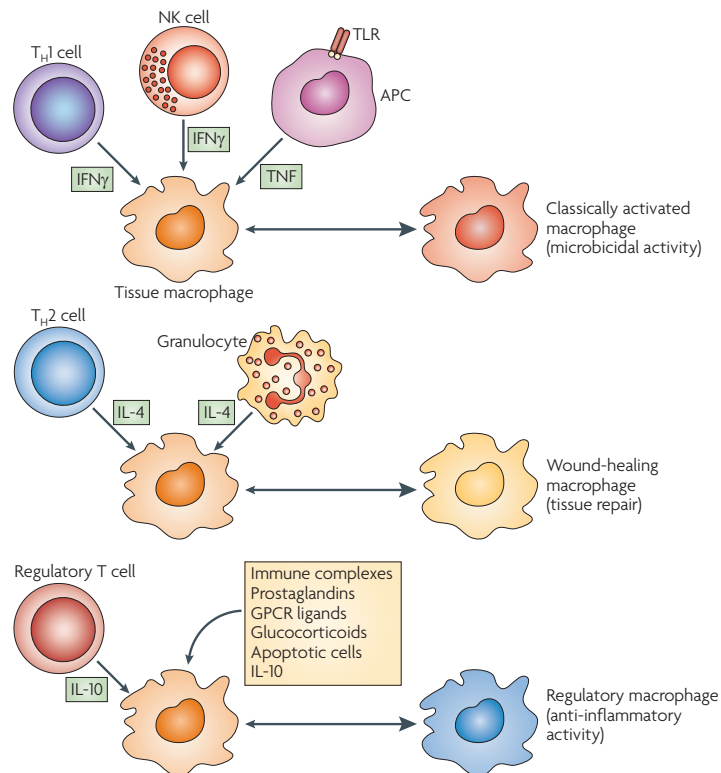
Figure 3. Macrophage activation states.

 T helper 1 (T_H1) cells or CD8+ T cells (not shown) from the adaptive immune system or Natural Killer (NK) cells, during an innate immune response produce Interferon-γ (IFN), leading the macrophage to classical activation. Production of Tumor-Necrosis Factor (TNF) by Antigen-Presenting Cells (APCs) also leads to classical activation.

 Production of Interleukin-4 (IL-4) by T_H2 cells, during adaptive response or by granulocytes leads to alternatively activated macrophages.   Several stimuli originate regulatory macrophages: immune complexes, prostaglandins, G-protein coupled receptor (GPCR) ligands, glucocorticoids, apoptotic cells or IL-10. TLR, Toll-like receptor. *Taken from reference (31)*

degrade them with a powerful arsenal of hydrolytic enzymes. Ingestion of particles for phagocytosis starts after activation of either scavenger or opsonic receptors (35).   Upon receptor activation, the cellular membrane engulfs the particle by one of three distinct processes: reaching (zipper), sinking or triggered (coiled) mechanisms (34). These mechanisms are morphologically distinct and have been postulated to use distinct components of the cytoskeleton (36, 37) and are thought to influence the outcome of the ingested particle (36). In every case, phagocytosis results in segregation of the ingested particle within a cytoplasmatic membrane-bound compartments. A sequential process of fusion of diverse vesicles from ER, Golgi, and lysosomal origin changes phagosome composition. This process is known as phagosome maturation, where phagosomes become acidic and enriched in hydrolytic enzymes and proteases.   Antimicrobial molecules are secreted into the

phagosome: free radicals, lactoferrin, lysozyme, defensins and histatins (38). NADPH oxidase in the phagosome will use O_2 to produce superoxide, which is then converted to toxic Reactive Oxygen Species (ROS) (39). More ROS can be produced by uncoupling of the mitochondrial respiratory chain and by 5-lipoxygenase (39). If inducible Nitric Oxide Synthase (iNOS) is active in the presence of ROS, equally toxic Reactive Nitrogen Species (RNS) are formed (39). Additional toxic molecules can be produced by other immune cells and used by macrophages. For example, myeloperoxidase enzyme exists only in monocytes and neutrophils, but if uptaken by macrophages it results in highly toxic hypochlorous acid (38). The same is true for defensins, peptides that are imported into the phagosome and create membrane pores in microbes (40). Although most of these molecules can be secreted into the extracellular space, the phagocytic compartment contains the pathogen and thus minimizes host damage. In addition to high levels of toxic molecules, the phagosome is assumed to be low in nutrients. This is achieved by active sequestration of elements, notably iron, and sources of carbon and nitrogen sources. The availability of little nutrients in the phagosome aims at restricting pathogen growth. In fact, engulfed yeasts induce starvation responses, for example Cn (41) and *Candida albicans* (42). Phagocytosis is a central mechanism of the immune response, since it is highly effective in pathogen inactivation and allows for microbe degradation for antigen presentation for subsequent immune response.

The genetic response of macrophages to foreign stimuli has been described (43). TLR stimulation, ingestion of latex beads or ingestion of live bacteria lead to a common response that affects transcription, cell cycle, and stress factors. This response occurs by the mere sensing of a non-self particle in the extracellular milieu. If the stimulation came from microbial ligands, but not inert latex beads, anti-apoptotic and cell cycle factors were additionally affected. If the particle was of enough size to be phagocytosed, more components are added: isoprenoid biosynthetic processes, cholesterol biosynthesis, and cell differentiation processes are modified (43). To complement the genetic approach, proteomics analysis showed down-regulation of proteins for metabolism, energy homeostasis and development after phagocytosis (44). This underscores the existence of a common core response to non-self. However this common core response is then complemented by a response that is specific to the type of non-self encountered. This is explained by activation of distinct combinations of receptors at all stages of phagocytosis (34, 43, 44) which reciprocate to influence the phagocytic process. This distinction is so detailed that it is capable of distinguishing between inert and pathogen particles or between opsonic and non-opsonic phagocytosis: ingestion through each opsonic receptor reflects different fates within the phagosome (45) while phagocytosis of inert beads leads to distinct phagosome maturation kinetics than those observed with live bacteria (43, 46). Even with simultaneous phagocytosis of opsonized and unopsonized beads, there is still separate processing of each individual phagosome (47). Host sensors of pathogen molecules

are aided by physical sensors. Size, shape, and rigidity of the particle are capable of influencing the phagocytic process (34, 48). The combination of these physical and molecular sensors is complex enough that the phagocytic synapse is able to distinguish between a soluble β-glucan, a particulate β-glucan or a live yeast (β-glucan associated to yeast cell wall) (34). Overall, macrophages possess a common activation response but also a ligand specific response. This allows the immune cell to distinguish, with great detail, what kind of danger it is encountering, and initiate an adequate response.

Life of the macrophage

Until recently, little was known about macrophage proliferation within tissues and its consequences for immunity. It was somewhat accepted that local proliferation could be enough for maintenance of homeostasis (49, 50), and it was thought that, upon and after inflammation, tissue compartments are replenished with circulating monocytes coming from the bone marrow (31, 49). It is now known that establishment of a resident population of macrophages can occur both from yolk sac progenitors and from bone marrow stem cells. In both cases the macrophages become tissue resident macrophages and can survive for years in the tissue.

In vitro, LPS stimulation is capable of arresting macrophages in G1 phase and so it was thought macrophage activation was synonymous with cell cycle arrest. Interestingly, concomitant activation with IFN-γ protects macrophages from LPS-induced cell cycle arrest and apoptosis (51). Furthermore, there is evidence that cell cycle phase influences macrophage behavior: drug-induced cell cycle arrest in G1 influences MHC class II expression (52) or prevents LPS-induced apoptosis (53). Evidence for the importance of cell cycle in immunity of macrophages is that pathogens have evolved to interfere with it. Bacterial products responsible for cell cycle interference are called cyclomodulins (54). These toxins cause DNA damage or interfere with the cytoskeleton in such a way that the host cell suffers cell cycle arrest. Other times, the host cell experiences defective mitosis, resulting in endomitosis and poliploidic nuclei, which can then lead to apoptosis (54). How cyclomodulins affect virulence has not been fully established, but cell cycle alterations by pathogens might promote appearance of cancer. Therefore, we can infer that the pathogen has an advantage to interfere with cell cycle, which must mean that cell cycle and proliferation have consequences for immunity.

There are several instances where activation of immunity is dependent on cellular proliferation. Note the case of T cells and B cells, which undergo clonal expansion in the lymph node upon activation. This did not seem the case for macrophages. However, reports of local macrophage proliferation have been available in the literature for a long time, in particular in lung alveolar macrophages (55-59), both in naive and inflammatory conditions. Resident macrophage proliferation in inflammatory conditions was firmly established by Jenkins *et.*

al (60), who observed proliferation, in the pleural cavity, after a Th2 inflammatory stimulus (60). The data showed that a Th1 inflammation did not cause macrophage proliferation, unless Il-4 (a hallmark of Th2 response) was also present. This was readily accepted as a consequence of the different macrophage activation states (61). Soon after, resident macrophage proliferation was reported in other experimental models: zymosan-induced peritonitis (62) and autoimmune encephalitis (63). These studies did extend macrophage proliferation to Th1-type response. Thus these discrepancies, compared in Figure 4, are probably attributed to the distinct inflammatory stimulus used. Because these studies also observed naive tissues, a complete picture of macrophage proliferation is now emerging. In 2 week old mice, infiltrating monocytes proliferate after arrival to the peritoneum, implicating local proliferation as a way to colonize tissues during infancy (62). Proliferation of resident macrophages increased after resolution of the inflammatory stimulus, as to restore the resident macrophage population (62). Last but not least, Janssen observed selective apoptosis of infiltrating monocytes at the resolution of infection (64). Resident macrophages were left untouched in his model. So it seems that in order to aid the immune response additional macrophages are recruited from infiltrating monocytes, but are
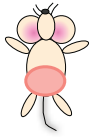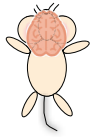
	Pleural cavity	Alveolar	Peritoneal	Microglia
Legend: ∅ None, + Slow, ++ Increased				
Naive tissue	Proliferation +	Proliferation +	Proliferation +	Proliferation ∅
Inflammatory stimuli	Helminth infection Th2 Il-4	Intratracheal LPS H1N1 Influenza pneumonia	Sterile Zymosan	Autoimmune encephalitis
Inflammation	Proliferation resident ++ Proliferation infiltrated ∅	Proliferation resident ++ Proliferation infiltrated ∅	------	Proliferation resident ++ Proliferation infiltrated ∅
Resolution	------	Survival resident Apoptosis infiltrated	Proliferation resident +	Survival resident Apoptosis of infiltrated
Additional findings	Il-4/Th2 dependent	Half life > 8 months Apoptosis dependent on FasL	Proliferation at development	------
Reference	Jenkins, 2011	Janssen, 2011	Davies, 2011	Ajami, 2011

Figure 4. Macrophage proliferation in tissues.

Recent studies have highlighted macrophage proliferation in response to different stimuli. Some report macrophage proliferation only in Th2 type inflammation, but other studies do not agree. Tissue specific mechanisms may be the base for these differences. *Based on references (62, 64-66)*

selectively killed upon resolution of damage.   Only in a case of extensive damage there is replenishment of tissue macrophages from the bone marrow compartment.   Resident macrophages are now accepted to be responsible for self renewal in tissue and to proliferate as a part of homeostasis and inflammation.

Death of the macrophage

When speaking of cell death, two main types of cell death are considered: necrosis and programmed cell death. Necrosis is a violent and inflammatory death that causes the cell membrane to lose integrity, releasing intracellular components into the milieu. On the other instance, programmed cell death is a tightly regulated, energy-dependent cellular suicide mechanism, where cellular organelles are decomposed and degraded before cell membrane loses integrity.   Programmed cell death was first described as apoptosis in 1972 (65). Morphological features of apoptosis include chromatin condensation, picknotic nuclei and vesiculation of the cytoplasm. Recently, mechanisms of programmed cell death other than apoptosis have come to light (66).

Apoptosis can proceed through 2 major pathways and its main effectors are a family of cysteinyl aspartate proteases (caspases) (67). Apoptosis is highly conserved and even yeasts can suffer a kind of programmed cell death. Pathways are well characterized and have been reviewed extensively (67). The first pathway is called the extrinsic pathway, since death receptors at the plasma membrane are activated by extracellular TNF-α or FasL signals.   For example, cytotoxic T cells use these signals to kill abnormal host cells. Activation of death receptors activates initiator caspase-8, which then activates effector caspase-3. In some cells, caspase-8 activation requires two extra steps, release of cytochrome c from the mitochondria and activation of initiator caspase-9. Only then, effector caspase-3 will be activated. The second pathways is dubbed intrinsic apoptosis. This occurs when DNA or cellular organelles are damaged. This damage activates initiator caspase-9, which directly activates caspase-3.

Other types of programmed cell death have surfaced in the past decade. One of them, pyroptosis seems to be exclusive to the immune system.   Activation of NLR by cytoplasmatic PAMPs and DAMPs leads to assembly of a multimolecular complex, the inflammasome.   In turn, the complex activates caspase-1 and secretion of Il-1β and Il-18. Caspase-1 activation causes permeability of the plasma cell membrane, while loss of cell viability is not immediate.   However, the permeability of the cell membrane leads to release of inflammatory molecules into the extracellular milieu, alerting other immune cells (68). Other newly identified death mechanisms are dubbed necroptosis. They are caspase independent programmed cell deaths that share morphological characteristics of necrosis and apoptosis.   Receptor- Interacting Kinase (RIP1) will activate
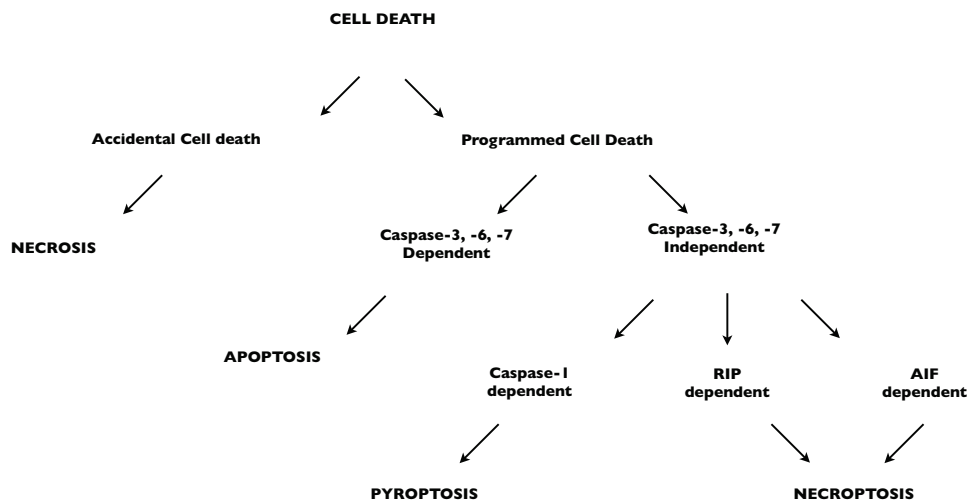
Figure 5. Hierarchy of cell death decision.

Proposed hierarchy of cell death decision. This model only encompasses molecular programs of death mentioned in this study and it is not exhaustive. *Based on references (68, 73)*

mitochondrial permeability and cell demise (69). When DNA damage is sensed, Apoptosis Inducing Factor (AIF) release from the mitochondria causes a DNA fragmentation and consequent death (70). These newly described death pathways have mixed morphological features and their identification has to rely instead on characterization of biochemical cascades (66), as illustrated in Figure 5.

It is important to note that inhibition of one form of death will not always result in inhibition of death, but can instead result in a rerouting of the pathway to an alternate pathway of death. Cell death pathways possess an extensive cross regulation between them, as outlined in Figure 6. Increasing the dose of the toxic stimulus alters which pathway of death is activated and more importantly, more than one pathway of death can coexist within the same milieu. Thus determining the pathways involved in programmed cell death becomes complex. Execution of their molecular program will lead to very distinct outcomes, because different signals are released into the extracellular milieu. The death of an immune cell upon infection reflects damage to the host and as such the death of immune cells has very relevant effects in immunity (66, 71). Death of the macrophage by necrosis will trigger inflammation, but might also release pathogen in the extracellular space, while death by apoptosis will be anti-inflammatory and maintain the pathogen contained within a lipid bilayer. Meanwhile, pyroptosis can lead to enhanced immunity by triggering release of inflammatory molecules (68). This explains why pathogens have evolved to subvert these cascades. Several examples are found in the bacterial kingdom:

Staphylococcus aureus phagocytosis is cytoprotective for macrophages (72) is one of many examples. Similarly, survival of *Mycobacterium tuberculosis* is affected by the mode of macrophage death (73). *M. tuberculosis* have evolved mechanisms to decrease host apoptosis, facilitating their intracellular lifestyle in the lung (74). In the fungal kingdom, survival to *Histoplasma capsulatum* infection is decreased when apoptosis is inhibited (75). In contrast, inhibition of NO signaling after *Candida albicans* infection leads to inhibition of apoptosis and host protection (76). It is clear that manipulation of cellular death pathways has widespread effects in infection.

Mitochondria and immunity

Mitochondria have been suggested as a place of integration of signals, concerning proliferation, death and immunity (77-80). Mitochondria's main function is to produce energy for the cell by oxidative phosphorylation. Oxidation of substrate by the electron transport chain creates a transmembrane potential across the inner mitochondrial membrane. This potential drives a proton gradient which in turn drives production of ATP. As such, mitochondrial function is commonly assessed by measuring the inner mitochondrial transmembrane potential ($\Delta\Psi_m$). Cells, with high energy demands, such as skeletal muscle, have alternative forms of obtaining ATP. This is achieved by lower efficiency glycolysis, resulting in the production of lactate. The balance between glycolysis and oxidative phosphorylation is a reflection not only of the cell's energy requirements at any given moment, but also of outside cues like hypoxia. Mitochondrial oxidative state is tightly regulated during cell cycle and proliferation (77). In fact, a reduction in oxidative phosphorylation is mandatory for cells to proliferate. The reason for this is unknown. Since mitochondria exist in a branching network that can suffer fusion or fission to serve cellular needs (78), regulation of energy production also affects mitochondrial organization. Because of their central role in producing energy, mitochondria are central for cellular functions.

However, mitochondria possess many other functions than energy factories. Mitochondria are responsible for production of amino acids and other molecules. A myriad of cytosolic events are dependent on mitochondrial components. One example is that cell death pathways are activated by release of mitochondrial cytochrome c or AIF into the cytosol (as discussed above). Release of mitochondrial DNA and N-formyl peptides, which reflect mitochondrial damage, activates the inflammasome. The same components, if released into the extracellular milieu, activate stress responses in neighboring cells. Damage to the mitochondria is used as a universal danger signal: mitochondrial DNA injection into the joints triggers inflammation, while nuclear DNA does not (78). Not only serving the cell's energy requirements, mitochondria are an integration site for

21
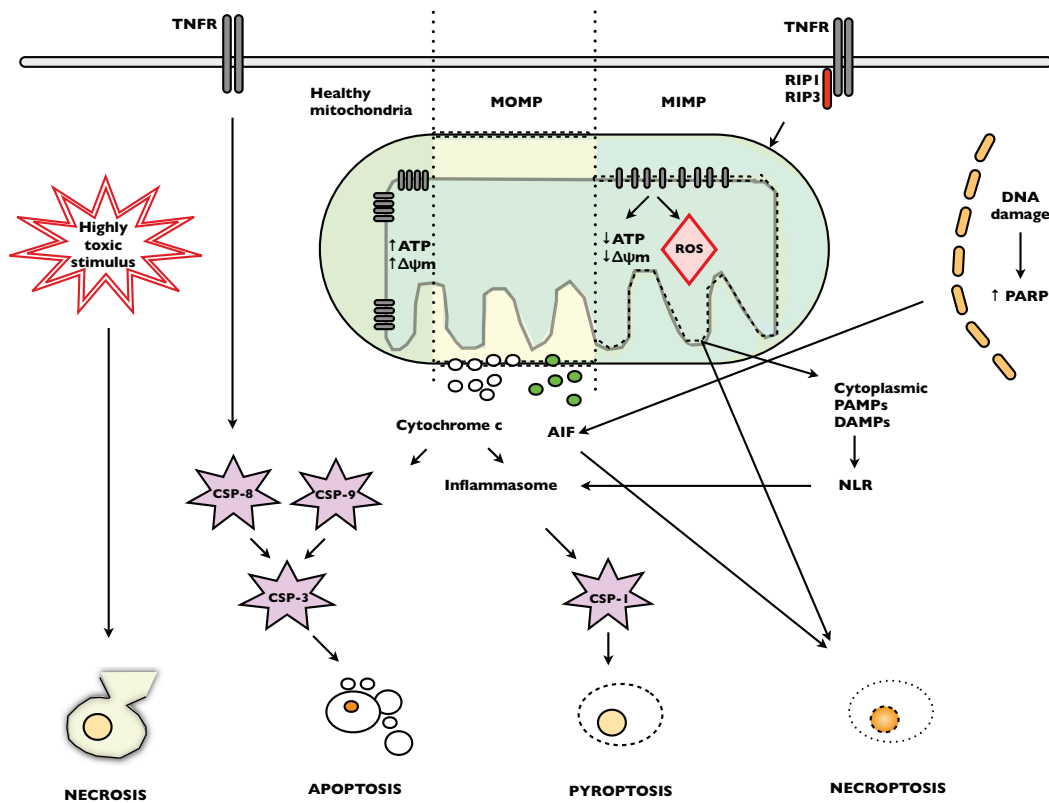
Figure 6. Mitochondria's central role in death pathways.

Mitochondrial components are involved in life and death decisions. An extensive crosstalk between pathways exists, making mitochondria one integration center for these decisions. Necrosis is caused by a highly toxic stimulus. There is causes abrupt cell rupture, releasing cytoplasmatic components into the extracellular milieu. Death receptors activate the extrinsic pathway of apoptosis. TNF-α Receptor 1 (TNFR), one of the death receptors, will cause activation of initiator caspase-8 (CSP-8) and subsequent effector caspase-3 (CSP-3). The intrinsic pathway senses intracellular damage, including mitochondrial damage. This will cause Mitochondrial Outer Membrane Permeability (MOMP) and consequent release of cytochrome c (cytoc c) and other mediators (not displayed), which then activates initiator caspase-9 (CSP-9) and effector caspase-3. Both apoptotic pathways share morphological features, with degradation of organelles, nuclear condensation and vesiculation of cytoplasm. Another type of death is necroptosis. DNA damage activates Poly(ADP)ribose-polymerase (PARP), causing Apoptosis Inducing Factor (AIF) release from the mitochondria and initiating AIF mediated-necroptosis. Ligation of TNFR activates Receptor Interacting Protein 1 (RIP1). RIP1 causes decoupling of oxidative phosphorylation, subsequent release of mitochondrial ROS and dissipation of the mitochondrial potential. This results in inner mitochondrial membrane permeability (MIMP). This process is RIP-dependent necroptosis. Independently of the effector molecule, necroptosis has intermediate characteristics of apoptosis and necrosis, where some organelle degradation exists but cellular components are released into the extracellular milieu. Both MOMP and MIMP will cause mitochondrial permeability to be increased and oxidative phosphorylation failure, which culminate in release of cytochrome c and mitochondrial ROS. These are known activators of the inflammasome. Activation of the inflammasome results in active caspase-1 and pyroptosis. Pores are opened in the cellular membrane, while maintaining cell viability and there is secretion of specific inflammatory molecules, such as IL-1β and IL-18. *Based on references (72,79,81, 247)*

cellular decisions.   Several cellular processes either have one mitochondrial step or require access to mitochondrial components, and thus mitochondrial damage impairs normal cell functioning.

Mitochondria have signaling and effector functions in immunity. In fact, virulence factors that interfere with mitochondria have been characterized in bacteria and virus (reviewed in (80), but not in fungi. Effector functions of mitochondria are best described at viral infection. It was found that one PRR, the Mitochondrial Antiviral Signaling Protein (MAVS), required association with the outer mitochondrial membrane for proper antiviral signaling. Proper mitochondrial fusion is required for subsequent antiviral response (Figure 7). In the case of bacteria, activation of TLR in the phagosome drives production of ROS, both from phagosomal NADPH oxidase and uncoupling of oxidative phosphorylation. Mitochondrial ROS (mtROS) are a substantial part of cellular ROS and serve the dual purpose of antimicrobial and signaling molecules. (79).   Firstly, mtROS production is necessary for maximum bacterial killing.   Increased mtROS production can be achieved by deleting UCP2.   Mice deficient in this protein have increased resistance to *Toxoplasma gondii* and *Listeria monocytogenes*. This is sufficient proof of the effector functions of mtROS. Secondly, cellular ROS have been suggested as the signaling molecule for inflammasome activation (81), antiviral signaling (78), mitogen-kinase protein activation (82) and many others (83).   Although ROS are a signaling molecule, the picture is not complete yet and more mitochondrial factors have to be characterized (79, 84).   A direct link between mitochondria and phagocytosis was discovered by Park (85).   Upon phagocytosis of an apoptotic cell, macrophages increase their mitochondrial potential in a process that is dependent on Uncoupling Protein 2 (UCP2).   Phagocytosis of *Shigella flexneri* and *Listeria monoctyogenes* pathogen decreases mitochondrial potential (86, 87).   Overall, many of the mitochondria regulatory decisions require ROS dependent signaling. Mitochondrial signaling and, in particular, mtROS influence the outcome of an infection.
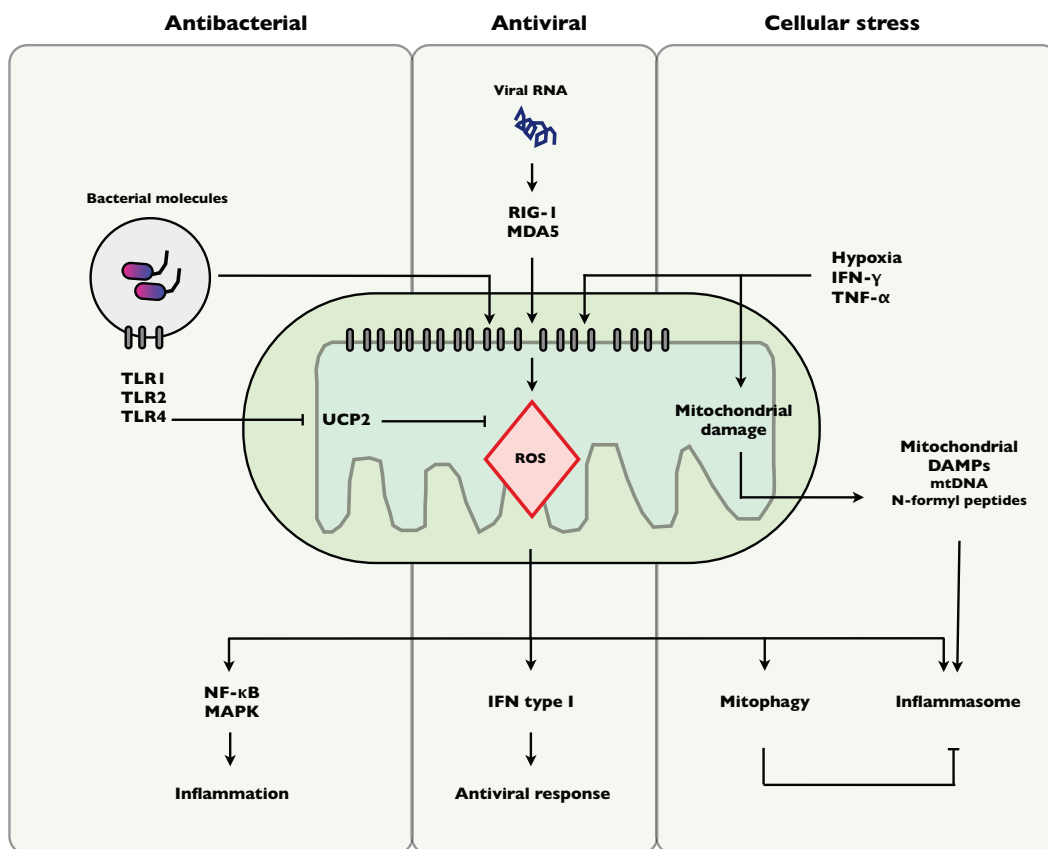
Figure 7. Mitochondrial role in innate immune responses.

Cytosolic viral RNA is recognized by retinoic acid-inducible gene (RIG-1) and melanoma differentiation-associated gene (MDA5), members of the RIG-I-like receptors (RLR) family. A complex signaling cascade results in increase of mtROS but also antiviral type -1 interferon antiviral responses. Activation of TLRs in the phagosome also results in uncoupling of the mitochondrial respiratory chain, resulting in mtROS and consequent Nf-kB and MAPK inflammatory signaling. For example LPS, through TLR4, can inhibit UCP2 which then inhibits ROS production. Extracellular signals, such as Hypoxia, IFN-γ and TNF-α also cause decoupling of mitochondrial respiration and the subsequent mitochondrial damage. The release of damaged mitochondrial components is recognized as danger signals, resulting in both increased mitophagy and inflammasome activation. Mitophagy can successfully remove damage mitochondria and brake inflammasome activation. *Based on references (80,86)*

Laser Scanning Cytometry

Phagocytosis has been extensively studied by many methods. Due to the size of Cn, plain observation of co-cultures of macrophages and Cn under a light microscope are enough to determine ingestion. Quantitation of additional parameters is facilitated by the addition of dyes and antibodies. The dye can indicate different metabolic parameters of the cells or a fluorescently labelled antibody can indicate expression of a protein. Later on, Flow Activated Cell Sorting (FACS) was developed allowing fluorescent quantitation of high number of cells and allowing for simultaneous multiparameter analysis. The development of Laser Scanning Cytometry (LSC) has brought all of these together (90). LSC is a combination of the Flow Cytometry analysis applied to microscopic images. When extensive amounts of microscopic images need to be analyzed specialized softwares is available for automated analysis, which serves the dual purpose of decreasing operator time and bias. LSC requests operator instructions for image acquisition and analysis and based on these parameters the data is displayed in bivariate plots to facilitate analysis of cell populations. LSC has allowed to measure more parameters with less input from the operator and as such allowed scaling-up of the experiments, without loss of information of microscopy. This technique has become very valuable for immunological studies (91, 92) and applications such as immunophenotyping of blood samples (93), DNA ploidy analysis (94), cell cycle (95), caspase activation (96) and phagocytosis of bacteria (97-99) and Cn (100).

Cn and the the immune system

The host side

The individuals most at risk for cryptococcosis are the ones with a defect in CMI, with a relevant but controversial contribution by humoral immunity (101). Both HIV infection and immunosuppressive therapy, such as transplant rejection therapy and cancer chemotherapy, lead to CD4+ T cell defects, impairing CMI. Patients with lymphoproliferative diseases and some cases of diabetes mellitus are also at high risk for cryptococcosis (15). Natural occurring deficiencies predisposing for Cn infection are hyper-IgM syndrome and autosomal dominant hyper IgE syndrome (102). Thus, it is widely accepted that the fungus lies dormant within the lungs and reactivates if defects in cellular immunity arise (12).

There are a myriad of PPR that can recognize fungi, but only some are important to Cn infection. Fungi are mostly recognized through the CLRs, which include dectin-1 and mannose receptor (25). These receptors recognize cell wall components, such as α-glucans, β-glucans and chitin. Dectin-1 recognizes zymosan, a β-glucan and it is one of the most studied receptors in fungal immunology. TLRs can recognize mannans and zymosan from the cell wall, as well as fungal nucleic acids. Macrophages/monocytes express CD36 and other scavenger receptors, which bind β-glucans. NLR recognize intracellular zymosan. Unencapsulated Cn is readily ingested through mannose and beta-glucan receptors (103). *In vitro,* the capsule is highly anti-phagocytic. It was hypothesized that the capsule would hide some, if not most of these PAMP. For phagocytosis to proceed *in vitro*, opsonization with antibody or complement is necessary, after which phagocytosis proceeds through both FcR and CR (104). However, *in vivo* phagocytosis readily occurs. Deposition of complement (105, 106) has long been described as opsonic. Lung bronchoalveolar lavage can be opsonic for *Aspergillus* conidia (107), and surfactant protein A binds Cn capsule, but only in the presence of antibody (108). Absence of this protein had no influence into Cn phagocytosis *in vivo* and overall mouse survival. Recently, additional components have been found to mediate phagocytosis in the lung (109). Defects in recognition of Cn by PRR will impair the correct activation of the innate immune response and hamper host immunity. Mice defective in mannose receptor (110) or complement receptor (105) are more susceptible to Cn infection. TLR2 and Myd88 defective mice are more susceptible than WT mice (111, 112). TLR2 is required for maximum cytokine production and mice lacking CD36 receptors are more susceptible than WT to Cn infection (109). However, mice defective in Dectin-1, a major β-glucan receptor (113) or TLR4 (111, 112) are not more susceptible than wild-type mice to Cn infection. Mannose receptor, CD36, complement receptor and TLR2 therefore cooperate for Cn recognition in the lung.

Control of Cn infection is not the exclusive responsibility of one immune cell type. It is their concerted efforts that allows the host to control infection. Neither granulocyte nor γδ-T cells are absolutely necessary for defense against Cn (114) and might even be detrimental. Neutrophils could be auxiliary cells in the activation of the adaptive immune response (15), can kill Cn through oxidative mechanisms and defensins (40), but mice deficient in neutrophils (115) are resistant to cryptococcosis. Eosinophils have been found in association with Cn in the lung (116), and persistent eosinophilia is detrimental (117) but studies with eosinophil deficient mice have not been performed. Overall, macrophages seem the one innate immune cell essential for Cn control (118, 119). Dendritic cells are fungicidal for Cn *in vitro*, and lysosomal extracts have direct killing activity (120), albeit through an unknown mechanism. T cells and NK cells have direct antifungal activity, at least *in vitro* (121, 122). In fact, NK and NK-T cells are necessary for fungal resistance *in vivo* (123). Survival to Cn

challenge in mice requires both Th1 and Th2 cells (124-126), which probably then recruit NK cells and macrophages as effector or auxiliary cells. The role for B cells is controversial and discussed below. It is the cooperation of Th1 and Th2 lymphocytes, together with effector NK and macrophages that seems essential for Cn killing *in vivo.*

It is accepted that the development of a Th1 response is crucial for mice survival to Cn challenge, while Th2 type response is detrimental. In mice, development of Th1 response requires IFN-γ and Il-12. Mice defective in either of these cytokines are more susceptible to Cn (127-131). Urokinase-deficient mice have defective IFN-γ and Il-12 activation, making them more susceptible to Cn infection (132). Mice treated with neutralizing antibody to Il-12 have a increased dissemination to the brain (133). TNF-α deficient mice show increased eosinophilia in the lung and increased susceptibility to infection (134, 135). Other Th1 type cytokines, Il-18 (136), Il-23 (137) and Il-6 (131) deficient mice have decreased survival to Cn. TGF-β is a critical cytokine that is anti-proliferative in many cell types, that antagonizes IFN-γ signaling. Administration of TGF-β decreases the fungal burden in rat infections. The suggested mechanism for TGF-β action was higher secretion of lysozyme by macrophages (138). It has also been shown that TGF-β administration control and ameliorate eosinophilic pathologies without effects on pathogen growth (139), but no mouse survival studies were performed for cryptococcosis. Consistent with a detrimental role of Th2 response, mice defective in Il-10 (131), Il-13 (117) and Il-4 (131, 140) survive longer after Cn challenge. Deficiency in Il-13 increases Th17 responses and classical activation of macrophages (117). Th17 type responses do not seem to influence outcome of primary infection or efficiency of vaccination (141), suggesting a less important role for Th17 in cryptococcal disease. While an impressive body of work has been done to characterize cytokine dependence, more studies would be necessary to establish complete protection. How cytokines influence fungal escape to the brain is also not known. Different mouse strains have varying susceptibility to cryptococcosis and to the protective efficacy of antibodies (142-144). Some studies have correlated this resistance with alveolar macrophage fungicidal capabilities (145), while others explain it by a genetic bias towards an Th1 or Th2 response (142). We should highlight that a critical balance between both Th1 and Th2 responses is fundamental: IL-4 and Il-13 double KO models displays a clear Th1 and Th17 mediated lung protection, but cannot prevent the dissemination of Cn to the brain, leaving the mouse to die by meningoencephalitis (146). Why excessive Th1 cytokines mediate higher brain invasion is unknown. The mechanism of Cn protection *in vivo* has been addressed very elegantly in a series of studies by Wormley and colleagues (141, 147-149). Inoculation with an IFN-γ producing H99, hallmark cytokine of Th1 response, was used as a vaccination strategy. After vaccination, there is complete protection to secondary challenge and a bias of the lung cytokine pattern towards

Th1 activation in both infections. This is accompanied by classical activation of macrophages and by an increase in production of NO (148). The authors have also shown development of complete protection in T cells depleted mice (141). This suggests that an increased production of IFN-γ by the vaccine strain is enough to bias immune response just enough to have a Th1 type protective response, without any of the detrimental effects of an exaggerated Th1 response.

The role of humoral immunity and antibodies in Cn infection has proven difficult to decipher (101). As discussed above, an excessive Th2-type response is detrimental. Immunity to Cn should be skewed to Th1, but complete abrogation of Th2 results in an increased brain fungal burden and consequent host death. Excessive IgM antibodies seem detrimental for infection, in human and mice. Human individuals with hyper-IgM syndrome are at risk for cryptococcosis, while mice deficient in IgM secretion are less susceptible (150). However, too little IgM is not beneficial: absence of serum IgM enhances susceptibility in a peritoneal disease model (151) and specific IgM can be protective (152). Reconciliation of these results implies that a critical concentration of IgM is necessary to improve outcome of cryptococcosis. Humoral immunity has not been correlated with protection in humans, however B-cell deficient mice are susceptible to cryptococcosis (153). IgG antibodies to capsule components mediate protection in murine models (154-156), through B-cell (153) and NO dependent mechanisms (157). In fact, there is one monoclonal IgG antibody in clinical trials for treatment of cryptococcosis (22). These results prove that both antibody administration and B-cells are beneficial for the host, but also suggest that the picture is not complete yet (101). In fact, humans with hypogamaglobinemia, who are at risk for infection, showed defects in CMI (158). These findings support immunoregulatory functions of antibodies, even towards CMI (101, 159, 160). While antibody administration is capable of influencing the outcome of Cn infection, Cn infection has also proven to be a model for novel antibody-mediated functions.

Another unanswered question is the mechanism of fungal killing. Not all phagosomes are created equal and not all immune cells have the same fungicidal capacity. Human neutrophils can kill Cn through defensins, while DC are fungicidal to Cn with their lysosomal components (120). The identity of the lysosomal component responsible for the killing is unknown. In infection, cooperation between immune cells exists and models of cooperation could elucidate fungal killing *in vivo*. Phagocytes are hypothesized to kill Cn in a oxidative stress-dependent manner. However, infected tissues are hypoxic, impairing the activity of NADPH oxidase and iNOS (84). It is then possible that ROS do not achieve concentrations necessary to be the fungicidal *in vivo.* In a model of NADPH oxidase-null mice, the infection is contained and the fungal load in both brain and lung is decreased (133), supporting a detrimental role of ROS. One antimicrobial molecule proven to be fungistatic or fungicidal to Cn is NO (161), either by addition to Cn or when produced by macrophages *in vivo* and *in vitro*

(157, 162). Protective antibodies might enhance production of NO and thus, provide the mechanism of antibody mediated protection to cryptococcosis (157). In the rat model, resistance has been associated with classical activation, which upregulates iNOS (163) while iNOS is present in Cn granulomas in the lung (163). The same has been shown in mice (148). NO has always a protective role in cryptococcosis, albeit mechanistic considerations are hampered by difficulty in separating between the direct fungicidal effects of NO and its immunoregulatory effects. Cn with defective nitrosative defenses is only slightly less virulent than WT Cn (164), potentially resolving this debate in favor of NO- mediated immunoregulation. An additional candidate for fungal killing is the the myeloperoxidase system since myeloperoxidase KO mice have a dramatically decreased survival to Cn challenge (165). In general, killing of Cn is favored by Th1 type responses, resulting in host protection, but it is not clear yet the precise fungicidal mechanisms that prevent cryptococcosis.

The fungal side

Cn possesses many characteristics that allow the fungus to survive and thrive within a host. These characteristics are called virulence factors, which are factors necessary for the fungus to survive within the host, resist attack of the host immunity and to cause damage to the host. The first essential factor is that Cn is able to grow at 37°C. Therefore, all the enzymes that allow for fitness at this temperature fit the definition of virulence factors (166). Importantly, growth at this temperature expands the range of Cn hosts to the majority of the endothermic animals (1, 10). Another inherent virulence factor is the fungal cell wall, who provides rigidity and protects the fungus from physical and oxidative stress (15). Cn possesses many other virulence factors, that explain its clinical importance.

The importance of the capsule in virulence is most convincingly illustrated by the fact that acapsular mutants are avirulent (167). Cn capsule is composed of long chains of glucuronoxylomannan (GXM), glucuronoxylomannogalactan (GalXM) and some mannoproteins. As discussed above, the capsule is highly anti-phagocytic *in vitro* (15) and can additionally quench reactive oxygen species and other free radicals (168, 169), and host derived complement and antibody(22). The capsular structure adapts to the environment, and the size of the capsule dramatically increases in response to infection, contributing to fungal cell gigantism (169, 170). Capsule is shed *in vivo* and *in vitro* (171-173) and the capsule as a whole has immunomodulatory properties (174), interfering with cytokine secretion and antigen presentation. Interaction of capsule with DC and T cells is capable of affecting Th1/Th2 balance (175). Isolated capsule components maintain the immunomodulatory properties (176-178). GXM induces macrophage expression of FasL, inducing death in

29

neighboring T cells (179). Similarly, GalXM down-regulates T cell response (175). Capsular immunomodulation might be a major factor on establishment of Cn as a latent infection.

Long polymer chains of GXM and GalXM can have a molecular weight up to 1 megadalton (180), but little is know about how the polymers are assembled into the capsular structure. Studies correlating GXM polymers to pathogenicity show that distinct capsular extracts mediate distinct biological effects, but it has not clearly been demonstrated to affect virulence of the organism in animal models (170, 181, 182). In short, it is not known if the capsule polymers are the sole responsible for its virulent properties or if the capsule structure, as a whole, has some emergent property required for full virulence. Del Poeta has raised some controversial points that deserve to be mentioned. The author argues that despite the fact that the capsule is anti-phagocytic *in vitro,* there is phagocytosis *in vivo*, and capsule anti-phagocytic properties cannot be discussed as a virulence trait (183). To illustrate his point, the capsule is important in immunocompetent mice but in mice deficient in cell mediated immunity an acapsular strain could be pathogenic(183). These are facts that should be kept in mind when addressing Cn virulence in immunosuppressed hosts. In any case, the capsule does confer considerable advantages to Cn survival in the host and it remains Cn most studied virulence factor.

Cn possesses 2 isoforms of laccase, the enzyme responsible for producing melanin (184). Melanin most likely acts as an potent antioxidant (185, 186), but it is also an adjuvant in cell wall structure (187) and makes yeast cells more resistant to amphotericin B (185). It also seems to have some iron oxidase activity and capacity to produce PGE2 (188). Like the polysaccharide capsule, it might also have some immumodulatory properties (189). Melanin deficient mutants were shown to have reduced virulence(190, 191), ascertaining laccase as a virulence factor.

Cn releases extracellular vesicles at infection, which contain GXM (192) and enzymes such as urease and laccase (193). Given that GXM has many immunomodulatory properties (176, 177) and since vesicles are readily disrupted in the presence of mammalian blood serum (193-195), they have been hypothesized to act as virulence bags (193, 196). Very recently, they have been shown to enhance invasion across blood-brain barrier (197).

There are many more examples of Cn proteins and enzymes with virulence properties. For example, App1 is a secreted protein with anti-phagocytic properties (198). Other authors have found identified Gat201 as transcription factor that mediates inhibition of phagocytosis. From Gat201 interacting genes, the authors proceed to identify capsule independent proteins that display anti-phagocytic capacity (199). The anti-phagocytic activity correlated with control of infection, underscoring yet again the importance of phagocytosis

in control of infection. Screens with mutants strains of Cn have identified proteins that contribute to differential lung/brain ratio(200, 201). Since it is the escape to the brain that implicates a poorer prognosis in cryptococcosis, these factors would be very attractive drug targets. Urease deficient strains have decreased BBB crossing and have reduced virulence (202, 203). Similarly phospholipase B (Plb1) mutants have also reduced virulence and invasion of the brain (204) and, recently, phospholipase B has been described to interact with Rac1 from the host cytoskeleton to promote brain invasion (205). Two copies of superoxide dismutase (SOD) enzymes are present in the Cn genome. In Cn, the SOD1 mutant is more susceptible to macrophage killing (206), while SOD2 does not grow at 37C (207). Several other enzymes that contribute to ROS defense have also been described (208). Despite this impressive array, of which the most impressive member is the capsule, we might have not reached the bottom of the well and other virulence factors might still be uncovered in the future.

Despite extensive tools that allow Cn intracellular growth, Cn possesses surprising mechanisms to escape host cells. Non-lytic exocytosis is the escape of Cn cells from the host which was simultaneously described by two groups (209, 210). The most surprising feature of non-lytic extrusion is an apparent lack of phagocyte damage. Mechanistic studies have shown non-lytic extrusion to be inhibited by lack of phagosomal maturation and it never occurs for heat-killed Cn or latex beads (209, 211-213). Curiously, actin flashes are necessary to inhibit fungal escape by non-lytic extrusion and phagosomal permeability precedes non-lytic extrusion (211). These evidence point for a very active role of Cn in extrusion, but leave us clueless to what mechanism is used for this unique process. Other mechanisms of Cn damage or escape from host phagocytes are titan cell formation (214, 215), cell to cell spread (216) and phenotypic switching (217, 218). Cn is commonly found within macrophages and it has evolved impressive array of virulence factors that allow him to both survive and escape phagocytes.

Interactions between Cn and macrophages

Macrophages play a central cell in immunity and are bound to influence the outcome of Cn infection. Macrophage depleted mice have shown increased susceptibility to Cn infection (118, 119). One possible explanation to why cryptococcosis and other lung infections are so prevalent in AIDS patients is that lung macrophages are particularly susceptible to HIV and free HIV virus is found in the bronchoalveolar lavage. The particularly weakened lung macrophage would then allow for reactivation of Cn infection. In fact, HIV infected

macrophages killed less Cn and *Pneumocystis carinii*, but the same amount of *Staphylococcus aureus* or *Streptococcus pneumoniae* (30).
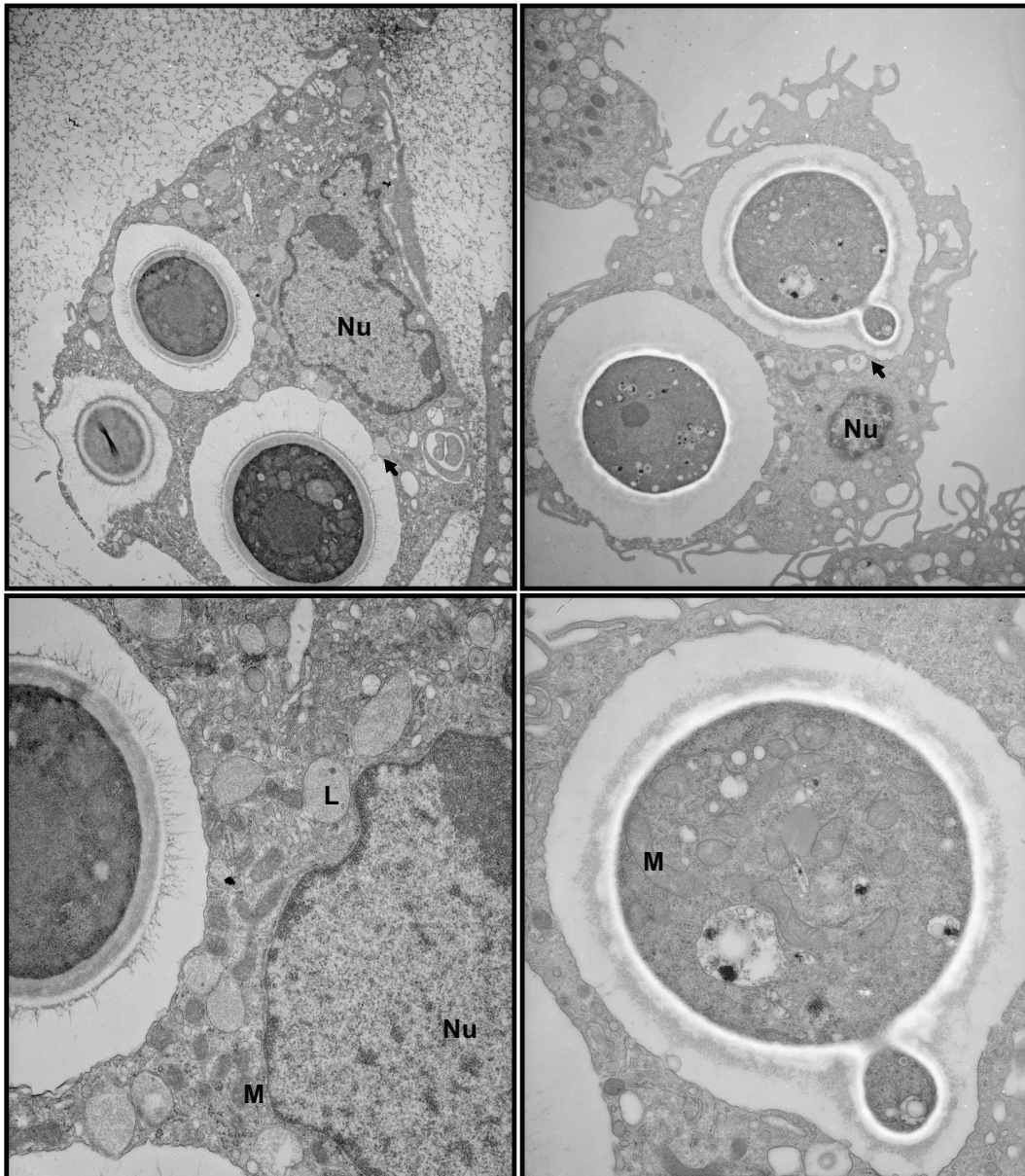
Figure 8. Electron micrographs showing Cn and macrophage interaction.

Bone marrow derived macrophages were infected with Cn for 24 hours. Left, top: Mitochondrial and autophagic events; left bottom: magnification of former showing lysosomes and mitochondria of the macrophage in proximity with the phagosome. Right, top: Cn budding within a phagosome; right, bottom: magnification of former, displaying Cn organelles;

Nu: Nucleous; M: Mitochondria; L: Lysosomes; arrows: possible lysosomal fusion events

Preferential targeting of lung macrophages by HIV would be a simple mechanism to explain the high incidence of pulmonary infections in AIDS patients. There are strong arguments in favor of macrophage explaining defense and susceptibility to Cn infection. When a yeast or a spore enters the lung, alveolar macrophages (AM) are likely the first immune cell that it encounters. In rats (219), mice (168), rabbits (220) and humans (221, 222), Cn was found associated with lung macrophages for months or years, without clinical symptoms. Therefore for intracellular residency to be true, Cn would literally be subverting the very function of macrophages. In fact, the macrophage would unwillingly carry the fungus throughout the body. It has been shown that if AM are depleted, brain dissemination is prevented (223), leading to formulation of the trojan horse hypothesis. Transport within macrophages would allow for evasion of the immune defenses and allow entry of the fungus into the brain (17).

Macrophage differential activation states correlates with distinct outcome of infection *in vivo* (145, 148). *In vitro,* alternative activation of macrophages (with Il-4 and Il-13) kills less Cn (224). Cn downregulates MHC molecule presentation upon phagocytosis by macrophages (225), thus impairing macrophage function as antigen-presenting cells. For proper Cn killing, macrophages seems dependent on a classically-activated phenotype by Th1 cells and cytokines (145, 148, 226). Macrophage activation is not as clear cut *in vivo* as *in vitro* (as stated above)*,* which limits the scope of *in vitro* findings. Arora *et al.,* established an simultaneous classical and alternative state of activation of macrophages in Cn infection *in vivo* and *in vitro* (227), in response to Cn. Macrophage activation and function has been associated with protection from Cn infection, implicating macrophages as a crucial cell in immunity to Cn, even if fungicidal capacities are not clearly demonstrated.

As discussed in the previous section, Cn is readily ingested *in vivo* by phagocytes*. In vitro*, opsonization is required, but after that phagocytosis is very efficient. In both cases, the fungus is able to replicate intracellularly, as illustrated by budding events in Figure 8. However there is some extent of fungal damage *in vitro*, since killing assays show restriction of Cn growth by macrophages up to 24 or more hours of infection (228). *In vivo,* the exact mechanism of fungal control has not been elucidated. The most likely case is that a synergy of mechanisms exists. , since within the phagosome, the yeast is exposed simultaneously to low pH, ROS, RNS and nutrient starvation (15). But Cn possesses several resources to counteract macrophage effector mechanisms. Several gene expression studies show that phagocytosed fungi upregulate oxidative stress and DNA repair. Nutritional starvation responses and autophagic machinery is increased (41, 208). Cn possesses multiple tools to avoid ROS attack. In fact, a NADPH oxidase null mice was less susceptible to Cn infection, arguing that ROS is not the fungicidal mechanism for Cn.

Cn has also not been shown to inhibit phagosomal maturation. Although the Cn phagosome has not been extensively characterized, it possesses EEA-1 (120), CD63 (229), mannose-6-phosphate receptor (M6PR), LAMP-1(229), and cathepsin D (230), showing no interference with normal phagosomal maturation. The ER marker calcireticulin was also found to associate with Cn phagosomes (230). A phagosome containing Cn is able to acidify in primary and immortalized macrophages and also in Drosophila S2 cells (230). Counter intuitively, inhibition of lysosomal acidification leads to decreased Cn replication (229-231), implicating that the fungus prefers an acidic environment. Despite no evidence of manipulation of the phagocytic machinery, macrophage phagosomes become leaky after Cn infection. This was measured by electron micrographs and by observation of dextran leaking into cytoplasm (232). Phagosomal leakiness can be caused very simply by gigantism of Cn cells, which might cause physical damage to macrophages (214). Leakiness of the phagosome would have a myriad of consequences: easy access to nutrients (38) and loss of acidity in phagosome; release of phagosomal components, that can activate the inflammasome; and release of capsular components which have potent immunomodulatory properties. It has been shown that a leaky phagosome is required for extrusion, facilitating hijack of the host cytoskeleton (211). *In vivo*, cells that have ingested Cn show features of affected lysosomes, showing an increase in cytoplasmatic vacuoles that result in a characteristic morphology, Hueco cell (168).

Cn phagocytosis interferes with other cellular processes, such as autophagy. Autophagy is a process where the cell is able to target its own components to a specialized compartment and degrade and recycle their components. Therefore, it is an essential process for cleaning damaged organelles or molecules and as such its degradative machinery could be useful for degradation of pathogens. Indeed autophagy has been implied in defense against several organisms (233), and particularly, Cn killing (234). However, no Cn has ever been reported to reside within an autophagic double membrane compartment, negating that Cn resides in an autophagic vacuole. Qin et al. has shown that decrease of authophagy decreases uptake of Cn by macrophages, but also decreases intracellular replication of Cn (230). *In vitro* LC3, Atg9a and Atg5 are recruited to the phagosome. An alternative explanation would be that an increased ratio of LC3-I/LC3-II, a marker for nutritional starvation within the macrophage, indicates nutritional starvation in response to Cn infection (230). The role of autophagy for *in vivo* infection, was surprisingly hard to predict and autophagy deficient mice were not ore susceptible to Cn killing (234). These findings show Cn interferes with macrophage metabolism, but none of them have been correlated with macrophage demise upon infection.
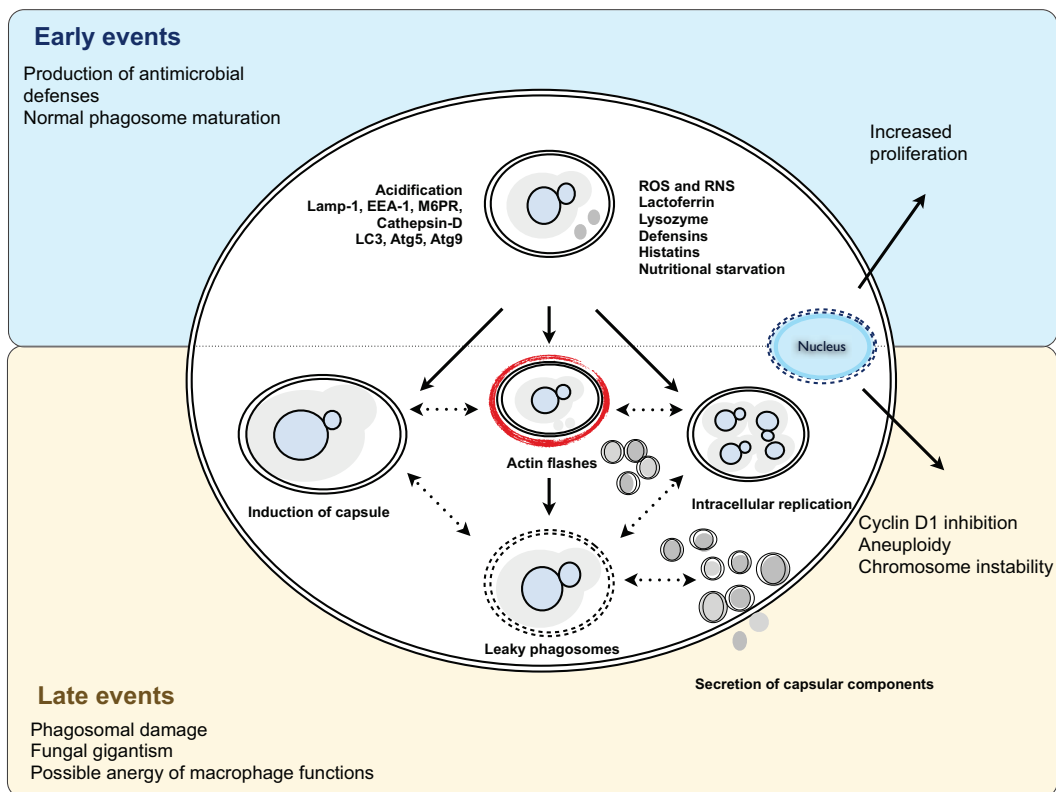
Figure 9. Phagocytic events upon Cn ingestion.

To date, manipulation of the phagocytic compartment by Cn has not been described. The interplay between macrophage fungicidal mechanisms and Cn results in host damage, mainly to the phagosomal compartment and to the integrity of nuclear genetic information. Abbreviations: ROS, reactive oxygen species; RNS, reactive nitrogen species.

Of particular interest for this thesis is the Cn interference with macrophage cell cycle. Luo et all (235, 236) has shown that crosslinking of FcR, either by ingestion of fungus, inert beads or frustrated phagocytosis, stimulated the replication of murine macrophages. Frustrated phagocytosis consists in coating of the cell culture surface with antibody or other opsonin, so that the macrophages are constantly trying to ingest a surface. This provides a very clean experimental model for phagocytosis, which was used to characterize the molecular pathways that link phagocytosis and cell cycle (236). However, continued proliferation after phagocytosis was difficult to reconcile with reports of macrophage death after prolonged Cn infection. Later work showed that ingestion of live yeast cells, and not latex beads, inhibited cyclin D1 expression (237). Since Cyclin D1 is a major checkpoint in the transition from G1 to S phase, the data supports a toxic effect of Cn in the macrophage cell cycle. An example in other models has shown cyclin D1 expression is inhibited in response to LPS,

triggering mitotic arrest (238). Other groups have reported toxic effects in the cell cycle after exposure to extracellular Cn (239). Presence of capsulated and acapsular yeast triggered aneuploidy and cell cycle impairment in macrophages. But only capsulated organisms could trigger apoptosis in macrophages, which agrees with studies that shown that isolated capsular components cause apoptosis in many immune cells (175, 176, 240, 241). Despite this work being performed in extracellular Cn, the observed aneuploidy once again supports fungal virulence through cell cycle or DNA integrity toxicity. *In vivo*, lungs infected with Cn were positive for Proliferating Cell Nuclear Antigen (PCNA) (242). It is clear that Cn phagocytosis causes widespread effects within a macrophage cell and elucidation of these effects is crucial for understanding fungal pathogenesis.

Rationale

Cryptococcosis is the fungal infection with the highest mortality rate. Although immunocompetent patients are generally not at risk, immunocompromised patients face a poor prognosis (16). Survival to Cn infection has been correlated both with an effective Th1-type response and with classical macrophage activation. In fact, without macrophages the host quickly succumbs to infection (118, 119, 145). However, the yeast can use macrophages to its advantage and persistence within macrophages seems to be a key to Cn latency (168, 219-222). Intracellular residence of Cn within macrophages has to signify host adaptations, even without obvious signs of cytotoxicity. Damage includes giant vacuole formation (243), cytosolic vaculoes in the form Hueco cell (168) and phagosomal leakage (232). It is hard to reconcile these findings with the observation of increased cell cycle progression after Cn ingestion (235). How is this compatible with the knowledge that the most likely outcome *in vitro* is death of the macrophage? Furthermore, if proliferation is a conserved response to phagocytosis, it has still to be demosntrated *in vivo.* If prolongued infection leads to macrophage death (228, 232), it is necessary to characterize this death. There is more than one way to die and macrophage modalities of deat influence the subsequent immune response differently. Perhaps more important, understanding death provides clues into the injury that triggered it. Thus, studying macrophage proliferation and death would provide insight into Cn mechanisms of intracellular survival. Cell and life decisions are often integrated in the mitochondria. Further, mitochondria have been shown to be important for antiviral and antibacterial immunity, but have not been characterized in the setting of a fungal infection. It is reasonable to assume they will have a role in antifungal immunity. Ultimately, it would provide us with immunological targets that are needed to improve poor prognosis of Cn infection (16).

References

1. **Barnett JA**. 2010. A history of research on yeasts 14: 1 medical yeasts part 2, Cryptococcus neoformans. Yeast **27**:875–904.

2. **Dromer F**, **Mathoulin-Pélissier S**, **Fontanet A**, **Ronin O**, **Dupont B**, **Lortholary O**, **French Cryptococcosis Study Group**. 2004. Epidemiology of HIV-associated cryptococcosis in France (1985-2001): comparison of the pre- and post-HAART eras. AIDS **18**:555–562.

3. **Mirza SA**, **Phelan M**, **Rimland D**, **Graviss E**, **Hamill R**, **Brandt ME**, **Gardner T**, **Sattah M**, **Ponce de Leon G**, **Baughman W**, **Hajjeh RA**. 2003. The Changing Epidemiology of Cryptococcosis: An Update from Population-Based Active Surveillance in 2 Large Metropolitan Areas, 1992–2000. Clin Infect Dis **36**:789–794.

4. **Park BJ**, **Wannemuehler KA**, **Marston BJ**, **Govender N**, **Pappas PG**, **Chiller TM**. 2009. Estimation of the current global burden of cryptococcal meningitis among persons living with HIV/AIDS. AIDS **23**:525.

5. **Lortholary O**, **Poizat G**, **Zeller V**, **Neuville S**, **Boibieux A**, **Alvarez M**, **Dellamonica P**, **Botterel F**, **Dromer F**, **Chêne G**. 2006. Long-term outcome of AIDS-associated cryptococcosis in the era of combination antiretroviral therapy. AIDS **20**:2183–2191.

6. **Jarvis JN**, **Harrison TS**. 2007. HIV-associated cryptococcal meningitis. AIDS **21**:2119–2129.

7. **Kwon-Chung KJ**, **Varma A**. 2006. Do major species concepts support one, two or more species within Cryptococcus neoformans? FEMS Yeast Res. **6**:574–587.

8. **Ikeda R**, **Shinoda T**, **Fukazawa Y**, **Kaufman L**. 1982. Antigenic characterization of Cryptococcus neoformans serotypes and its application to serotyping of clinical isolates. J Clin Microbiol **16**:22–29.

9. **Kwon-Chung KJ**, **Bennett JE**. 1984. Epidemiologic differences between the two varieties of Cryptococcus neoformans. Am. J. Epidemiol. **120**:123–130.

10. **Lin X**, **Heitman J**. 2006. The biology of the Cryptococcus neoformans species complex. Annu. Rev. Microbiol. **60**:69–105.

11. **Goldman DL**, **Khine H**, **Abadi J**, **Lindenberg DJ**, **Pirofski La**, **Niang R**, **Casadevall A**. 2001. Serologic evidence for Cryptococcus neoformans infection in early childhood. Pediatrics **107**:E66.

12. **Lindell DM**, **Ballinger MN**, **McDonald RA**, **Toews GB**, **Huffnagle GB**. 2006. Immunologic homeostasis during infection: coexistence of strong pulmonary cell-mediated immunity to secondary Cryptococcus neoformans infection while the primary infection still persists at low levels in the lungs. J Immunol **177**:4652–4661.

13. **Goldman DL**, **Davis J**, **Bommarito F**, **Shao X**, **Casadevall A**. 2006. Enhanced allergic inflammation and airway responsiveness in rats with chronic Cryptococcus neoformans infection: potential role for fungal pulmonary infection in the pathogenesis of asthma. J Infect Dis **193**:1178–1186.

14. **Jain AV**, **Zhang Y**, **Fields WB**, **McNamara DA**, **Choe MY**, **Chen G-H**, **Erb-Downward J**, **Osterholzer JJ**, **Toews GB**, **Huffnagle GB**, **Olszewski MA**. 2009. Th2 but Not Th1 Immune Bias Results in Altered Lung Functions in a Murine Model of Pulmonary Cryptococcus neoformans Infection. Infect Immunit **77**:5389–5399.

15. **Shoham S**, **Levitz SM**. 2005. The immune response to fungal infections. Br J of Haem **129**:569–582.

16. **Longo D**, **Fauci A**, **Kasper D**, **Hauser S**, **Jameson J**, **Loscalzo J**. 2011. Harrison's Principles of Internal Medicine: Volumes 1 and 2, 18th Edition, 18 ed. McGraw-Hill Professional.

17. **Charlier C**, **Nielsen K**, **Daou S**, **Brigitte M**, **Chrétien F**, **Dromer F**. 2009. Evidence of a role for monocytes in dissemination and brain invasion by Cryptococcus neoformans. Infect Immunit **77**:120–127.

18. **Charlier C**, **Chrétien F**, **Baudrimont M**, **Mordelet E**, **Lortholary O**, **Dromer F**. 2005. Capsule Structure Changes Associated with Cryptococcus neoformans Crossing of the Blood-Brain Barrier. Am J Pathol **166**:421–432.

19. **Majid Z**, **Ali ZM**. 2010. Central nervous system fungal infections; a review article. Jundishapur J Microbiol **3**:41–47.

20. **Powderly WG**. 2006. Antifungal treatment for cryptococcal meningitis. Intern Med J **36**:404–405.

21. **Casadevall A**, **Feldmesser M**, **Pirofski L-A**. 2002. Induced humoral immunity and vaccination against major human fungal pathogens. Curr Opin Microbiol **5**:386–391.

22. **Casadevall A**, **Perfect JR**. 1998. Cryptococcus Neoformans, 1st ed. American Society for Clinical Investigation.

23. **Casadevall A**, **Pirofski L-A**. 1999. Host-pathogen interactions: redefining the basic concepts of virulence and pathogenicity. **67**:3703–3713.

24. **Casadevall A**, **Pirofski L-A**. 2003. The damage-response framework of microbial pathogenesis. Nat Rev Microbiol **1**:17–24.

25. **Romani L**. 2011. Immunity to fungal infections. Nat Rev Immunol **11**:275–288.

26. **Kawai T**, **Akira S**. 2007. Antiviral signaling through pattern recognition receptors. J Biochem **141**:137–145.

27. **Jouault T**, **Sarazin A**, **Martinez-Esparza M**, **Fradin C**, **Sendid B**, **Poulain D**. 2009. Host responses to a versatile commensal: PAMPs and PRRs interplay leading to tolerance or infection by Candida albicans. Cell Microbiol **11**:1007–1015.

28. **Schulz C**, **Gomez Perdiguero E**, **Chorro L**, **Szabo-Rogers H**, **Cagnard N**, **Kierdorf K**, **Prinz M**, **Wu B**, **Jacobsen SEW**, **Pollard JW**, **Frampton J**, **Liu KJ**, **Geissmann F**. 2012. A lineage of myeloid cells independent of Myb and hematopoietic stem cells. Science **336**:86–90.

29. **Gordon S**, **Taylor PR**. 2005. Monocyte and macrophage heterogeneity. Nat Rev Immunol **5**:953–964.

30. **Gordon SB**, **Read RC**. 2002. Macrophage defences against respiratory tract infections. Br. Med. Bull. **61**:45–61.

31. **Mosser DM**, **Edwards JP**. 2008. Exploring the full spectrum of macrophage activation. Nat Rev Immunol **8**:958–969.

32. **Gordon S**. 2003. Alternative activation of macrophages. Nat Rev Immunol **3**:23–35.

33. **Jutras I**, **Desjardins M**. 2005. Phagocytosis: at the crossroads of innate and adaptive immunity. Annu. Rev. Cell Dev. Biol. **21**:511–527.

34. **Underhill DM**, **Goodridge HS**. 2012. Information processing during phagocytosis. Nat Rev Immunol **12**:492–502.

35. **Groves E**, **Dart AE**, **Covarelli V**, **Caron E**. 2008. Molecular mechanisms of phagocytic uptake in mammalian cells. Cell Mol Life Sci **65**:1957–1976.

36. **Niedergang F**, **Chavrier P**. 2005. Regulation of phagocytosis by Rho GTPases. Curr Top Microbiol Immunol **291**:43–60.

37. **Hoppe AD**, **Swanson JA**. 2004. Cdc42, Rac1, and Rac2 display distinct patterns of activation during phagocytosis. Mol Biol Cell **15**:3509–3519.

38. **Brown GD**. 2011. Innate antifungal immunity: the key role of phagocytes. Annu Rev Immunol **29**:1–21.

39. **Novo E**, **Parola M**. 2008. Redox mechanisms in hepatic chronic wound healing and fibrogenesis. Fibrogenesis Tiss Repair **1**:5.

40. **Mambula SS**, **Simons ER**, **Hastey R**, **Selsted ME**, **Levitz SM**. 2000. Human neutrophil-mediated nonoxidative antifungal activity against Cryptococcus neoformans. Infect Immunit **68**:6257–6264.

41. **Fan W**, **Kraus PR**, **Boily M-J**, **Heitman J**. 2005. Cryptococcus neoformans gene expression during murine macrophage infection. Eukaryot Cell **4**:1420–1433.

42. **Fernández-Arenas E**, **Cabezón V**, **Bermejo C**, **Arroyo J**, **Nombela C**, **Diez-Orejas R**, **Gil C**. 2007. Integrated proteomics and genomics strategies bring new insight into Candida albicans response upon macrophage interaction. Mol. Cell Proteomics **6**:460–478.

43. **McDermott JE**, **Archuleta M**, **Thrall BD**, **Adkins JN**, **Waters KM**. 2011. Controlling the response: predictive modeling of a highly central, pathogen-targeted core response module in macrophage activation. PLoS ONE **6**:e14673.

44. **Hoffmann E**, **Marion S**, **Mishra BB**, **John M**, **Kratzke R**, **Ahmad SF**, **Holzer D**, **Anand PK**, **Weiss DG**, **Griffiths G**, **Kuznetsov SA**. 2010. Initial receptor-ligand interactions modulate gene expression and phagosomal properties during both early and late stages of phagocytosis. Eur. J. Cell Biol. **89**:693–704.

45. **Vieira OV**, **Botelho RJ**, **Grinstein S**. 2002. Phagosome maturation: aging gracefully. Biochem J **366**:689–704.

46. **Blander JM**, **Medzhitov R**. 2004. Regulation of phagosome maturation by signals from toll-like receptors. Science **304**:1014–1018.

47. **Hoffmann E**, **Kotsias F**, **Visentin G**, **Bruhns P**, **Savina A**, **Amigorena S**. 2012. Autonomous phagosomal degradation and antigen presentation in dendritic cells. Proc Natl Acad Sci USA **109**:14556–14561.

48. **Doshi N**, **Mitragotri S**. 2010. Macrophages recognize size and shape of their targets. PLoS ONE **5**:e10051.

49. **Merad M**, **Manz MG**, **Karsunky H**, **Wagers A**, **Peters W**, **Charo I**, **Weissman IL**, **Cyster JG**, **Engleman EG**. 2002. Langerhans cells renew in the skin throughout life under steady-state conditions. Nat Immunol **3**:1135–1141.

50. **Landsman L**, **Jung S**. 2007. Lung macrophages serve as obligatory intermediate between blood monocytes and alveolar macrophages. J Immunol **179**:3488–3494.

51. **Xaus J**, **Cardó M**, **Valledor AF**, **Soler C**, **Lloberas J**, **Celada A**. 1999. Interferon gamma induces the expression of p21waf-1 and arrests macrophage cell cycle, preventing induction of apoptosis. Immunity **11**:103–113.

52. **Xaus J**, **Comalada M**, **Barrachina M**, **Herrero C**, **Goñalons E**, **Soler C**, **Lloberas J**, **Celada A**. 2000. The expression of MHC class II genes in macrophages is cell cycle dependent. J Immunol **165**:6364–6371.

53. **Xaus J**, **Comalada M**, **Valledor AF**, **Lloberas J**, **López-Soriano F**, **Argilés JM**, **Bogdan C**, **Celada A**. 2000. LPS induces apoptosis in macrophages mostly through the autocrine production of TNF-alpha. Blood **95**:3823–3831.

54. **Nougayrède J-P**, **Taïeb F**, **Rycke JD**, **Oswald E**. 2005. Cyclomodulins: bacterial effectors that modulate the eukaryotic cell cycle. Trends Microbiol **13**:103–110.

55. **Bitterman PB**, **Saltzman LE**, **Adelberg S**, **Ferrans VJ**, **Crystal RG**. 1984. Alveolar macrophage replication. One mechanism for the expansion of the mononuclear phagocyte population in the chronically inflamed lung. J Clin Invest **74**:460–469.

56. **Spector WG**, **Wynne KM**. 1976. Proliferation of macrophages in inflammation. Agents Actions **6**:123–126.

57. **Spurzem JR**, **Saltini C**, **Rom W**, **Winchester RJ**, **Crystal RG**. 1987. Mechanisms of macrophage accumulation in the lungs of asbestos-exposed subjects. Am Rev Respir Dis **136**:276–280.

58. **Tarling JD**, **Lin HS**, **Hsu S**. 1987. Self-renewal of pulmonary alveolar macrophages: evidence from radiation chimera studies. J Leukoc Biol **42**:443–446.

59. **Hornby SB**, **Kellington JP**. 1990. DNA synthesis in alveolar macrophages and other changes in lavaged cells following exposure of CBA/H mice to cigarette smoke. Environ Health Perspect **85**:107–112.

60. **Jenkins SJ**, **Ruckerl D**, **Cook PC**, **Jones LH**, **Finkelman FD**, **van Rooijen N**, **MacDonald AS**, **Allen JE**. 2011. Local macrophage proliferation, rather than recruitment from the blood, is a signature of TH2 inflammation. Science **332**:1284–1288.

61. **Randolph GJ**. 2011. Immunology. No need to coax monocytes. Science **332**:1268–1269.

62. **Davies LC**, **Rosas M**, **Smith PJ**, **Fraser DJ**, **Jones SA**, **Taylor PR**. 2011. A quantifiable proliferative burst of tissue macrophages restores homeostatic macrophage populations after acute inflammation. Eur J Immunol **41**:2155–2164.

63. **Ajami B**, **Bennett JL**, **Krieger C**, **McNagny KM**, **Rossi FMV**. 2011. Infiltrating monocytes trigger EAE progression, but do not contribute to the resident microglia pool. Nat Neurosci **14**:1142–1149.

64. **Janssen WJ**, **Barthel L**, **Muldrow A**, **Oberley-Deegan RE**, **Kearns MT**, **Jakubzick C**, **Henson PM**. 2011. Fas determines differential fates of resident and recruited macrophages during resolution of acute lung injury. Am J Respir Crit Care Med **184**:547–560.

65. **Kerr JF**, **Wyllie AH**, **Currie AR**. 1972. Apoptosis: a basic biological phenomenon with wide-ranging implications in tissue kinetics. Br. J. Cancer **26**:239–257.

66. **Galluzzi L**, **Vitale I**, **Abrams JM**, **Alnemri ES**, **Baehrecke EH**, **Blagosklonny MV**, **Dawson TM**, **Dawson VL**, **El-Deiry WS**, **Fulda S**, **Gottlieb E**, **Green DR**, **Hengartner MO**, **Kepp O**, **Knight RA**, **Kumar S**, **Lipton SA**, **Lu X**, **Madeo F**, **Malorni W**, **Mehlen P**, **Nuñez G**, **Peter ME**, **Piacentini M**, **Rubinsztein DC**, **Shi Y**, **Simon H-U**, **Vandenabeele P**, **White E**, **Yuan J**, **Zhivotovsky B**, **Melino G**, **Kroemer G**. 2012. Molecular definitions of cell death subroutines: recommendations of the Nomenclature Committee on Cell Death 2012. Cell Death Differ. **19**:107–120.

67. **Siegel RM**. 2006. Caspases at the crossroads of immune-cell life and death. Nat Rev Immunol **6**:308–317.

68. **Bergsbaken T**, **Fink SL**, **Cookson BT**. 2009. Pyroptosis: host cell death and inflammation. Nat Rev Microbiol **7**:99–109.

69. **Degterev A**, **Hitomi J**, **Germscheid M**, **Ch'en IL**, **Korkina O**, **Teng X**, **Abbott D**, **Cuny GD**, **Yuan C**, **Wagner G**, **Hedrick SM**, **Gerber SA**, **Lugovskoy A**, **Yuan J**. 2008. Identification of RIP1 kinase as a specific cellular target of necrostatins. Nat Chem Biol **4**:313–321.

70. **Boujrad H**, **Gubkina O**, **Robert N**, **Krantic S**, **Susin SA**. 2007. AIF-mediated programmed necrosis: a highly regulated way to die. Cell Cycle **6**:2612–2619.

71. **Duprez L**, **Wirawan E**, **Vanden Berghe T**, **Vandenabeele P**. 2009. Major cell death pathways at a glance. Microbes Infect **11**:1050–1062.

72. **Koziel J**, **Maciag-Gudowska A**, **Mikolajczyk T**, **Bzowska M**, **Sturdevant DE**, **Whitney AR**, **Shaw LN**, **DeLeo FR**, **Potempa J**. 2009. Phagocytosis of Staphylococcus aureus by macrophages exerts cytoprotective effects manifested by the upregulation of antiapoptotic factors. PLoS ONE **4**:e5210.

73. **Briken V**. 2012. "With a Little Help from My Friends": Efferocytosis as an Antimicrobial Mechanism. Cell Host Microbe **12**:261–263.

74. **Dockrell DH**, **Whyte MKB**. 2006. Regulation of phagocyte lifespan in the lung during bacterial infection. J Leukoc Biol **79**:904–908.

75. **Allen HL**, **Deepe GS**. 2005. Apoptosis modulates protective immunity to the pathogenic fungus Histoplasma capsulatum. J Clin Invest **115**:2875–2885.

76. **Hosogi S**, **Iwasaki Y**, **Yamada T**, **Komatani-Tamiya N**, **Hiramatsu A**, **Kohno Y**, **Ueda M**, **Arimoto T**, **Marunaka Y**. 2008. Effect of inducible nitric oxide synthase on apoptosis in Candida-induced acute lung injury. Biomed. Res. **29**:257–266.

77. **Antico Arciuch VG**, **Elguero ME**, **Poderoso JJ**, **Carreras MC**. 2012. Mitochondrial regulation of cell cycle and proliferation. Antioxid. Redox Signal. **16**:1150–1180.

78. **West AP**, **Shadel GS**, **Ghosh S**. 2011. Mitochondria in innate immune responses. Nat Rev Immunol **11**:389–402.

79. **Tschopp J**. 2011. Mitochondria: Sovereign of inflammation? Eur J Immunol **41**:1196–1202.

80. **Arnoult D**, **Carneiro L**, **Tattoli I**, **Girardin SE**. 2009. The role of mitochondria in cellular defense against microbial infection. Semin Immunol **21**:223–232.

81. **Mariathasan S**, **Monack DM**. 2007. Inflammasome adaptors and sensors: intracellular regulators of infection and inflammation. Nat Rev Immunol **7**:31–40.

82. **Emre Y**, **Nübel T**. 2010. Uncoupling protein UCP2: when mitochondrial activity meets immunity. FEBS Lett. **584**:1437–1442.

83. **Sena LA**, **Chandel NS**. 2012. Physiological Roles of Mitochondrial Reactive Oxygen Species. Molecular Cell **48**:158–167.

84. **Wiese M**, **Gerlach RG**, **Popp I**, **Matuszak J**, **Mahapatro M**, **Castiglione K**, **Chakravortty D**, **Willam C**, **Hensel M**, **Bogdan C**, **Jantsch J**. 2012. Hypoxia-mediated impairment of the mitochondrial respiratory chain inhibits the bactericidal activity of macrophages. Infect Immunit **80**:1455–1466.

85. **Park D**, **Han CZ**, **Elliott MR**, **Kinchen JM**, **Trampont PC**, **Das S**, **Collins S**, **Lysiak JJ**, **Hoehn KL**, **Ravichandran KS**. 2011. Continued clearance of apoptotic cells critically depends on the phagocyte Ucp2 protein. Nature **477**:220–224.

86. **Koterski JF**, **Nahvi M**, **Venkatesan MM**, **Haimovich B**. 2005. Virulent Shigella flexneri causes damage to mitochondria and triggers necrosis in infected human monocyte-derived macrophages. Infect Immunit **73**:504–513.

87. **Stavru F**, **Bouillaud F**, **Sartori A**, **Ricquier D**, **Cossart P**. 2011. Listeria monocytogenes transiently alters mitochondrial dynamics during infection. Proc Natl Acad Sci USA **108**:3612–3617.

88. **Nicola AM**, **Casadevall A**. 2012. In vitro measurement of phagocytosis and killing of Cryptococcus neoformans by macrophages. Methods Mol Biol **844**:189–197.

89. **Chaka W**, **Scharringa J**, **Verheul AF**, **Verhoef J**, **Van Strijp AG**, **Hoepelman IM**. 1995. Quantitative analysis of phagocytosis and killing of Cryptococcus neoformans by human peripheral blood mononuclear cells by flow cytometry. Clin Diagn Lab Immunol **2**:753–759.

90. **Kamentsky L**. 2001. Laser scanning cytometry. Methods Cell Biol **63**:51–87.

91. **Harnett MM**. 2007. Laser scanning cytometry: understanding the immune system in situ. Nat Rev Immunol **7**:897–904.

92. **Luther E**, **Kamentsky L**, **Henriksen M**, **Holden E**. 2004. Next-generation laser scanning cytometry. Methods Cell Biol **75**:185–218.

93. **Gerstner A**, **Laffers W**, **Bootz F**, **Tárnok A**. 2000. Immunophenotyping of peripheral blood leukocytes by laser scanning cytometry. J Immunol Methods **246**:175–185.

94. **Wojcik E**, **Saraga S**, **Jin J**, **Hendricks J**. 2001. Application of laser scanning cytometry for evaluation of DNA ploidy in routine cytologic specimens. Diagn Cytopatol **24**:200–205.

95. **Kawasaki M**, **Sasaki K**, **Satoh T**, **Kurose A**, **Kamada T**, **Furuya T**, **Murakami T**, **Todoroki T**. 1997. Laser scanning cytometry (LCS) allows detailed analysis of the cell cycle in PI stained human fibroblasts (TIG-7). Cell Proliferation **30**:139–147.

96. **Telford WG**, **Komoriya A**, **Packard BZ**. 2002. Detection of localized caspase activity in early apoptotic cells by laser scanning cytometry. Cytomet **47**:81–88.

97. **Brodin P**, **Poquet Y**, **Levillain F**, **Peguillet I**, **Larrouy-Maumus G**, **Gilleron M**, **Ewann F**, **Christophe T**, **Fenistein D**, **Jang J**, **Jang M-S**, **Park S-J**, **Rauzier J**, **Carralot J-P**, **Shrimpton R**, **Genovesio A**, **Gonzalo-Asensio JA**, **Puzo G**, **Martin C**, **Brosch R**, **Stewart GR**, **Gicquel B**, **Neyrolles O**. 2010. High Content Phenotypic Cell-Based Visual Screen Identifies Mycobacterium tuberculosis Acyltrehalose-Containing Glycolipids Involved in Phagosome Remodeling. PLoS Pathog **6**:e1001100.

98. **DeLoid GM**, **Sulahian TH**, **Imrich A**, **Kobzik L**. 2009. Heterogeneity in macrophage phagocytosis of Staphylococcus aureus strains: high-throughput scanning cytometry-based analysis. PLoS ONE **4**:e6209.

99. **Steinberg BE**, **Scott CC**, **Grinstein S**. 2007. High-throughput assays of phagocytosis, phagosome maturation, and bacterial invasion. Am J Physiol, Cell Physiol **292**:C945–52.

100. **Srikanta D**, **Yang M**, **Williams M**, **Doering TL**. 2011. A sensitive high-throughput assay for evaluating host-pathogen interactions in Cryptococcus neoformans infection. PLoS ONE **6**:e22773.

101. **Casadevall A**, **Pirofski L-A**. 2012. Immunoglobulins in defense, pathogenesis, and therapy of fungal diseases. Cell Host Microbe **11**:447–456.

102. **Vinh DC**. 2011. Insights into human antifungal immunity from primary immunodeficiencies. Lancet Infect Dis **11**:780–792.

103. **Cross CE**, **Bancroft GJ**. 1995. Ingestion of acapsular Cryptococcus neoformans occurs via mannose and beta-glucan receptors, resulting in cytokine production and increased phagocytosis of the encapsulated form. Infect Immunit **63**:2604–2611.

104. **Taborda CP**, **Casadevall A**. 2002. CR3 (CD11b/CD18) and CR4 (CD11c/CD18) are involved in complement-independent antibody-mediated phagocytosis of Cryptococcus neoformans. Immunity **16**:791–802.

105. **Shapiro S**, **Beenhouwer DO**, **Feldmesser M**, **Taborda C**, **Carroll MC**, **Casadevall A**, **Scharff MD**. 2002. Immunoglobulin G monoclonal antibodies to Cryptococcus neoformans protect mice deficient in complement component C3. Infect Immunit **70**:2598–2604.

106. **Rhodes JC**. 1985. Contribution of complement component C5 to the pathogenesis of experimental murine cryptococcosis. Sabouraudia **23**:225–234.

107. **Faro-Trindade I**, **Willment JA**, **Kerrigan AM**, **Redelinghuys P**, **Hadebe S**, **Reid DM**, **Srinivasan N**, **Wainwright H**, **Lang DM**, **Steele C**, **Brown GD**. 2012. Characterisation of innate fungal recognition in the lung. PLoS ONE **7**:e35675.

108. **Giles SS**, **Zaas AK**, **Reidy MF**, **Perfect JR**, **Wright JR**. 2007. Cryptococcus neoformans is resistant to surfactant protein A mediated host defense mechanisms. PLoS ONE **2**:e1370.

109. **Means TK**, **Mylonakis E**, **Tampakakis E**, **Colvin RA**, **Seung E**, **Puckett L**, **Tai MF**, **Stewart CR**, **Pukkila-Worley R**, **Hickman SE**, **Moore KJ**, **Calderwood SB**, **Hacohen N**, **Luster AD**, **Khoury El J**. 2009. Evolutionarily conserved recognition and innate immunity to fungal pathogens by the scavenger receptors SCARF1 and CD36. J Exp Med **206**:637–653.

110. **Dan JM**, **Kelly RM**, **Lee CK**, **Levitz SM**. 2008. Role of the mannose receptor in a murine model of Cryptococcus neoformans infection. Infect Immunit **76**:2362–2367.

111. **Biondo C**, **Midiri A**, **Messina L**, **Tomasello F**, **Garufi G**, **Catania MR**, **Bombaci M**, **Beninati C**, **Teti G**, **Mancuso G**. 2005. MyD88 and TLR2, but not TLR4, are required for host defense against Cryptococcus neoformans. Eur J Immunol **35**:870–878.

112. **Yauch LE**, **Mansour MK**, **Shoham S**, **Rottman JB**, **Levitz SM**. 2004. Involvement of CD14, toll-like receptors 2 and 4, and MyD88 in the host response to the fungal pathogen Cryptococcus neoformans in vivo. Infect Immunit **72**:5373–5382.

113. **Nakamura K**, **Kinjo T**, **Saijo S**, **Miyazato A**, **Adachi Y**, **Ohno N**, **Fujita J**, **Kaku M**, **Iwakura Y**, **Kawakami K**. 2007. Dectin-1 is not required for the host defense to Cryptococcus neoformans. Microbiol. Immunol. **51**:1115–1119.

114. **Brown GD**, **Netea MG**. 2007. Immunology of Fungal Infections, 1st ed. Springer.

115. **Mednick AJ**, **Feldmesser M**, **Rivera J**, **Casadevall A**. 2003. Neutropenia alters lung cytokine production in mice and reduces their susceptibility to pulmonary cryptococcosis. Eur J Immunol **33**:1744–1753.

116. **Feldmesser M**, **Casadevall A**, **Kress Y**, **Spira G**, **Orlofsky A**. 1997. Eosinophil-Cryptococcus neoformans interactions in vivo and in vitro. Infect Immunit **65**:1899–1907.

117. **Müller U**, **Stenzel W**, **Köhler G**, **Werner C**, **Polte T**, **Hansen G**, **Schütze N**, **Straubinger RK**, **Blessing M**, **McKenzie ANJ**, **Brombacher F**, **Alber G**. 2007. IL-13 induces disease-promoting type 2 cytokines, alternatively activated macrophages and allergic inflammation during pulmonary infection of mice with Cryptococcus neoformans. J Immunol **179**:5367–5377.

118. **Monga DP**. 1981. Role of macrophages in resistance of mice to experimental cryptococcosis. Infect Immunit **32**:975–978.

119. **Osterholzer JJ**, **Milam JE**, **Chen G-H**, **Toews GB**, **Huffnagle GB**, **Olszewski MA**. 2009. Role of dendritic cells and alveolar macrophages in regulating early host defense against pulmonary infection with Cryptococcus neoformans. Infect Immunit **77**:3749–3758.

120. **Wozniak KL**, **Levitz SM**. 2008. Cryptococcus neoformans enters the endolysosomal pathway of dendritic cells and is killed by lysosomal components. Infect Immunit **76**:4764–4771.

121. **Murphy JW**, **Hidore MR**, **Wong SC**. 1993. Direct interactions of human lymphocytes with the yeast-like organism, Cryptococcus neoformans. J Clin Invest **91**:1553–1566.

122. **Levitz SM**, **Dupont MP**, **Smail EH**. 1994. Direct activity of human T lymphocytes and natural killer cells against Cryptococcus neoformans. Infect Immunit **62**:194–202.

123. **Levitz SM**, **Dupont MP**. 1993. Phenotypic and functional characterization of human lymphocytes activated by interleukin-2 to directly inhibit growth of Cryptococcus neoformans in vitro. J Clin Invest **91**:1490–1498.

124. **Lindell DM**, **Ballinger MN**, **McDonald RA**, **Toews GB**, **Huffnagle GB**. 2006. Diversity of the T-cell response to pulmonary Cryptococcus neoformans infection. Infect Immunit **74**:4538–4548.

125. **Huffnagle GB**, **Yates JL**, **Lipscomb MF**. 1991. Immunity to a pulmonary Cryptococcus neoformans infection requires both CD4+ and CD8+ T cells. J Exp Med **173**:793–800.

126. **Lim TS**, **Murphy JW**. 1980. Transfer of immunity to cryptococcosis by T-enriched splenic lymphocytes from Cryptococcus neoformans-sensitized mice. Infect Immunit **30**:5–11.

127. **Hoag KA**, **Lipscomb MF**, **Izzo AA**, **Street NE**. 1997. IL-12 and IFN-gamma are required for initiating the protective Th1 response to pulmonary cryptococcosis in resistant C.B-17 mice. Am J Respir Cell Mol Biol **17**:733–739.

128. **Decken K**, **Köhler G**, **Palmer-Lehmann K**, **Wunderlin A**, **Mattner F**, **Magram J**, **Gately MK**, **Alber G**. 1998. Interleukin-12 is essential for a protective Th1 response in mice infected with Cryptococcus neoformans. Infect Immunit **66**:4994–5000.

129. **Chen G-H**, **McDonald RA**, **Wells JC**, **Huffnagle GB**, **Lukacs NW**, **Toews GB**. 2005. The gamma interferon receptor is required for the protective pulmonary inflammatory response to Cryptococcus neoformans. Infect Immunit **73**:1788–1796.

130. **Arora S**, **Hernandez Y**, **Erb-Downward JR**, **McDonald RA**, **Toews GB**, **Huffnagle GB**. 2005. Role of IFN-gamma in regulating T2 immunity and the development of alternatively activated macrophages during allergic bronchopulmonary mycosis. J Immunol **174**:6346–6356.

131. **Beenhouwer DO**, **Shapiro S**, **Feldmesser M**, **Casadevall A**, **Scharff MD**. 2001. Both Th1 and Th2 cytokines affect the ability of monoclonal antibodies to protect mice against Cryptococcus neoformans. Infect Immunit **69**:6445–6455.

132. **Gyetko MR**, **Sud S**, **Chen G-H**, **Fuller JA**, **Chensue SW**, **Toews GB**. 2002. Urokinase-type plasminogen activator is required for the generation of a type 1 immune response to pulmonary Cryptococcus neoformans infection. J Immunol **168**:801–809.

133. **Snelgrove RJ**, **Edwards L**, **Williams AE**, **Rae AJ**, **Hussell T**. 2006. In the absence of reactive oxygen species, T cells default to a Th1 phenotype and mediate protection against pulmonary Cryptococcus neoformans infection. J Immunol **177**:5509–5516.

134. **Herring AC**, **Lee J**, **McDonald RA**, **Toews GB**, **Huffnagle GB**. 2002. Induction of interleukin-12 and gamma interferon requires tumor necrosis factor alpha for protective T1-cell-mediated immunity to pulmonary Cryptococcus neoformans infection. Infect Immunit **70**:2959–2964.

135. **Huffnagle GB**, **Toews GB**, **Burdick MD**, **Boyd MB**, **McAllister KS**, **McDonald RA**, **Kunkel SL**, **Strieter RM**. 1996. Afferent phase production of TNF-alpha is required for the development of protective T cell immunity to Cryptococcus neoformans. J Immunol **157**:4529–4536.

136. **Kawakami K**, **Koguchi Y**, **Qureshi MH**, **Kinjo Y**, **Yara S**, **Miyazato A**, **Kurimoto M**, **Takeda K**, **Akira S**, **Saito A**. 2000. Reduced host resistance and Th1 response to Cryptococcus neoformans in interleukin-18 deficient mice. FEMS Microbiol. Lett. **186**:121–126.

137. **Kleinschek MA**, **Müller U**, **Brodie SJ**, **Stenzel W**, **Köhler G**, **Blumenschein WM**, **Straubinger RK**, **McClanahan T**, **Kastelein RA**, **Alber G**. 2006. IL-23 enhances the inflammatory cell response in Cryptococcus neoformans infection and induces a cytokine pattern distinct from IL-12. J Immunol **176**:1098–1106.

138. **Shao X**, **Rivera J**, **Niang R**, **Casadevall A**, **Goldman DL**. 2005. A dual role for TGF-beta1 in the control and persistence of fungal pneumonia. J Immunol **175**:6757–6763.

139. **Williams AE**, **Humphreys IR**, **Cornere M**, **Edwards L**, **Rae A**, **Hussell T**. 2005. TGF-beta prevents eosinophilic lung disease but impairs pathogen clearance. Microbes Infect **7**:365–374.

140. **Blackstock R**, **Murphy JW**. 2004. Role of interleukin-4 in resistance to Cryptococcus neoformans infection. Am J Respir Cell Mol Biol **30**:109–117.

141. **Wozniak KL**, **Young ML**, **Wormley FL**. 2011. Protective immunity against experimental pulmonary cryptococcosis in T cell-depleted mice. CVI **18**:717–723.

142. **Zaragoza O**, **Alvarez M**, **Telzak A**, **Rivera J**, **Casadevall A**. 2007. The relative susceptibility of mouse strains to pulmonary Cryptococcus neoformans infection is associated with pleiotropic differences in the immune response. Infect Immunit **75**:2729–2739.

143. **Feldmesser M**, **Mednick A**, **Casadevall A**. 2002. Antibody-mediated protection in murine Cryptococcus neoformans infection is associated with pleotrophic effects on cytokine and leukocyte responses. Infect Immunit **70**:1571–1580.

144. **Rivera J**, **Casadevall A**. 2005. Mouse genetic background is a major determinant of isotype-related differences for antibody-mediated protective efficacy against Cryptococcus neoformans. J Immunol **174**:8017–8026.

145. **Shao X**, **Mednick A**, **Alvarez M**, **van Rooijen N**, **Casadevall A**, **Goldman DL**. 2005. An innate immune system cell is a major determinant of species-related susceptibility differences to fungal pneumonia. J Immunol **175**:3244–3251.

146. **Zhang Y**, **Wang F**, **Tompkins KC**, **McNamara A**, **Jain AV**, **Moore BB**, **Toews GB**, **Huffnagle GB**, **Olszewski MA**. 2009. Robust Th1 and Th17 immunity supports pulmonary clearance but cannot prevent systemic dissemination of highly virulent Cryptococcus neoformans H99. Am J Pathol **175**:2489–2500.

147. **Hardison SE**, **Wozniak KL**, **Kolls JK**, **Wormley FL**. 2010. Interleukin-17 is not required for classical macrophage activation in a pulmonary mouse model of Cryptococcus neoformans infection **78**:5341–5351.

148. **Hardison SE**, **Herrera G**, **Young ML**, **Hole CR**, **Wozniak KL**, **Wormley FL**. 2012. Protective Immunity against Pulmonary Cryptococcosis Is Associated with STAT1-Mediated Classical Macrophage Activation. J Immunol **189**:4060–4068.

149. **Hardison SE**, **Ravi S**, **Wozniak KL**, **Young ML**, **Olszewski MA**, **Wormley FL**. 2010. Pulmonary infection with an interferon-gamma-producing Cryptococcus neoformans strain results in classical macrophage activation and protection. Am J Pathol **176**:774–785.

150. **Subramaniam KS**, **Datta K**, **Marks MS**, **Pirofski L-A**. 2010. Improved survival of mice deficient in secretory immunoglobulin M following systemic infection with Cryptococcus neoformans. Infect Immunit **78**:441–452.

151. **Subramaniam KS**, **Datta K**, **Quintero E**, **Manix C**, **Marks MS**, **Pirofski L-A**. 2010. The absence of serum IgM enhances the susceptibility of mice to pulmonary challenge with Cryptococcus neoformans. J Immunol **184**:5755–5767.

152. **Casadevall A**, **Pirofski L**. 2005. Insights into mechanisms of antibody-mediated immunity from studies with Cryptococcus neoformans. Curr. Mol. Med. **5**:421–433.

153. **Rivera J**, **Zaragoza O**, **Casadevall A**. 2005. Antibody-mediated protection against Cryptococcus neoformans pulmonary infection is dependent on B cells. Infect Immunit **73**:1141–1150.

154. **Dromer F**, **Charreire J**, **Contrepois A**, **Carbon C**, **Yeni P**. 1987. Protection of mice against experimental cryptococcosis by anti-Cryptococcus neoformans monoclonal antibody. Infect Immunit **55**:749–752.

155. **Fleuridor R**, **Zhong Z**, **Pirofski L**. 1998. A human IgM monoclonal antibody prolongs survival of mice with lethal cryptococcosis. J Infect Dis **178**:1213–1216.

156. **Casadevall A**, **Cleare W**, **Feldmesser M**, **Glatman-Freedman A**, **Goldman DL**, **Kozel TR**, **Lendvai N**, **Mukherjee J**, **Pirofski LA**, **Rivera J**, **Rosas AL**, **Scharff MD**, **Valadon P**, **Westin K**, **Zhong Z**. 1998. Characterization of a murine monoclonal antibody to Cryptococcus neoformans polysaccharide that is a candidate for human therapeutic studies. Antimicrob Agents Chemother **42**:1437–1446.

157. **Rivera J**, **Mukherjee J**, **Weiss LM**, **Casadevall A**. 2002. Antibody efficacy in murine pulmonary Cryptococcus neoformans infection: a role for nitric oxide. J Immunol **168**:3419–3427.

158. **Oliveira FR**, **Louzada PL Jr**, **Martinez R**. 2000. Hypogammaglobulinemia as risk factor for Cryptococcus neoformans infection: report of 2 cases]. Revista da Sociedade ….

159. **Casadevall A**, **Pirofski L-A**. 2006. A reappraisal of humoral immunity based on mechanisms of antibody-mediated protection against intracellular pathogens. Adv Immunol **91**:1–44.

160. **Casadevall A**, **Pirofski L-A**. 2003. Antibody-mediated regulation of cellular immunity and the inflammatory response. Trends Immunol **24**:474–478.

161. **Alspaugh JA**, **Granger DL**. 1991. Inhibition of Cryptococcus neoformans replication by nitrogen oxides supports the role of these molecules as effectors of macrophage-mediated cytostasis. Infect Immunit **59**:2291–2296.

162. **Aguirre KM**, **Gibson GW**. 2000. Differing requirement for inducible nitric oxide synthase activity in clearance of primary and secondary Cryptococcus neoformans infection. Med Mycol **38**:343–353.

163. **Goldman D**, **Cho Y**, **Zhao M**, **Casadevall A**, **Lee SC**. 1996. Expression of inducible nitric oxide synthase in rat pulmonary Cryptococcus neoformans granulomas. Am J Pathol **148**:1275–1282.

164. **de Jesús-Berríos M**, **Liu L**, **Nussbaum JC**, **Cox GM**, **Stamler JS**, **Heitman J**. 2003. Enzymes that Counteract Nitrosative Stress Promote Fungal Virulence. Current Biology **13**:1963–1968.

165. **Aratani Y**. 2006. Contribution of the myeloperoxidase-dependent oxidative system to host defence against Cryptococcus neoformans. J. Med. Microbiol. **55**:1291–1299.

166. **Robert VA**, **Casadevall A**. 2009. Vertebrate endothermy restricts most fungi as potential pathogens. J Infect Dis **200**:1623–1626.

167. **Chang YC**, **Kwon-Chung KJ**. 1994. Complementation of a capsule-deficient mutation of Cryptococcus neoformans restores its virulence. Mol Cell Biol **14**:4912–4919.

168. **Feldmesser M**, **Kress Y**, **Novikoff P**, **Casadevall A**. 2000. Cryptococcus neoformans is a facultative intracellular pathogen in murine pulmonary infection. Infect Immunit **68**:4225–4237.

169. **Zaragoza O**, **Rodrigues ML**, **De Jesus M**, **Frases S**, **Dadachova E**, **Casadevall A**. 2009. The capsule of the fungal pathogen Cryptococcus neoformans. Adv Appl Microbiol **68**:133–216.

170. **McFadden DC**, **Fries BC**, **Wang F**, **Casadevall A**. 2007. Capsule structural heterogeneity and antigenic variation in Cryptococcus neoformans. Eukaryot Cell **6**:1464–1473.

171. **Feldmesser M**, **Casadevall A**. 1997. Effect of serum IgG1 to Cryptococcus neoformans glucuronoxylomannan on murine pulmonary infection. J Immunol **158**:790–799.

172. **Levitz SM**, **Nong SH**, **Seetoo KF**, **Harrison TS**, **Speizer RA**, **Simons ER**. 1999. Cryptococcus neoformans resides in an acidic phagolysosome of human macrophages. Infect Immunit **67**:885–890.

173. **Lee SC**, **Casadevall A**, **Dickson DW**. 1996. Immunohistochemical localization of capsular polysaccharide antigen in the central nervous system cells in cryptococcal meningoencephalitis. Am J Pathol **148**:1267–1274.

174. **Lupo P**, **Chang YC**, **Kelsall BL**, **Farber JM**, **Pietrella D**, **Vecchiarelli A**, **Leon F**, **Kwon-Chung KJ**. 2008. The Presence of Capsule in Cryptococcus neoformans Influences the Gene Expression Profile in Dendritic Cells during Interaction with the Fungus. Infect Immunit **76**:1581–1589.

175. **Vecchiarelli A**, **Pericolini E**, **Gabrielli E**, **Chow S-K**, **Bistoni F**, **Cenci E**, **Casadevall A**. 2011. Cryptococcus neoformans galactoxylomannan is a potent negative immunomodulator, inspiring new approaches in anti-inflammatory immunotherapy. Immunother **3**:997–1005.

176. **Chiapello LS**, **Baronetti JL**, **Garro AP**, **Spesso MF**, **Masih DT**. 2008. Cryptococcus neoformans glucuronoxylomannan induces macrophage apoptosis mediated by nitric oxide in a caspase-independent pathway. Int Immunol **20**:1527–1541.

177. **Chang ZL**, **Netski D**, **Thorkildson P**, **Kozel TR**. 2006. Binding and internalization of glucuronoxylomannan, the major capsular polysaccharide of Cryptococcus neoformans, by murine peritoneal macrophages. Infect Immunit **74**:144–151.

178. **Murphy JW**, **Mosley RL**, **Cherniak R**, **Reyes GH**, **Kozel TR**, **Reiss E**. 1988. Serological, electrophoretic, and biological properties of Cryptococcus neoformans antigens. Infect Immunit **56**:424–431.

179. **Monari C**, **Pericolini E**, **Bistoni G**, **Casadevall A**, **Kozel TR**, **Vecchiarelli A**. 2005. Cryptococcus neoformans capsular glucuronoxylomannan induces expression of fas ligand in macrophages. J Immunol **174**:3461–3468.

180. **McFadden DC**, **De Jesus M**, **Casadevall A**. 2006. The physical properties of the capsular polysaccharides from Cryptococcus neoformans suggest features for capsule construction. J Biol Chem **281**:1868–1875.

181. **Cordero RJB**, **Frases S**, **Guimaräes AJ**, **Rivera J**, **Casadevall A**. 2011. Evidence for branching in cryptococcal capsular polysaccharides and consequences on its biological activity. Mol Microbiol **79**:1101–1117.

182. **Fonseca FL**, **Nohara LL**, **Cordero RJB**, **Frases S**, **Casadevall A**, **Almeida IC**, **Nimrichter L**, **Rodrigues ML**. 2010. Immunomodulatory effects of serotype B glucuronoxylomannan from Cryptococcus gattii correlate with polysaccharide diameter. Infect Immunit **78**:3861–3870.

183. **Del Poeta M**. 2004. Role of phagocytosis in the virulence of Cryptococcus neoformans. Eukaryot Cell **3**:1067–1075.

184. **Polacheck I**, **Hearing VJ**, **Kwon-Chung KJ**. 1982. Biochemical studies of phenoloxidase and utilization of catecholamines in Cryptococcus neoformans. J Bacteriol **150**:1212–1220.

185. **Wang Y**, **Casadevall A**. 1994. Susceptibility of melanized and nonmelanized Cryptococcus neoformans to nitrogen- and oxygen-derived oxidants. Infect Immunit **62**:3004–3007.

186. **Wang Y**, **Aisen P**, **Casadevall A**. 1995. Cryptococcus neoformans melanin and virulence: mechanism of action. Infect Immunit **63**:3131–3136.

187. **Williamson PR**. 1997. Laccase and melanin in the pathogenesis of Cryptococcus neoformans. Front. Biosci. **2**:e99–107.

188. **Erb-Downward JR**, **Huffnagle GB**. 2007. Cryptococcus neoformans produces authentic prostaglandin E2 without a cyclooxygenase. Eukaryot Cell **6**:346–350.

189. **Mednick AJ**, **Nosanchuk JD**, **Casadevall A**. 2005. Melanization of Cryptococcus neoformans affects lung inflammatory responses during cryptococcal infection. Infect Immunit **73**:2012–2019.

190. **Rhodes JC**, **Polacheck I**, **Kwon-Chung KJ**. 1982. Phenoloxidase activity and virulence in isogenic strains of Cryptococcus neoformans. Infect Immunit **36**:1175–1184.

191. **Kwon-Chung KJ**, **Polacheck I**, **Popkin TJ**. 1982. Melanin-lacking mutants of Cryptococcus neoformans and their virulence for mice. J Bacteriol **150**:1414–1421.

192. **Rodrigues ML**, **Nimrichter L**, **Oliveira DL**, **Frases S**, **Miranda K**, **Zaragoza O**, **Alvarez M**, **Nakouzi A**, **Feldmesser M**, **Casadevall A**. 2007. Vesicular polysaccharide export in Cryptococcus neoformans is a eukaryotic solution to the problem of fungal trans-cell wall transport. Eukaryot Cell **6**:48–59.

193. **Rodrigues ML**, **Nakayasu ES**, **Oliveira DL**, **Nimrichter L**, **Nosanchuk JD**, **Almeida IC**, **Casadevall A**. 2008. Extracellular vesicles produced by Cryptococcus neoformans contain protein components associated with virulence. Eukaryot Cell **7**:58–67.

194. **Oliveira DL**, **Nimrichter L**, **Miranda K**, **Frases S**, **Faull KF**, **Casadevall A**, **Rodrigues ML**. 2009. Cryptococcus neoformans cryoultramicrotomy and vesicle fractionation reveals an intimate association between membrane lipids and glucuronoxylomannan. Fungal Genet Biol **46**:956–963.

195. **Wolf JM**, **Rivera J**, **Casadevall A**. 2012. Serum albumin disrupts Cryptococcus neoformans and Bacillus anthracis extracellular vesicles. Cell Microbiol **14**:762–773.

196. **Oliveira DL**, **Freire-de-Lima CG**, **Nosanchuk JD**, **Casadevall A**, **Rodrigues ML**, **Nimrichter L**. 2010. Extracellular vesicles from Cryptococcus neoformans modulate macrophage functions. Infect Immunit **78**:1601–1609.

197. **Huang S-H**, **Wu C-H**, **Chang YC**, **Kwon-Chung KJ**, **Brown RJ**, **Jong A**. 2012. Cryptococcus neoformans-Derived Microvesicles Enhance the Pathogenesis of Fungal Brain Infection. PLoS ONE **7**:e48570.

198. **Stano P**, **Williams V**, **Villani M**, **Cymbalyuk ES**, **Qureshi A**, **Huang Y**, **Morace G**, **Luberto C**, **Tomlinson S**, **Del Poeta M**. 2009. App1: an antiphagocytic protein that binds to complement receptors 3 and 2. J Immunol **182**:84–91.

199. **Chun CD**, **Brown JCS**, **Madhani HD**. 2011. A major role for capsule-independent phagocytosis-inhibitory mechanisms in mammalian infection by Cryptococcus neoformans. Cell Host Microbe **9**:243–251.

200. **He X**, **Lyons DM**, **Toffaletti DL**, **Wang F**, **Qiu Y**, **Davis MJ**, **Meister DL**, **Dayrit JK**, **Lee A**, **Osterholzer JJ**, **Perfect JR**, **Olszewski MA**. 2012. Virulence factors identified by Cryptococcus neoformans mutant screen differentially modulate lung immune responses and brain dissemination. Am J Pathol **181**:1356–1366.

201. **Rao PK**, **Rao PK**, **Singh CR**, **Singh CR**, **Jagannath C**, **Jagannath C**, **Li Q**. 2009. A systems biology approach to study the phagosomal proteome modulated by mycobacterial infections. Int J Clinic Exp Med **2**:233–247.

202. **Cox GM**, **Mukherjee J**, **Cole GT**, **Casadevall A**, **Perfect JR**. 2000. Urease as a virulence factor in experimental cryptococcosis. Infect Immunit **68**:443–448.

203. **Shi M**, **Li SS**, **Zheng C**, **Jones GJ**, **Kim KS**, **Zhou H**, **Kubes P**, **Mody CH**. 2010. Real-time imaging of trapping and urease-dependent transmigration of Cryptococcus neoformans in mouse brain. J Clin Invest **120**:1683–1693.

204. **Cox GM**, **McDade HC**, **Chen SC**, **Tucker SC**, **Gottfredsson M**, **Wright LC**, **Sorrell TC**, **Leidich SD**, **Casadevall A**, **Ghannoum MA**, **Perfect JR**. 2001. Extracellular phospholipase activity is a virulence factor for Cryptococcus neoformans. Mol Microbiol **39**:166–175.

205. **Maruvada R**, **Zhu L**, **Pearce D**, **Zheng Y**, **Perfect J**, **Kwon-Chung KJ**, **Kim KS**. 2012. Cryptococcus neoformans phospholipase B1 activates host cell Rac1 for traversal across the blood-brain barrier. Cell Microbiol **14**:1544–1553.

206. **Cox GM**, **Harrison TS**, **McDade HC**, **Taborda CP**, **Heinrich G**, **Casadevall A**, **Perfect JR**. 2003. Superoxide dismutase influences the virulence of Cryptococcus neoformans by affecting growth within macrophages. Infect Immunit **71**:173–180.

207. **Giles SS**, **Batinić-Haberle I**, **Perfect JR**, **Cox GM**. 2005. Cryptococcus neoformans mitochondrial superoxide dismutase: an essential link between antioxidant function and high-temperature growth. Eukaryot Cell **4**:46–54.

208. **Seider K**, **Heyken A**, **Lüttich A**, **Miramón P**, **Hube B**. 2010. Interaction of pathogenic yeasts with phagocytes: survival, persistence and escape. Curr Opin Microbiol **13**:392–400.

209. **Alvarez M**, **Casadevall A**. 2006. Phagosome extrusion and host-cell survival after Cryptococcus neoformans phagocytosis by macrophages. Curr Biol **16**:2161–2165.

210. **Schepetkin IA**, **Quinn MT**. 2006. Botanical polysaccharides: macrophage immunomodulation and therapeutic potential. Int Immunopharmacol **6**:317–333.

211. **Johnston SA**, **May RC**. 2010. The human fungal pathogen Cryptococcus neoformans escapes macrophages by a phagosome emptying mechanism that is inhibited by Arp2/3 complex-mediated actin polymerisation. PLoS Pathog **6**:e1001041.

212. **Nicola AM**, **Robertson EJ**, **Albuquerque P**, **Derengowski LDS**, **Casadevall A**. 2011. Nonlytic exocytosis of Cryptococcus neoformans from macrophages occurs in vivo and is influenced by phagosomal pH. MBio **2**:e00167–11.

213. **Ma H**, **Croudace JE**, **Lammas DA**, **May RC**. 2006. Expulsion of live pathogenic yeast by macrophages. Curr Biol **16**:2156–2160.

214. **Zaragoza O**, **García-Rodas R**, **Nosanchuk JD**, **Cuenca-Estrella M**, **Rodríguez-Tudela JL**, **Casadevall A**. 2010. Fungal Cell Gigantism during Mammalian Infection. PLoS Pathog **6**:e1000945.

215. **Zaragoza O**, **Chrisman CJ**, **Castelli MV**, **Frases S**, **Cuenca-Estrella M**, **Rodríguez-Tudela JL**, **Casadevall A**. 2008. Capsule enlargement in Cryptococcus neoformans confers resistance to oxidative stress suggesting a mechanism for intracellular survival. Cell Microbiol **10**:2043–2057.

216. **Alvarez M**, **Burn T**, **Luo Y**, **Pirofski L-A**, **Casadevall A**. 2009. The outcome of Cryptococcus neoformans intracellular pathogenesis in human monocytes. BMC Microbiol. **9**:51.

217. **Fries BC**, **Goldman DL**, **Cherniak R**, **Ju R**, **Casadevall A**. 1999. Phenotypic switching in Cryptococcus neoformans results in changes in cellular morphology and glucuronoxylomannan structure. Infect Immunit **67**:6076–6083.

218. **Goldman DL**, **Fries BC**, **Franzot SP**, **Montella L**, **Casadevall A**. 1998. Phenotypic switching in the human pathogenic fungus Cryptococcus neoformans is associated with changes in virulence and pulmonary inflammatory response in rodents. Proc Natl Acad Sci USA **95**:14967–14972.

219. **Goldman DL**, **Lee SC**, **Mednick AJ**, **Montella L**, **Casadevall A**. 2000. Persistent Cryptococcus neoformans pulmonary infection in the rat is associated with intracellular parasitism, decreased inducible nitric oxide synthase expression, and altered antibody responsiveness to cryptococcal polysaccharide. Infect Immunit **68**:832–838.

220. **Nessa K**, **Gross NT**, **Jarstrand C**, **Johansson A**, **Camner P**. 1997. In vivo interaction between alveolar macrophages and Cryptococcus neoformans. Mycopathologia **139**:1–7.

221. **Baker RD**, **Haugen RK**. 1955. Tissue changes and tissue diagnosis in cryptococcosis; a study of 26 cases. Am J Clin Pathol **25**:14–24.

222. **Schwartz DA**. 1988. Characterization of the biological activity of Cryptococcus infections in surgical pathology. The Budding Index and Carminophilic Index. Ann. Clin. Lab. Sci. **18**:388–397.

223. **Kechichian TB**, **Shea J**, **Del Poeta M**. 2007. Depletion of alveolar macrophages decreases the dissemination of a glucosylceramide-deficient mutant of Cryptococcus neoformans in immunodeficient mice. Infect Immunit **75**:4792–4798.

224. **Voelz K**, **Lammas DA**, **May RC**. 2009. Cytokine signaling regulates the outcome of intracellular macrophage parasitism by Cryptococcus neoformans. Infect Immunit **77**:3450–3457.

225. **Siegemund S**, **Alber G**. 2008. Cryptococcus neoformans activates bone marrow-derived conventional dendritic cells rather than plasmacytoid dendritic cells and down-regulates macrophages. FEMS Immunol Med Microbiol **52**:417–427.

226. **Luberto C**, **Martinez-Mariño B**, **Taraskiewicz D**, **Bolaños B**, **Chitano P**, **Toffaletti DL**, **Cox GM**, **Perfect JR**, **Hannun YA**, **Balish E**, **Del Poeta M**. 2003. Identification of App1 as a regulator of phagocytosis and virulence of Cryptococcus neoformans. J Clin Invest **112**:1080–1094.

227. **Arora S**, **Olszewski MA**, **Tsang TM**, **McDonald RA**, **Toews GB**, **Huffnagle GB**. 2011. Effect of cytokine interplay on macrophage polarization during chronic pulmonary infection with Cryptococcus neoformans. Infect Immunit **79**:1915–1926.

228. **Levitz SM**, **Farrell TP**. 1990. Growth inhibition of Cryptococcus neoformans by cultured human monocytes: role of the capsule, opsonins, the culture surface, and cytokines. Infect Immunit **58**:1201–1209.

229. **Artavanis-Tsakonas K**, **Love JC**, **Ploegh HL**, **Vyas JM**. 2006. Recruitment of CD63 to Cryptococcus neoformans phagosomes requires acidification. Proc Natl Acad Sci USA **103**:15945–15950.

230. **Qin Q-M**, **Luo J**, **Lin X**, **Pei J**, **Li L**, **Ficht TA**, **de Figueiredo P**. 2011. Functional Analysis of Host Factors that Mediate the Intracellular Lifestyle of Cryptococcus neoformans. PLoS Pathog **7**:e1002078.

231. **Levitz SM**, **Harrison TS**, **Tabuni A**, **Liu X**. 1997. Chloroquine induces human mononuclear phagocytes to inhibit and kill Cryptococcus neoformans by a mechanism independent of iron deprivation. J Clin Invest **100**:1640–1646.

232. **Tucker SC**, **Casadevall A**. 2002. Replication of Cryptococcus neoformans in macrophages is accompanied by phagosomal permeabilization and accumulation of vesicles containing polysaccharide in the cytoplasm. Proc Natl Acad Sci USA **99**:3165–3170.

233. **Kuballa P**, **Nolte WM**, **Castoreno AB**, **Xavier RJ**. 2012. Autophagy and the Immune System. Annu Rev Immunol **30**:611–646.

234. **Nicola AM**, **Albuquerque P**, **Martinez LR**, **Dal-Rosso RA**, **Saylor C**, **De Jesus M**, **Nosanchuk JD**, **Casadevall A**. 2012. Macrophage Autophagy in Immunity to Cryptococcus neoformans and Candida albicans. Infect Immunit **80**:3065–3076.

235. **Luo Y**, **Tucker SC**, **Casadevall A**. 2005. Fc- and complement-receptor activation stimulates cell cycle progression of macrophage cells from G1 to S. J Immunol **174**:7226–7233.

236. **Luo Y**, **Pollard JW**, **Casadevall A**. 2010. Fcgamma receptor cross-linking stimulates cell proliferation of macrophages via the ERK pathway. J Biol Chem **285**:4232–4242.

237. **Luo Y**, **Casadevall A**. 2010. Intracellular cryptococci suppress Fc-mediated cyclin D1 elevation. Commun Integr Biol **3**:390–391.

238. **Vadiveloo PK**. 1999. Macrophages--proliferation, activation, and cell cycle proteins. J Leukoc Biol **66**:579–582.

239. **Ben-Abdallah M**, **Sturny-Leclère A**, **Avé P**, **Louise A**, **Moyrand F**, **Weih F**, **Janbon G**, **Mémet S**. 2012. Fungal-induced cell cycle impairment, chromosome instability and apoptosis via differential activation of NF-κB. PLoS Pathog **8**:e1002555.

240. **Villena SN**, **Pinheiro RO**, **Pinheiro CS**, **Nunes MP**, **Takiya CM**, **DosReis GA**, **Previato JO**, **Mendonça-Previato L**, **Freire-de-Lima CG**. 2008. Capsular polysaccharides galactoxylomannan and

glucuronoxylomannan from Cryptococcus neoformans induce macrophage apoptosis mediated by Fas ligand. Cell Microbiol **10**:1274–1285.

241. **Pericolini E**, **Cenci E**, **Monari C**, **De Jesus M**, **Bistoni F**, **Casadevall A**, **Vecchiarelli A**. 2006. Cryptococcus neoformans capsular polysaccharide component galactoxylomannan induces apoptosis of human T-cells through activation of caspase-8. Cell Microbiol **8**:267–275.

242. **Goldman D**, **Lee SC**, **Casadevall A**. 1994. Pathogenesis of pulmonary Cryptococcus neoformans infection in the rat. Infect Immunit **62**:4755–4761.

243. **Alvarez M**, **Casadevall A**. 2007. Cell-to-cell spread and massive vacuole formation after Cryptococcus neoformans infection of murine macrophages. BMC Immunol. **8**:16.

244. **Declercq W**, **Vanden Berghe T**, **Vandenabeele P**. 2009. RIP kinases at the crossroads of cell death and survival. Cell **138**:229–232.

245. **Hull CM**, **Heitman J**. 2002. Genetics of Cryptococcus neoformans. Annu. Rev. Genet. **36**:557–615.

246. **Murray PJ**, **Wynn TA**. 2011. Protective and pathogenic functions of macrophage subsets. Nat. Rev. Immunol. **11**:723–737.

247. **Declercq W**, **Vanden Berghe T**, **Vandenabeele P**. 2009. RIP kinases at the crossroads of cell death and survival. Cell **138**:229–232.

Chapter 2

_____

Analysis of Cell Cycle and Replication of Mouse Macrophages after *In Vivo* and *In Vitro Cryptococcus neoformans* Infection Using Laser Scanning Cytometry

Abstract

We investigated the outcome of the interaction of *Cryptococcus neoformans* (Cn) with murine macrophages using Laser Scanning Cytometry (LSC). Previous results in our lab had shown that phagocytosis of Cn promoted cell cycle progression. LSC allowed us to simultaneously measure the phagocytic index, macrophage DNA content and 5-ethynyl-2'-deoxyuridine (EdU) incorporation such that it was possible to study host cell division as a function of phagocytosis. LSC proved to be robust, reliable and high throughput method for quantifying phagocytosis. Phagocytosis of Cn promoted cell cycle progression but infected macrophages were significantly less likely to complete mitosis. Hence we report a new cytotoxic effect associated with intracellular Cn residence that manifested itself in impaired cell cycle completion as a consequence of a block in the G2/M stage of the mitotic cell cycle. Cell cycle arrest was not due to increased cell membrane permeability or to DNA damage. We investigated alveolar macrophage replication *in vivo* and demonstrated that these cells are capable of low levels of cell division in the presence and absence of Cn infection. In summary, we studied simultaneously phagocytosis, cell cycle state of the host cell and pathogen cytotoxicity, demonstrating new cytotoxic effects of Cn infection on murine macrophages: fungal induced cell cycle arrest. Finally we provide evidence for alveolar macrophage proliferation *in vivo*.

Introduction

The interaction of the human pathogenic fungus Cryptococcus neoformans (Cn) with macrophages is thought to be a key event in the outcome of cryptococcal infection (10, 13, 17, 28, 29). Cn is a facultative intracellular pathogen and, once within a macrophage, Cn can replicate intracellularly with outcomes that range from host cell lysis to non-lytic exocytosis (2, 3, 23). Previous work in our laboratory has established that phagocytosis of Cn by murine macrophages could lead macrophages into cell cycle progression, namely into the S phase of the cell cycle (21). Later work established that Fcγ Receptor (FcγR) crosslinking triggered cell cycle progression resulting in increased proliferation of murine macrophages (20). However, while FcγR crosslinking (20) or ingestion of antibody coated beads led to cyclin D1 activation, phagocytosis of live yeasts suppressed cyclin D1 activation (18), possibly reflecting fungal-mediated host cell damage. Cyclin D1 is a major checkpoint in the passage from G1 to S phase. Hence fungal- macrophage interaction could influence host cell cycle machinery. Consequently, there is considerable interest in the relationship between macrophage cell cycle and phagocytic function.

Macrophages are derived from monocytes that migrate into tissues, where they acquire tissue-specific characteristics and can live as resident tissue cells for years (25, 26). Resident tissue macrophage proliferation plays an unknown role in the maintenance of tissue specific macrophages. Evidence of resident macrophage proliferation has been available for some time (30). In the lung, specifically, site of initial infection in human cryptococcosis, there is evidence for *in vivo* alveolar macrophages (AM) proliferation (4, 31, 32). AM recovered from mice exposed to cigarette smoke manifested increased proliferation *in vitro* suggesting that cell division could be increased in response to a damaging stimuli (12). Nevertheless, many questions still remain as to the relative contribution of local macrophage proliferation versus influx of blood monocytes in response to infection. In recent months several studies have appeared in the literature investigating this phenomenon and how macrophage life, replication and death are balanced at the onset and resolution of tissue insult and damage (1, 9, 14, 15). These studies suggest that macrophage proliferation contributes to normal tissue homeostasis and that macrophages can replicate at the site of inflammation.

In this work we show that Laser Scanning Cytometry (LSC) can be adapted to study phagocytosis and have used this technique to explore how phagocytosis of yeast cells influenced macrophage cell cycle progression and mitosis. LSC was developed to scan, analyze and compare images from microscopic preparations in a fully automated form. It enables users to perform analysis similar to Flow Cytometry using various quantitative parameters extracted from the scanned images (11). The ability of LSC to perform microscopic correlations of

61

cellular and sub cellular events in a large population of cells makes it a highly attractive technique for studying intracellular processes. LSC is routinely used in several applications such as microarray analysis, tissue section analysis and immunophenotyping and cell cycle or mitosis analysis (16, 42). It is generally accepted that the results of LSC are equivalent to Flow Cytometry and that for certain assays it can be more sensitive than Flow Cytometry, such as detecting cells in transition between mitotic phases, or very early apoptosis (33, 42). Hence LSC can be a powerful tool for studying pathogen interactions with macrophages.

Materials and Methods

Yeast strains, cell lines and reagents

C. neoformans var. *grubii* strain H99 (serotype A) was obtained from John Perfect (Durham, NC) and *C. neoformans* var. *neoformans* strain 24067 (serotype D) was obtained from the American Type Tissue Collection (Rockville, MD). Strain H99 was used for all *in vitro* studies. Both strains were cultured in Sabouraud dextrose broth (Difco, Carlsbad, California) for 2 d at 37°C with agitation (150–180 rpm). Yeast cells were washed three times with sterile PBS, counted on a hemocytometer and suspended at the appropriate cell density in cell culture media.

The IgG1 monoclonal antibody (mAb) 18B7 was described previously (5) and was used as an opsonin at 10 μg/mL, unless otherwise noted. The macrophage-like murine cell line J774.16, which was originally derived from a reticulum sarcoma was used for most experiments. Macrophages were grown in media consisting of Dulbecco's minimal essential medium (DMEM) (CellGro, Mediatech, Manassas, Virginia, USA), 10% NCTC-109 Gibco medium (Invitrogen, Carlsbad, California, USA), 10% heat-inactivated FCS (Atlanta Biologicals, Lawrenceville, Georgia, USA), and 1% non-essential amino acids (CellGro, Mediatech, Manassas, Virginia, USA).

Bone marrow derived macrophages (BMDM) were obtained from wild-type 6-8 weeks BALB/C female mice (National Cancer Institute, Bethesda, Maryland, USA). Briefly, mice were killed by CO_2 asphyxiation and bone marrow cells were harvested from the hind leg bones by flushing them with DMEM. The harvested cells were cultured at 37°C with 5% CO_2 in DMEM media with 20% L-929 cell conditioned media, 10% fetal bovine serum, 2 mM L-glutamine (CellGro, Mediatech, Manassas, Virginia, USA), 1% non-essential amino acids (CellGro, Mediatech, Manassas, Virginia, USA), 1% HEPES buffer (CellGro, Mediatech, Manassas, Virginia, USA) and β-mercaptoethanol (Gibco, Carlsbad, California, USA). Macrophages where allowed to grow for 6 to 8 d before plating at the desired density for the experiments.

All animal experiments were conducted according to ethical guidelines, with the approval of the Institutional Animal Care and Use Committee (IACUC) of Albert Einstein College of Medicine.

In vitro phagocytosis assays

For LSC experiments, J774.16 and BMDM cells were seeded in a 96-well glass bottom plate with dark edges (MGB096-1-2-HG-L, Matrical Biosciences, Spokane, Washington, USA). The macrophages were plated at a density of 2.4 x 10^4 cells/well and used for phagocytosis studies after adhering to the microtiter plate for either 2 h or overnight. Yeasts were added at a Multiplicity of Infection (MOI) of 1:2 and the opsonic mAb was added at 10 μg/ml in a final volume of 200 μL per well. When necessary, Cn was heat-killed (HK Cn) by

incubating at 56 °C for 60 min. Phagocytosis was allowed to proceed for 2 h at 37° C, under 5% CO_2 atmosphere.

After phagocytosis the wells were washed twice with 200 μL of PBS, fixed in ice-cold methanol for 30 min at -20° C and washed again. Wheat Germ Agglutinin (WGA) conjugated to Alexa 633 (Invitrogen, Carlsbad, California, USA) was used at 10 μg/mL and incubated overnight at 4° C. We found no instances of Cn staining with WGA in our experimental conditions. Uvitex 2B (Polysciences, Inc, Warrington, PA, USA) was added at a 0.1 μg/mL and allowed to stain for 1 min. Propidium Iodide (PI) (Sigma-Aldrich, St. Louis, Missouri, USA) was added at a concentration of 5 μg/mL in a total volume of 400 μL per well. Cells were analyzed in PI solution.

Alternative protocols were designed according to experimental conveniences. When using antibodies for detection, preparations were blocked for 30 min at room temperature with 2% FCS in PBS. In one protocol, detection of yeasts was done by detecting the opsonizing antibody bound to the capsule with an Alexa 488-conjugated goat antibody to murine IgG (Invitrogen, Carlsbad, California, USA) at a 1:50 dilution. Macrophage contour could also be successfully was detected with Alexa 633-conjugated antibody to mouse F4/80 (Invitrogen, Carlsbad, California, USA) at a dilution of 1:25.

Confirmation of successful internalization can be achieved by immunostaining extracellular Cn previous to permeabilization, followed by Uvitex staining of total Cn. Staining of Cn nuclei with PI occurred, but given the smaller size of Cn nuclei and the dimmer fluorescent signal it was not enough to interfere with DNA quantification. Irrespective of this we established an independent nucleus contour, such that the staining of the Cn nuclei is automatically excluded from the macrophage nuclei contour, to assure that it did not interfere with our determination of macrophage nuclei and DNA quantification.

Additionally, cell cycle plots were performed with Nucleus contour that corresponded only to the macrophage nuclei.

Images were acquired in LSC by imaging 35-60 fields in each well with the 40x objective at 0.5 μm resolution, allowing a field size of 500 μm x 192 μm. For phagocytosis assays, at least 1000 cells were imaged for each experimental replicate.

After acquisition of fluorescent images in LSC, preparations were stained by incubating with Giemsa dye solution for 2 h at room temperature, and washed with PBS to remove excess stain. Phagocytic index was quantified by direct observation using an inverted microscope, for a total of three fields per well, with at least 100 cells/field. Macrophages with internalized Cn were readily distinguishable from cells that had not ingested

64

Cn, or from cells where Cn was simply attached to the outside, due to the visible vacuole containing engulfed Cn.

In vitro replication studies

A protocol to study replication *in vitro* was adapted from the work of Darzynkiewicz (8). Briefly, J774.16 macrophages were plated at 2.4 x 10^4 cells/well and allowed to adhere for 2 h. In all conditions a 10 μM solution of EdU in cell media was added for 2 h, unless otherwise noted, then removed by washing with warm media. For pre-labeling studies cells were labeled with EdU, then allowed to ingest Cn for 15 min at a MOI of 1:5 and afterwards the extracellular Cn was removed by washing twice with warm media. For post labeling studies Cn phagocytosis was done in the same manner but EdU was added after Cn was removed. After 2 h, cell media was replaced with fresh media and cells allowed to cycle for an additional 2 h. Co incubation studies consisted of phagocytosis of Cn at MOI 1:2 in the presence of EdU for 2 h. Cells were fixed in methanol and non-specific signal was blocked with 2% FBS in PBS. EdU labeling was performed following manufacturer's instructions. Briefly, this labeling strategy coupled the thymidine analogue 5-ethynyl-2'-deoxyuridine (EdU) with an azide-conjugated Alexa 488 for detection, via the Click-it Chemistry reaction (Invitrogen, Carlsbad, California, USA). Macrophages were counterstained with WGA-Alexa 633, PI and yeast detected with Uvitex. LSC images were obtained with the 40x objective at 0.5 μm resolution, allowing a field size of 500 μm x 192 μm. For cell cycle analysis, 49-100 fields were imaged to information from at least 2000 cells in each experimental replicate.

Experiments with BMDM were performed alike, except that the time for EdU incubation was extended to 6 h due to slower replication rate of these cells relative to J774.16 cells . When indicated, BMDM were incubated with IFN-γ at 400 U/mL or LPS at 1 ng/mL for 18h before phagocytosis and the stimuli were renovated after each media change. Taxol (Tocris Bioscience, Ellisville, Missouri, USA) was added at 250 nM for 18 h.

DNA fragmentation and permeability assays

Phagocytic experiments were carried out as described above for 2, 6 and 18 h. Valinomycin (Tocris Bioscience, Ellisville, Missouri, USA) was added at a concentration of 400 nM for 18h to induce apoptosis through DNA damage, serving as a positive control for both experiments. Cell membrane permeability was measured by adding 100 nM of Image-iT® DEAD Green (Invitrogen, Carlsbad, California, USA) to cells 30 min before fixation with 4% paraformaldehyde. Cells were counterstained with Alexa 633 conjugated-WGA and DAPI. Experiment was performed twice for J774.16 cells and once for BMDMD in triplicate wells.

TUNEL staining (Invitrogen, Carlsbad, California, USA) was performed according to manufacturer's instructions. Briefly, wells were fixed with paraformaldehyde 4% and 100 μL of TdT reaction cocktail added for

1h at 37°C, washed and developed by incubating with Click-iT reaction cocktail that will couple TdT to Alexa 647 allowing for fluorescent detection. Cells were counterstained with PI and yeast cells labeled with Uvitex. This experiment was performed twice for J774.16 cells and once for BMDMD with one single experimental replicate. LSC images were obtained with a 40x objective at 0.5 μm resolution, allowing a field size of 500 μm x 192 μm. At least 1000 cells were imaged for each experimental replicate.

In vivo replication studies

Alveolar macrophage (AM) labeling was performed as described previously (17, 19). Briefly 100 μL of 40 mM PKH26 (PKH) was dissolved into 300 μL diluent B (Sigma-Aldrich, St. Louis, Missouri, USA) in order to label phagocytic cells and injected into the tail vein of Balb/C mice.   After 2 d, mice were infected with the virulent strain 24067.   *In vivo* studies were performed with strain 24067 because this strain is better characterized in our lab in the context of the mouse model of intratracheal infection (41).   Mice were anesthetized with ketamine (10 mg/kg) and xylazine (125 mg/kg) intraperitoneally (i.p.) in PBS, and a midline incision over the trachea was performed and an inoculum of 1×10^6 Cn in 50-100 μL was injected into the trachea. The incision was closed with VetBOND (3M, St. Paul, Minnesota, USA). At 4 d post-infection, mice were injected i.p. with 100 μg of EdU in PBS 20% DMSO or vehicle alone, as described previously (24). Mice were sacrificed 6 h post EdU administration by CO_2 asphyxiation and bronchoalveolar lavage (BAL) performed to extract AM.   Briefly, the trachea was exposed and the lungs were lavaged 10 times with 0.8 mL sterile calcium and magnesium-free HBSS (Life Technologies, Grand Island, NY, USA) supplemented with 1 mM EGTA (Sigma-Aldrich, St. Louis, Missouri, USA). BAL was spun and resuspended in cell culture media and allowed to adhere for 2 h at 37° C, 5% CO_2. Cells were treated with a hypotonic solution of NH_4Cl for 10 min on ice to remove red blood cells and subsequently fixed for 30 min at -20° C. Preparations were then blocked with 2% FCS in PBS and EdU staining developed following manufacturer's instructions (Invitrogen, Carlsbad, California, USA).   Nuclei were counterstained with DAPI.   Images were acquired in LSC by imaging 156 fields/well with a 60x objective that allowed 0.15 μm resolution. Additional confirmation was performed by inspecting the entire area of the negative control wells, in an inverted epifluorescent microscope at 20x magnification. No positive events were ever found in the negative control samples.

Data collection and analysis

The iCys® Research Imaging Cytometer (CompuCyte Corporation, Westwood, Massachusetts, USA) was used for the experiments. Instrument control, data acquisition and analysis were performed using the software the iCys Cytometric Analysis Software®, provided with the instrument. The instrument was calibrated using an empty 96-well plate to allow use of the autofocus feature.

For image analysis three different type of events were defined: the 'Cell' event was the combined image of the nuclear PI signal plus cell membrane Wheat Germ Agglutinin (WGA); the Nuclear signal generated 'Nucleus' event and the 'Uvitex' event was used for the Uvitex stained yeasts (Fig. 1).

The creation of these channels was the first step in analyzing cell fluorescence so that cells could be recognized and contoured by the software and translated into events. The 'Cell' channel contoured macrophages using a merged PI and WGA image. Clusters of positive pixels were delimited creating the threshold contour, which allowed the software to identify a single macrophage cell as one 'event'. Association of separate events like 'Cell' or 'Nucleus' or 'Yeast' was the last step, allowing quantification of the number of 'Yeast' events localized within the contour of the 'Cell' event, i.e. the number of phagocytosed particles inside each macrophage.

Events are represented in a scatter plot or histograms, where different regions could be defined. Statistics of the number of events occurring in each of the regions of interest were obtained and used to calculate phagocytic index and fungal burden.

Statistical analysis and plotting

Graphs and statistical analysis were performed in Prism version 5.00 for Mac OS X, GraphPad Software, San Diego, California, USA.

Results

Development of the LSC Detection Protocol

The first objective of this work was to establish whether LSC could be adapted to study phagocytosis of Cn by macrophages. The irregular shape of a macrophage cell was successfully detected by merging PI nuclear staining with Wheat Germ Agglutinin (Fig. 1). Yeast cells were successfully detected with either the fungal cell wall stain Uvitex or with specific capsule-binding antibody staining. The method was first established in the macrophage-like immortalized cell line J774.16 and then adapted to primary cells, including bone marrow derived macrophages and alveolar macrophages and subsequently to *in vivo* phagocytosis post-intratracheal instillation of Cn (data not shown).

We ascertained LSC accuracy by inspecting the images created by the instrument (Supplemental Fig. 1). LSC correctly identified over 90% of the macrophages. In addition to detecting number of phagocytic macrophages, LSC quantified the number of yeasts that each macrophage Ingested with 85% accuracy and distinguished up to 10 yeasts inside each cell. LSC could analyze over 1000 cells within the time frame were a human operator could only analyze 100-300 cells, while greatly reducing operator time investment.

Cell cycle analysis was performed by two measurements: DNA content quantification after Propidium Iodide (PI) staining and new DNA synthesis through nucleoside analogue 5-ethynyl-2'-deoxyuridine (EdU) incorporation, as recently published (4), and as illustrated in Fig.1B. Hence, we concluded that LSC quantification was a fast, versatile and reliable method for studying cell cycle in phagocytic macrophages.

LSC measurements using different Cn staining protocols

To insure that LSC was compatible with a wide range of fluorescent tools we established and compared two separate Cn staining protocols. Cell wall specific stain Uvitex is available in only one fluorescent color. Since a capsular antibody was used as an opsonin to mediate phagocytosis, we investigated whether the same antibody could also be used for Cn detection. The advantage of antibody detection is that it would allow us to choose a wide range of commercially available fluorophores. Consequently, we compared Immunostaining to Uvitex staining and compared both to human Operator visual quantification after Giemsa staining (Fig.2A), over a range of opsonizing mAb concentrations. Uvitex staining was effective independently of the concentration of opsonizing antibody used. In contrast, immunostaining was effective only when opsonizing mAb
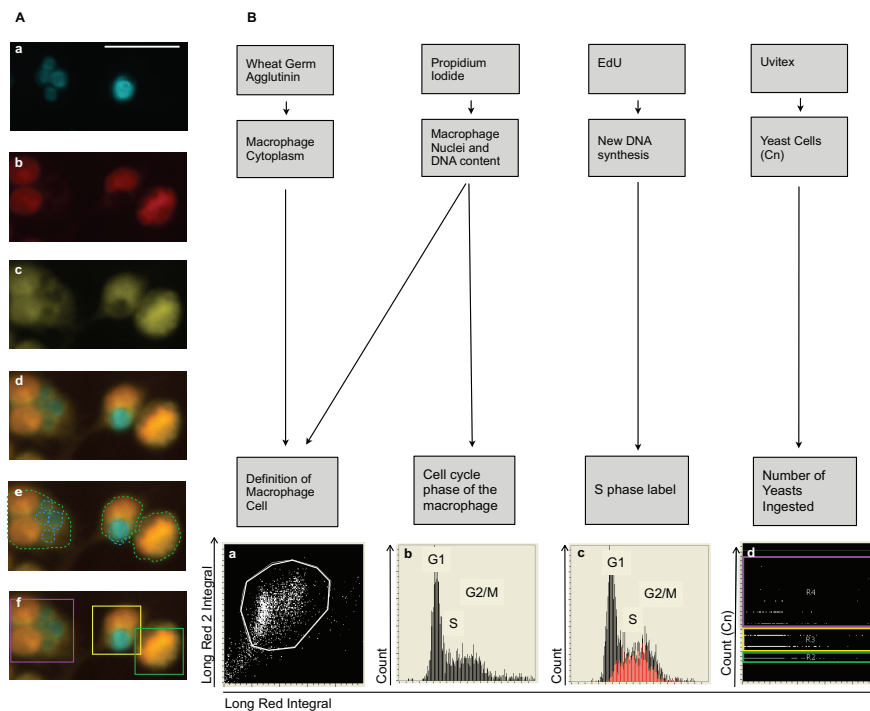
Figure 1. Quantification of phagocytosis and cell cycle phase in macrophages by LSC.

A) Phagocytic Quantification. Fluorescent image of: a) Uvitex stained Cn; b) PI stained Nuclei; c) Wheat Germ Agglutinin stained Cytoplasm; d) merged Uvitex, PI and Wheat Germ Agglutinin; e) Contours encircling fluorescent areas (light green line) will define the macrophage area and contours encircling Uvitex singal will define the Cn area (cyan line) and f) *Cryptococcus neoformans* yeast (Cn) subcontours inside each macrophage are quantified. Categories were created and translated into color coded boxes: No Cn, Green; One and Two (1-2) Cn, Yellow and More than Three (>3) Cn, Magenta, allowing verification of software identification. Scale bar represents 20 μm. B) Cell cycle status and correlation with phagocytosis. The association of different fluorescent markers allowed the identification of macrophages and the study of intracellular events within each macrophage. Macrophages were classified according to the number of yeasts that they had ingested and then sub-classified according to the their cell cycle phase. a) Cytoplasmatic signal and nuclear signals were merged to delineate the macrophage and define the macrophage population (white box). b) PI staining quantifies the amount of DNA, producing a histogram with 3 regions that reflected cell cycle stage: G1, S and G2/M phase. c) EdU labeling (Red) will identify cells actively synthesizing DNA (S phase). d) Number of Cn events inside each macrophage was plotted and divided into 3 categories: No Cn, Green; One and Two (1-2) Cn, Yellow and More than Three (>3) Cn, Magenta. The experiment was performed with primary macrophages infected with Cn strain H99 at MOI 1:2. concentrations ≥ 10 μg/mL were used. Concentrations of opsonizing antibody <10 μg/mL promoted effective phagocytosis but the phagocytic index determined by Ab staining was half of the value detected by other stains, since this method is dependent on a certain amount of antibody bound to fungal cells. Concerns that adhered yeasts could be mistakenly measured as internalized yeasts were addressed by combining both Cn detection techniques, where one of the stains was applied before methanol permeabilization, and the other post permeabilization. We determined that at 2 h measurement of total yeasts (single staining) or differentiation of bound and internalized yeast (double staining) produced similar results (for example, both methods quantified 19% of non-phagocytic macrophages) (Supplemental Fig. 2), thus discarding the need to use differential staining when performing phagocytic measurements for longer than 2 hours. However when shorter time intervals were used or when internalization of Cn was blocked (incubation of cells at 4ºC promotes binding without internalization), measurement of total yeasts had a higher phagocytic rate than when double staining was performed. Hence, only in some conditions it was necessary to perform double staining to differentiate adherent Cn and avoid biasing phagocytic index.

We inquired whether LSC quantification correlated with microscopic counting performed by a human operator, which is currently the standard in the field. Furthermore, we investigated human-to-human variation in phagocytic index determinations given the same preparation to quantify. A comparison of the LSC count with that obtained by 5 human operators was done using in the same triplicate wells of one phagocytic assay (Fig. 2B). The phagocytic rate for triplicate wells obtained by LSC protocol (31%) was comparable to that measured by different human operators (from 15% to 30%), as was the standard deviation obtained. Curiously, there was no statistical difference between the counts between operators, as assessed by one-way analysis of variance (p = 0.4). These results show that LSC was adaptable to a wide variety of phagocytic indexes and experimental conditions and that operator bias should not be a concern in fungal phagocytic determinations.
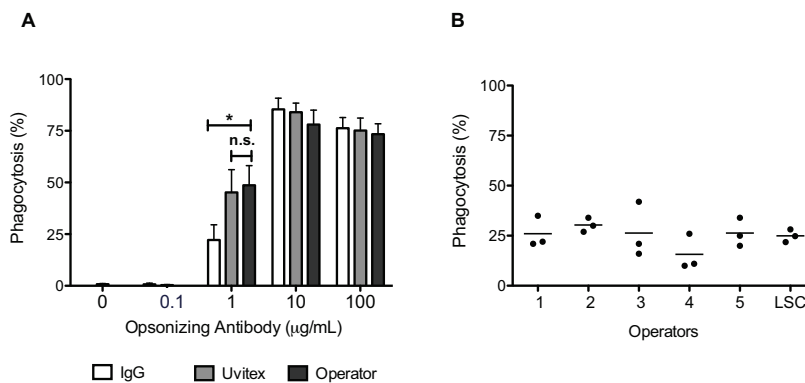

Figure 2. Comparison of LSC staining strategies with reference methods.

LSC quantification correlated with human operator quantification of a Giemsa-stained preparation. A) BMDM phagocytic rate was detected by LSC by staining with a fluorescent labeled antibody against the opsonizing antibody and simultaneously by Uvitex cell wall stain. The same preparations were subsequently stained with Giemsa stain and quantified by a human operator. The experiment was performed twice counting triplicate wells. Mean ± SD of triplicate wells of one representative experiment are shown. Two tailed t-test with a 95% confidence interval (*, p < 0.01; n.s., non-significant). B) Human operator quantification was compared to LSC in J774.16 macrophages. Triplicate wells were analyzed by LSC and subsequently stained by Giemsa and quantified by 5 independent human operators. The operators were blind to the conditions of the assay. Operators were instructed to choose 50% confluent fields but were left free to define their fields of analysis. Mean ± SD of triplicate wells are shown. Groups were compared using one-way analysis of variance. p=0.04 for a 95% confidence interval.

Cell cycle correlation with ingestion of yeast cells

Previous work in our lab had established that phagocytosis of Cn or inert latex beads drives macrophage cells into S phase (15). We investigated this result further by studying cell cycle progression as a function of intracellular fungal burden. In concordance with our prior study, ingestion of Heat-Killed (HK) or Live Cn cells was associated with a decrease in the proportion of G1 phase cells (56% in No Cn vs 33% in cells with 1-2 yeasts; and 42% when cells contained ≥ 3 yeasts) and a concomitant increase in the proportion of cells in S and G2/M phases for Live Cn (15% in No Cn vs 17% in 1-2 yeasts and 20% when ≥ 3 yeasts were ingested) (Fig. 3A and B). Note that cell cycle progression increased as fungal burden increased, suggesting that a higher fungal burden had a stronger effect in driving the macrophage into S phase.

To expand and confirm our findings we used EdU incorporation as an alternative to DNA quantification. In contrast to PI staining which reflects total DNA content, EdU incorporation labels cells with active DNA synthesis, thus cells in the S phase of cell cycle (Fig. 3C). When J774.16 macrophages ingested Cn, the rate of EdU incorporation was equal to macrophages that did not phagocytose Cn. In other experiments, macrophages were allowed to ingest more Cn, at a multiplicity of infection (MOI, macrophage:yeast ratio) of 1:10 and still there was no significant increase in Edu+ cells relative to cells with No Cn. Furthermore, when phagocytosis was allowed to proceed for 4 h there was still no increase in the rate of EdU positive cells (results not shown).

In vitro J774.16 macrophage proliferation after ingestion of yeast cells

To investigate the apparent discordance between DNA quantification and EdU incorporation we carried out pulse labeling experiments to track cycling macrophages. Macrophages were labeled with EdU for a 2 h period, EdU was removed and cells left to complete cell cycle, such that EdU labeled macrophages would now be in the G1 phase of cell cycle. Some macrophages were pre-labeled with EdU for 2 h, allowed to phagocytose Cn for 15 min and left for additional 4 h to complete cell cycle. Post-labeled cells were allowed to phagocytose first for 2 h, then incubated with EdU for 2 h and given an additional 2 h to progress through the cycle. Both pre and post-labeled cells that phagocytosed Cn had a percentage of Edu+ cells that was similar to uninfected macrophages (44% in No Cn vs 43% in Live CN and 44% for HK Cn) (Fig. 4A), similar to results in Fig.3C. In uninfected macrophages 27% of pre-labeled macrophages were now in G1 gate of DNA histogram, but when Live Cn was present only 12% of Edu+ macrophages had reached G1 (Fig. 4B). These results were consistent with an increase in Edu+ cells located in G2/M (Fig.4C) when macrophages ingest Cn, such that 22% of macrophages that ingested Live Cn were still in the G2/M phase while uninfected macrophages had only 11%.
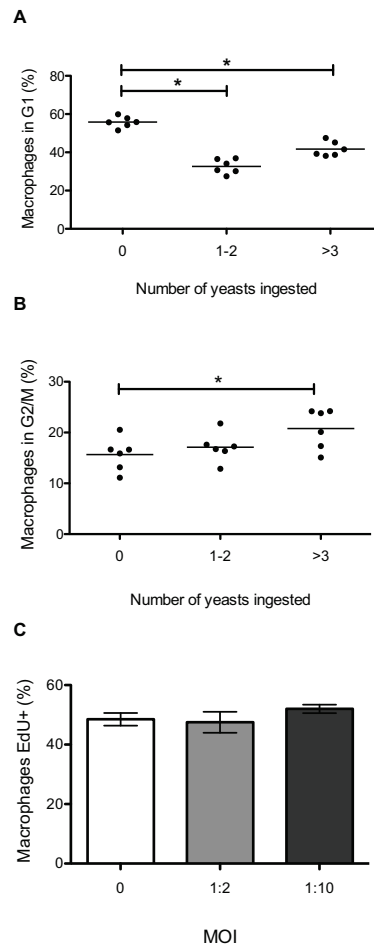
71

Figure 3. Association of cell cycle state in J774.16 macrophages with fungal burden. Macrophage progression to G2/M phase of cell cycle correlated with fungal burden within the macrophage. Macrophages were grouped according to the number of yeasts ingested and their cell cycle phase. A) Percentage of macrophages in G1 phase and; B) in G2/M. Experiments were performed three times, with 6 replicate wells. Data points and average are shown. C) Percentage of EdU+ macrophages during phagocytosis. Macrophages were allowed to incorporate EdU for 2 h with a Multiplicity Of Infection (macrophage:yeast ratio) (MOI) of zero (no yeasts), 1:2 or 1:10. Experiment was repeated twice in duplicate wells with similar results. Shown is mean ± SD of duplicate wells of one representative experiment.

Both results combined reflect an accumulation of macrophages at G2/M and decreased rate of successful mitosis. To validate that our experimental approach, we treated J774.16 cells with taxol, known to arrest cells at G2/M phase. We observed that taxol treatment does not affect overall EdU incorporation, but results in a marked increase in the number of Edu+ cells in G2/M phase (data not shown). Hence, the apparent discordance between PI and EdU was caused by cell cycle block at G2/M phase, such that cells are able to proceed through S

phase and stop in G2/M. Our experimental data implied that antibody-opsonized Cn ingestion caused macrophage cell cycle arrest at G2/M phase.
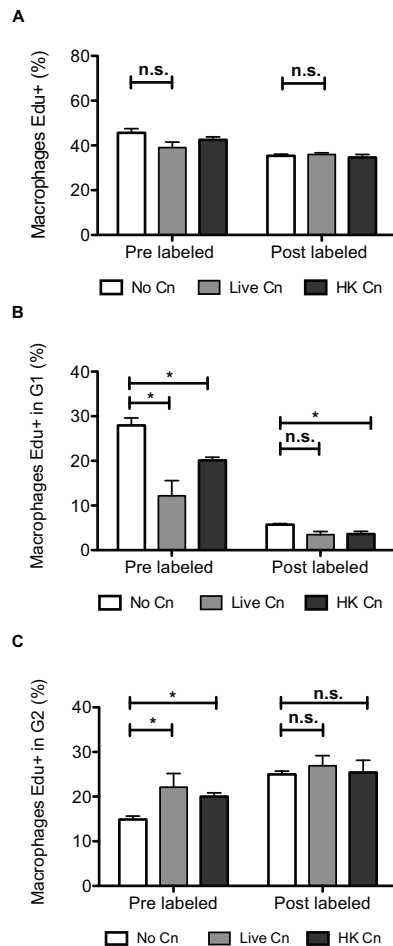

Figure 4. EdU incorporation and J774.16 macrophage completion of cycle.

Ingestion of Cn decreased the number of macrophages that successfully divided and returned to G1 phase. These macrophages were retained at G2/M phase. Macrophages that had not ingested Cn (No Cn) after 2 h of Cn phagocytosis were allowed to incorporate EdU for 6 h. A) Percentage of total macrophages that incorporated EdU. B) Percentage of macrophages that incorporated EdU, underwent mitotic division and subsequently reached G1 phase. C) Percentage of macrophages that incorporated EdU and reached G2/M phase. Experiments were performed three times. Shown is mean ± SD of triplicate wells of a representative experiment. Groups were compared using two tailed t-test with 95% confidence interval. (* $p<0.05$, n.s., not-significant).

BMDM proliferation after ingestion of yeast cells

To investigate the relevance of our results in primary cells, our experiments were adapted to BMDM, which have a much slower rate of proliferation than the J774.16 macrophage-like cell line. Some of these BMDM were stimulated with IFN-γ, which is known to arrest macrophages in G1 phase (38). After 6 h of phagocytosis,

there was a decrease in G1 phase accompanied by an increase in G2/M phase (Fig. 5A). This difference, however, was not statistically significant (p = 0.3), possibly because of the slower rate of replication of primary macrophages resulted in far fewer events. We studied macrophages treated with IFN-γ, which is known to suppress cell cycle and in those cells phagocytosis of Cn overcame IFN-γ-induced cell cycle arrest such that macrophages to progress into S phase, resulting in a statistically significant difference (p=0.0078). EdU was added to BMDM in the same conditions and for these cells we measured increased EdU incorporation when macrophages ingested Cn (10% vs 21% for No Cn vs Live Cn conditions). In IFN-γ stimulated macrophages there was a higher fold-increase in the percentage of Edu+ cells (4% vs 12% in No Cn vs Live Cn) (Fig. 5B). Next, we allowed Cn infection to proceed for 24 h (Fig. 5C) and labeled new DNA synthesis at the last 6 h of infection (Fig. 5D). The percentage of macrophages in G1 phase was reduced when macrophages ingested Cn, compared to control conditions (p=0.02). Additionally, in the presence of IFN-γ, there was a decrease in percentage of macrophages in G1 phase and a significant increase in the percentage of macrophages in G2/M phase (p<0.0001), suggesting that cell cycle arrest occurred in BMDM 24 h after phagocytosis. Similarly, EdU incorporation was increased at 24 h when macrophages had ingested Live Cn or HK Cn (10.1% in non infected macrophages vs 50.5% in macrophages with Live Cn). In IFN-γ treated wells the fold-increase in EdU incorporation was more drastic (1.19% vs 13.9%). We repeated these experiments for LPS-activated macrophages. Cn phagocytosis was able to override the cell cycle arrest provoked by LPS (data not shown). In the absence of growth factors, there was always a complete cell cycle arrest and no EdU incorporation (data not shown). We conclude that Cn infection provokes a sustained proliferative response in BMDM, as measured by incorporation of labeled DNA nucleotides. However, at 24 h post phagocytosis, IFN-γ treated BMDM are arrested at G2/M phase, as measured in cell cycle plots, implying that proliferative response was arrested and replication was not successful. Unlike the J774.16 cells, in BMDM there is an increase in the rate of EdU incorporation, mainly because BMDM have a much slower replication rate that might be subject to modulation. In contrast, J774.16 cells replicate more rapidly. However, for both J774.16 and BMDM our results indicate cell cycle arrest in the G2/M phase after Cn phagocytosis.
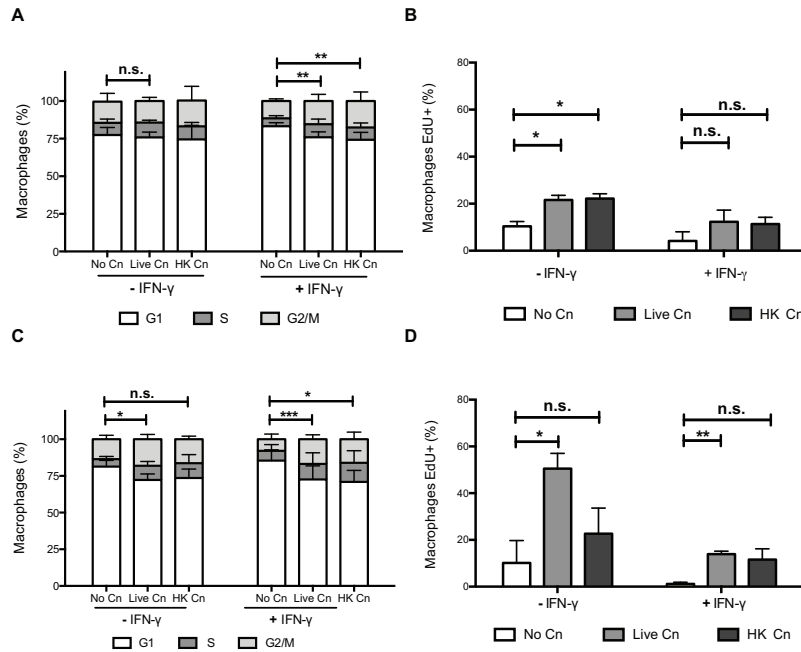
Figure 5. Progression in cell cycle and new DNA synthesis in BMDM.

BMDM progressed into S phase, as demonstrated by cell cycle analysis and EdU incorporation, when Cn was ingested. A) Cell cycle plot after 6 h phagocytosis. B) Incorporation of EdU after 6 h phagocytosis. C) Cell cycle plot after 24 h phagocytosis. D) Incorporation of EdU 24 h after phagocytosis. Macrophages were infected with Live and HK Cn for 6 h or 24 h and EdU was added in the last 6 h of the experiment. Phagocytosis occurred in the presence of growth factors, with and without IFN-γ (to induce cell cyle arrest in G1 phase). The experiment was repeated 4 times using triplicate wells. Shown is mean ± SD of triplicate wells of two experiments. Groups were compared using two tailed p-test with 95% confidence interval. (*** p<0.001, ** p<o.01, * p<0.05, n.s., not significant).

Alteration of nuclear morphology

Cyclomodulins are bacterial products that interfere with host cell cycle by mechanisms that usually involve direct effects to cell cycle machinery or indirectly by disturbing the cytoskeletal organization. Cyclomodulin usually results in host cell endonucleation (multiple nuclei inside the same cell), enlargement of the nuclei or of the cell or inhibition of cytokinesis that ultimately leads to cell death (Nougayrede, 2005). Hence, we inspected LSC images for altered nuclear morphology. We observed several events of nuclear enlargement, binucleate cells and cells that seemed to result from fusion of several macrophages (Supplemental Fig.3) both in not infected and infected wells. Cell cycle plots did not show an increase in ploidy over > 4n (data not shown) for any of the conditions studied. Hence, the cell cycle arrest observed for Cn does not appear comparable to that observed with cyclomodulins.
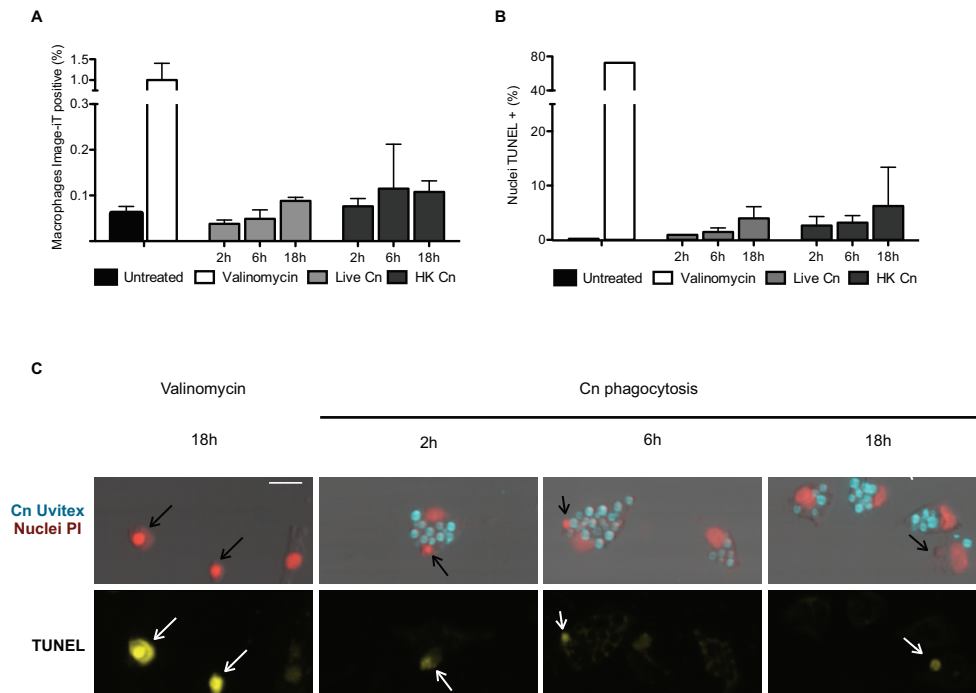
Figure 6. DNA fragmentation and membrane permeability in J774.16 macrophages.

J774.16 macrophages did not manifest increased membrane permeability or DNA fragmentation after phagocytosis of Cn. A) Quantification of the number of cells positive for membrane permeability; or B) DNA fragmentation. Treatment with valinomycin at 400 nM for 18 h was used as a positive control while uninfected macrophages were used as the negative control. C) Representative images of macrophages positive for TUNEL staining after treatment with 400 nM valinomycin (positive control) or after infection with Live Cn (HK Cn not shown). Nuclei positive for DNA fragmentation have apoptotic cell morphology and are rapidly engulfed by a neighboring cell (arrows). Scale bar represents 20 μm. Experiments were performed in duplicate wells for DNA fragmentation or in triplicate wells for membrane permeability measurements. Experiments were performed twice in J774.16 macrophages and one experiment is shown. Experiments were performed once for BMDM and same results as observed for J774.16 were obtained.

Causes of cell cycle arrest

Cell cycle arrest could be caused by interference directly in the cell cycle or by Cn indirect toxic effects. To investigate the cause of the cell cycle arrest we stained macrophages with the nuclear stain Image-iT green, which is impermeable for intact membranes. Bright Image-iT fluorescence indicates a permeable cellular membrane, characteristic of either late apoptosis or necrosis (Fig. 6A). In both J774.16 and BMDM there was an increase in the number of membrane permeable macrophages when Cn was ingested. However very few macrophages were membrane permeable suggesting that cell damage involving cell membrane integrity does not explain cell cycle arrest.

76

Next we measured DNA fragmentation by the TUNEL assay. DNA damage will activate cell cycle checkpoints and prevent cell cycle progression and, if DNA damage is extensive enough, it can trigger apoptosis. We observed an increase in TUNEL+ cells for macrophages with ingested Cn relative to control macrophages: 0% in uninfected macrophages vs 1.4% in Live Cn vs 3.2% in HK Cn (Fig. 6B). Most frequently we found TUNEL+ nuclei already ingested by a neighboring macrophage (Fig 6C, note arrows), suggesting that, in our system, the apoptotic cells are promptly removed by neighboring cells. Images show that every TUNEL+ nuclei had morphology consistent with very late apoptosis or even nuclei debris. From this we conclude cell cycle arrest is unlikely to be caused by direct DNA damage, as measured by DNA fragmentation.

In vivo macrophage proliferation in the presence and absence of Cn infection

Alveolar macrophages are considered the first line of defense for Cn infection. The lipophilic dye PKH, when suspended in a buffer that causes its aggregation, can be used to label phagocytic cells. This strategy has been used by Maus et al (24) to label alveolar macrophages *in vivo*. At the same time intraperitoneal injection of EdU will label proliferating cells *in vivo* (28). Hence, we decided to combine both these strategies together with the LSC technology to investigate AM replication in the lung.
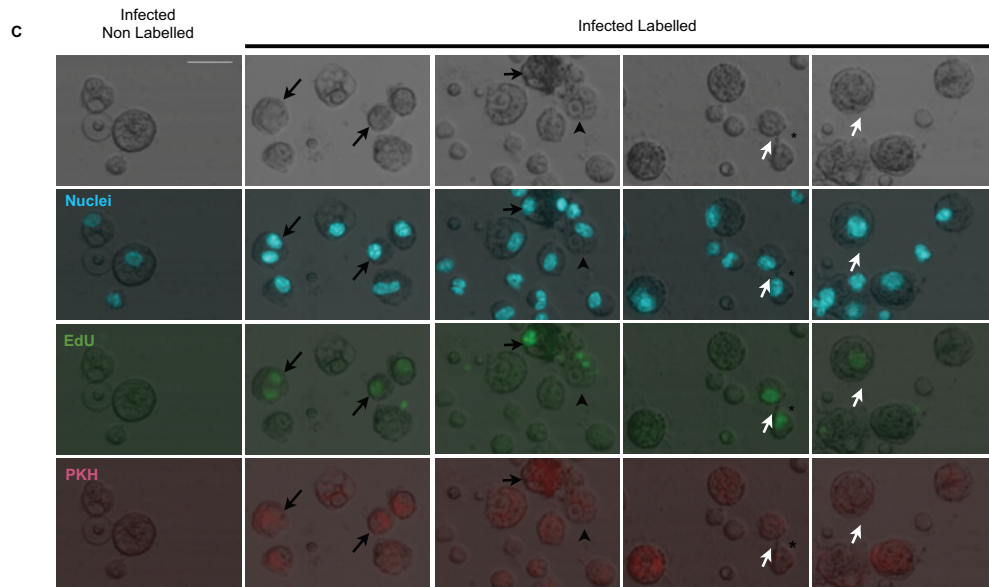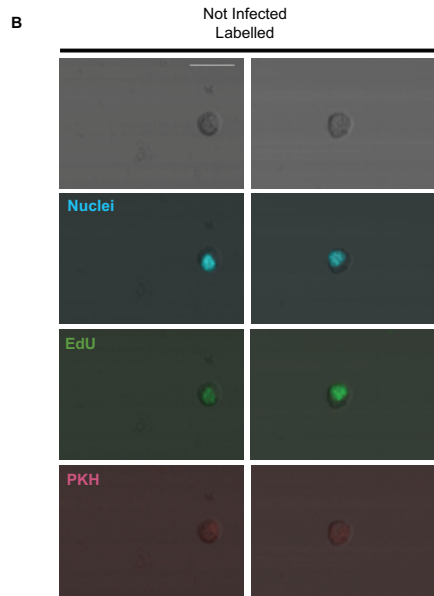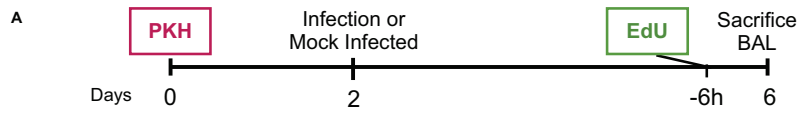
A suspension of PKH was administered to mice. Blood, bone marrow and alveolar macrophages from BAL were collected 2 and 6 d post PKH injection (Fig. 7A). At both time intervals only BAL cells showed PKH staining. PKH + cells constituted 30-50% of the recovered population with 15% being very brightly stained (Table 1). For mice that were intratracheally infected with Cn only BAL cells had PKH + staining. Due to infection there is a massive immune infiltration into the bronchoalveolar space leading to a decrease in the percentage of PKH+ cells to 4-20%. These cells could be assumed to be AM. However the absolute number of PKH + cells was higher in infected mice. The reason for this discrepancy is unknown. In our view this could be due to PKH labeling lung macrophages, other than AM. These cells could infiltrate the bronchoalveolar space in response to infection or, alternatively, infection could change adhesion characteristics of AM allowing higher recovery of AM. Other explanations are also possible. Consequently we caution the interpretation of PKH as an AM label in the setting of infection and inflammation.

To study proliferation mice were administered EdU 4 d post infection (or mock infection with sterile PBS). Mice were sacrificed 6 h later and BAL performed. We estimate that we imaged 1/20 and 1/60 of the recovered BAL cells, for mock-infected and infected mice, respectively. In mock infected mice (steady state conditions) we found 1-4 EdU+ cells per mouse (Table 1 and Figure 7B). In Cn-infected mice we found 13-18 events per mouse and of these only 1-2 were were double positive PKH+ Edu+ (Table 1 and Figure 7C). These results

show that AM in non-infected mice proliferate, suggesting that resident macrophage proliferation plays a role in tissue homeostasis. Furthermore AM proliferation was found in the cells recovered from the bronchoalveolar space after Cn infection. The rates of division seem to not be altered in the infected mice, although the low number of events does not allow us to make definitive conclusions.

Figure 7. Alveolar macrophage (AM) proliferation *in vivo*. (see next page)

Macrophages in the bronchoalveolar space replicated both in steady state and in the context of intratracheal Cn infection. A) Timeline of the experiment. PKH was administered to mice to label AM macrophages, 2 days before mice were infected with Cn strain 24067 intratracheally. Mock infected mice (sterile PBS) and infected mice were administered EdU to label cells in S phase at day 4 and 6 h later mice were sacrificed and bronchoalveolar lavage (BAL) performed. B) Representative image of alveolar macrophage replication recovered in a mock infected mice. C) Representative images of BAL recovered cells from mice Cn infected. First column displays cells from non labeled mouse. Following columns show cells from labeled mice. Alveolar macrophages (PKH positive) can incorporate EdU (arrows). Cells with macrophage morphology but PKH - can also incorporate EdU (open arrows). Note that one of the macrophages initiating replication has ingested Cn (arrowheads) and adjacent positive cells suggestive of recently completed mitosis (∗). See Table 1 for the frequency of events. Scale bars represent 20 μm. Experiment was repeated three times with 2-4 mice per group and representative images are shown.

A

PKH — Infection or Mock Infected — EdU — Sacrifice BAL

Days: 0 2 -6h 6

B

Not Infected Labelled

Nuclei

EdU

PKH

C

Infected Non Labelled — Infected Labelled

Nuclei

EdU

PKH

79

Discussion

This study established the usefulness and adaptability of LSC for the study of macrophage-fungal interactions. Microscopy protocols usually require a significant amount of operator input, both in the acquisition of images and analysis of those. LSC automates data acquisition but more importantly it allowed for automated and quantitative data analysis (11, 33, 37). LSC was shown to be comparable to human counting for measuring phagocytosis and provides significant advantages that were exploited for the study of the relationship of phagocytosis and cell cycle progression. LSC allows the use of images to quantify DNA content, in other words, to study cell cycle in adherent cells and correlate it with intracellular processes (6, 22). Hence, LSC allowed us to study cell cycle alterations induced by phagocytosis of Cn by murine macrophages.

Previous results from our lab showed that FcγR-mediated ingestion of yeast cells was associated with increased cell cycle progression (18, 20, 21). Both complement-mediated Cn phagocytosis and ingestion of inert latex beads were also effective at stimulating cell cycle progression (21). These effects could be reproduced using a model of frustrated phagocytosis mediated by FcγR (20), whereby continuous stimulation of receptors without particle ingestion triggered cell cycle progression and allowed dissection of signaling pathways involved in the proliferative response. It is known that macrophages could divide after Cn ingestion and even divide after non-lytic exocytosis (3, 23), but there has been no study of how macrophage replication is affected by Cn ingestion. Later work showed that ingestion of live yeast cells, but not latex beads, inhibited cyclin D1 expression (18), producing an apparent paradox, not resolved in their work. Cyclin D1 is a major checkpoint in the transition from G1 to S phase and cyclin D1 expression is inhibited in response to LPS, triggering mitotic arrest (35). In addition, there is evidence that cell cycle phase influences macrophage behavior: cell cycle arrest in G1 influences MHC class II expression (39) or prevents LPS induced apoptosis (40).

In this study, we have revisited this problem using LSC. Our experiments confirmed cell cycle progression in both J774.16 cells and primary macrophages using LSC. However, LSC provided additional information into this phenomenon by establishing that the likelihood of the effect increased with increasing intracellular fungal burden. Furthermore, cell cycle progression was observed after ingestion of Live and HK Cn, demonstrating that cell cycle progression does not require fungal viability, but is a consequence of FcγR activation and subsequent phagocytosis (20). DNA content quantification and a pulse labeling strategy revealed a reduction in the number of cells that cycled back into G1 phase, suggesting that macrophage-like cells containing Cn were less likely to complete mitosis, or, in other words, were arrested at G2/M phase of cell cycle. Pulse labeling experiments could not be performed in primary cells due to longer replication times, but when primary cells

were treated with IFN-γ, which is known to produce cell cycle arrest in dividing cells, we observed that phagocytosis was associated with an initial cell cycle progression that proceeded to arrest in G2/M. We conjectured that cell division impairment could be a consequence of fungal mediated host cell damage or a by-product of the macrophage's attempt to degrade a high load of large foreign particles. It is know that the phagosome of macrophages becomes permeabilized after Cn infection (34) and it is conceivable that the spill of phagosomal contents into the cytoplasm produces damage that translates into cell cycle arrest. Consequently, we explored several potential mechanisms of macrophage damage. Analysis of TUNEL staining and of membrane permeability in both J774.16 and BMDM cells revealed that neither of these mechanisms was likely the responsible for cell cycle arrest. We considered the possibility that the mitotic defect was a consequence of a fungal product analogous to bacterial cyclomodulins (27), which are known to provoke cell cycle arrest, alter DNA content or nuclear morphology. However we found no evidence of such an effect in our experiments. In this regard we note that taxol prevents mitosis by stabilizing cytoskeletal microtubules and that Cn has been reported to interfere with host cell cytoskeleton (7, 19). We conclude that despite Cn phagocytosis causing macrophages to progress in cell cycle, the yeast cells produced toxic effects that had widespread effects in the host cell cycle, resulting in G2/M phase arrest (this work) and cyclin D1 inhibition (18). Defining the mediator of the cell cycle interference remains an outstanding question for future studies.

In this study, we made the unexpected but relevant observation was that IFN-γ- and LPS-mediated cell cycle arrest could be overcome by phagocytosis-derived cell cycle progression. Both IFN-γ and LPS are known to arrest cell division in the presence of M-CSF (36, 40). This observation raised the possibility that microbial ingestion and macrophage effector functions *in vivo* in conditions where IFN-γ is made do not necessarily lead to cell cycle arrest. Further, macrophages might respond to infection in a way similar to other types of immune cells that undergo clonal expansion to generate additional effector cells to fight infection. We note that an increase in the proliferative ability of alveolar macrophages was reported in humans, following exposure to asbestos or in chronic inflammatory disorders (4, 31) and mice exposed to cigarette smoke (12).

To date, replication of alveolar macrophages *in vivo* has not been definitively established given the difficulties of distinguishing between resident alveolar macrophages and the infiltrating inflammatory cells by standard methods. A very recently published study reported macrophage proliferation in response to infection in the peritoneal and pleural cavity after an inflammatory stimulus (15). These studies were quickly followed by reports of macrophage proliferation in other experimental models: zymosan-induced peritonitis (9) and autoimmune encephalitis (1). Given that Cn establishes chronic pulmonary infection, we attempted to search for alveolar macrophage proliferation in a mouse model of cryptococcal pneumonia. Consequently, we

developed a double labeling strategy to investigate the problem of AM replication in the presence and absence of Cn infection. Our labeling strategy took advantage of the relative specificity of PKH for AM and EdU for replicating cells (24, 28). Our results demonstrated synthesis of new DNA in alveolar macrophage in both infected and non-infected mice. Both the resident population and the newly arrived blood derived macrophages incorporated EdU and showed features of mitotic division. This observation provides an important confirmation of the Jenkins *et al* report (15). Our results, albeit in a different model, suggest that macrophage proliferation occurs in the bronchoalveolar space after Cn infection, as reported in macrophages from other tissues (1, 9, 15). Furthermore we show that the resident alveolar macrophage population is capable of proliferation as part of normal tissue homeostasis, meaning in the absence of any infection. We were unable to demonstrate an increased rate of alveolar macrophage replication *in vivo* as a consequence of Cn infection. One explanation for the low rate of replication *in vivo* could be impairment of mitosis completion, meaning that what we observed *in vitro* for Cn-containing macrophages also occurs *in vivo*. Hence, it is conceivable that the rate of lung macrophage proliferation would be higher in other inflammatory conditions where there is not mitotic arrest, such as the presence of inert particles in the lungs (4, 31) or the inhalation of cigarette smoke (12). Proliferation of alveolar macrophages occurred at a low rate in the presence and absence of infection but is likely to make only a small contribution to inflammatory cell numbers during pulmonary cryptococcosis. Our observations can also be integrated with the recent report that upon resolution of lung infection newly recruited cells die by apoptosis while leaving PKH labeled resident alveolar macrophages untouched (14). Interpretation of our data in conjunction with the aforementioned works (1, 9, 15) suggests that resident macrophage numbers are supported by both local proliferation and the infiltration of new cells. In the event of an injury or inflammation the equilibrium between these processes is changed until a new equilibrium is established.

In summary, LSC confirmed that macrophage-like cells progressed in cell cycle after phagocytosis, as reported earlier (21), and allowed us to explore this process in significantly greater detail. We now report that despite increased cell cycle progression there completion of mitosis is less efficient, possibly as a result of phagocytosis dependent toxicity after ingestion of large microbial particles. Furthermore, we observed that phagocytosis of Cn is sufficient to suppress IFN-γ and LPS cell cycle arrest. Lastly, we established a protocol to study proliferation of resident phagocytic cells *in vivo* which allowed us to demonstrate that resident AM are capable of proliferation, both as part of tissue homeostasis and of the inflammatory process. These enhance our understanding of macrophage biology in the setting of phagocytosis and Cn infection.
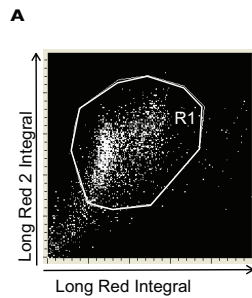
Supplemental Figures

A

Table 1. Accuracy of macrophage identification by LSC and a human operator

Well #	Macrophage Events		R1 Macrophage	
	LSC	Operator[b]	LSC	Operator[b]
1	100	89	84	100
2	100	78	84	94
3	100	96	89	97
4	100	97	86	97
5	100	95	84	96
Mean ± SD		91 ± 7	85 ± 2	96 ± 2

[a]Count of cells present in each of the categories, as identified by LSC, for a total of 100 macrophages per well. [b] % accurate values, measured by human operator observing LSC images.

B
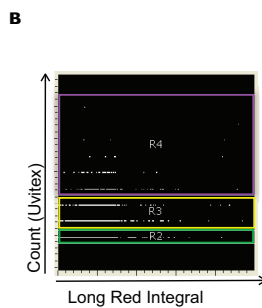
Table 2. Accuracy of number of ingested yeast cells by LSC and a human operator

Well #	No yeasts		1 yeast		2 yeasts		1-2 Yeasts		>3 Yeasts	
	LSC[a]	Correct[b]	LSC[a]	Correct[b]	LSC[a]	Correct[b]	LSC[a]	Correct[b]	LSC[a]	Correct[b]
1	40	93	21	90	6	50	27	81	5	80
2	36	94	21	76	2	50	23	96	8	75
3	32	97	25	96	17	100	42	95	3	100
4	27	93	24	92	13	77	37	86	5	60
5	21	86	22	86	13	85	35	91	8	100
Mean ± SD	31 ± 7	92 ± 4	23 ± 2	88 ± 8	10 ± 6	72 ± 21	33 ± 8	90 ± 6	6 ± 2	83 ± 17

[a]Count of cells present in each of the categories, as identified by LSC, for a total of 100 macrophages per well. [b] % accurate values, measured by human operator observing LSC images.

Supplemental Figure 1. Accuracy of LSC identification.

A) Macrophage Identification. Scatter plot of Macrophage events leads to definition of a region (in analogy to Flow Citometry) where the majority of macrophages will be located. Counts are displayed in Table 1. B) Fungal Burden Quantification. Number of Uvitex events inside each macrophage were divided into categories and translated into color coded boxes: Zero Yeasts, Green; One or Two Yeasts, Yellow and More than Three, Magenta, allowing verification of software identification. Counts are displayed in Table 2. LSC could distinguish up to 10 yeasts cells ingested by a macrophage cell but for our experimental conditions definition of 2 categories was sufficient.

A
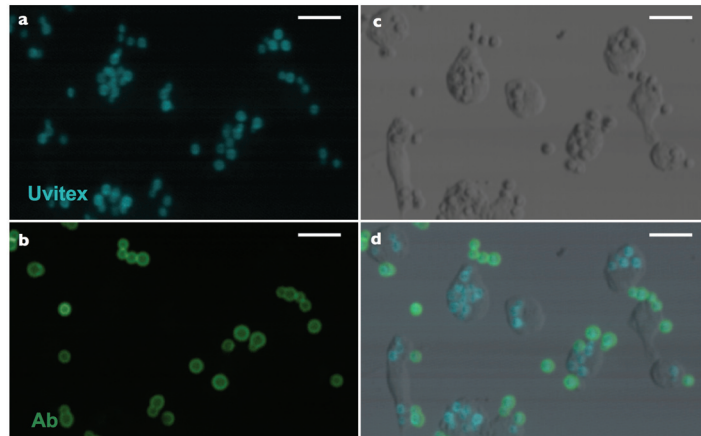
B

Table 3. Comparison between using Uvitex staining alone or combined with Immunostaining (Ab)

Uvitex + Ab

Uvitex + Ab

Uvitex + Ab

Well #	No yeasts		1-2 Yeasts		>3 Yeasts	
	Uvitex	Uvitex+Ab	Uvitex	Uvitex+Ab	Uvitex	Uvitex+Ab
Phagocytosis 2 h						
1	16	15	23	22	62	63
2	26	25	40	40	34	35
3	20	20	37	38	43	42
4	16	17	38	39	45	44
5	17	17	37	39	45	44
Mean ± SD	19 ± 4	19 ± 4	35 ± 7	36 ± 8	46 ± 10	46 ± 10
Phagocytosis 15 min						
1	19	34	36	39	45	27
2	12	36	30	36	58	27
3	5	24	18	39	77	37
4	17	37	37	42	46	21
5	34	49	42	38	24	13
Mean ± SD	17 ± 11	36 ± 9*	32 ±9	39 ± 28*	50 ±19	25 ± 9*
Incubation at 4ºC No phagocytosis						
1	73	99	22	1	5	0
2	91	99	8	1	1	0
3	95	100	5	0	0	0
4	86	100	13	0	2	0
5	66	94	26	6	7	0
Mean ± SD	82 ± 12	98 ± 2*	15 ±9	2 ± 2*	3 ±3	0 ± 0*

* $p < 0.05$, Two-tailed Student t-test for paired observations, 95% confidence interval.

Distinction between internalized and adhered Cn can be made by combining Uvitex with Immunostaining. Extracellular Cn will stain with Uvitex and Alexa 488 conjugated antibody to recognize capsule bound opsonin. A) Illustrative images of staining strategy: a) Uvitex staining of total Cn; b) Extracellular Cn using capsular immunostaing; c) Brightfield image of the same field and d) Merge of three previous images. Scale bars represent 20 μm. B) Illustrative images showing differentially stained Cn to test reliability of phagocytic quantification using Uvitex alone (Uvitex) or Uvitex combined with Immunostaining (Uvitex+Ab) in three different conditions. Images are a merge of Uvitex (cyan), Immunostaining (green) and Brightfield (grey). Arrow points to bound Cn and arrowheads points to ingested Cn. Scale bars represent 10 μm. Counts are displayed in Table 3.
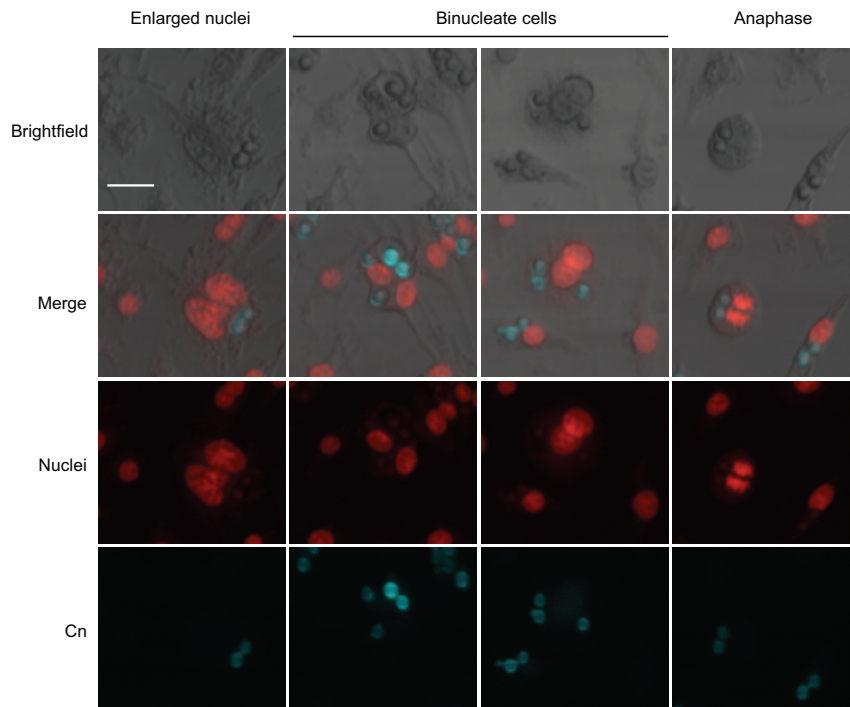
Supplemental Figure 3. Nuclear morphology of BMDM infected with Cn.

Nuclear morphology of BMDM infected with Cn did not display significant changes from uninfected wells. Binucleate cells and nuclei enlargement were found but those events were rare and could not be quantified above the non infected wells (not shown). Mitotic figures were also observed. Experiments were repeated at least 4 times with triplicate wells for each condition. Original magnification 40x at 0.5 μm resolution. Scale bar represents 20 μm.

Tables

Table 1. Alveolar Macrophages incorporation of EdU *in vivo*

Not infected		Total cells [a]	PKH+ (%)	EdU+	PKH+ EdU+
Experiment 1					
Mouse #	1	63	35 (55%)	1	1
	2	134	46 (34%)	2	2
Experiment 2					
Mouse #	1	178	55 (30%)	1	1
	2	209	41 (30%)	4	2

[a]Analyzed cells correspond to 1/20 of the BAL recovered cells.

Cn infected		Total cells [a]	PKH+ (%)	EdU+ [b]	PKH+ EdU+
Experiment 1					
Mouse #	1	4730	205 (4%)	16	1
	2	2787	663(23%)	8	2
Experiment 2					
Mouse #	1	875	191(22%)	13	2
	2	1896	181(10%)	13	1
	3	3539	751 (21%)	15	2
	4	2817	574 (20%)	18	2

[a]Analyzed cells correspond to 1/60 of the BAL recovered cells.

[b]Edu+ PKH- cells are of unknown origin.

References

1. **Ajami, B., J. L. Bennett, C. Krieger, K. M. McNagny, and F. M. Rossi.** 2011. Infiltrating monocytes trigger EAE progression, but do not contribute to the resident microglia pool. Nat Neurosci **14:**1142-9.

2. **Alvarez, M., T. Burn, Y. Luo, L. A. Pirofski, and A. Casadevall.** 2009. The outcome of Cryptococcus neoformans intracellular pathogenesis in human monocytes. BMC Microbiol **9:**51.

3. **Alvarez, M., and A. Casadevall.** 2006. Phagosome extrusion and host-cell survival after Cryptococcus neoformans phagocytosis by macrophages. Curr Biol **16:**2161-5.

4. **Bitterman, P. B., L. E. Saltzman, S. Adelberg, V. J. Ferrans, and R. G. Crystal.** 1984. Alveolar macrophage replication. One mechanism for the expansion of the mononuclear phagocyte population in the chronically inflamed lung. J Clin Invest **74:**460-9.

5. **Casadevall, A., W. Cleare, M. Feldmesser, A. Glatman-Freedman, D. L. Goldman, T. R. Kozel, N. Lendvai, J. Mukherjee, L. A. Pirofski, J. Rivera, A. L. Rosas, M. D. Scharff, P. Valadon, K. Westin, and Z. Zhong.** 1998. Characterization of a murine monoclonal antibody to Cryptococcus neoformans polysaccharide that is a candidate for human therapeutic studies. Antimicrob Agents Chemother **42:**1437-46.

6. **Chakraborty, A. A., and W. P. Tansey.** 2009. Inference of cell cycle-dependent proteolysis by laser scanning cytometry. Exp Cell Res **315:**1772-8.

7. **Chen, S. H., M. F. Stins, S. H. Huang, Y. H. Chen, K. J. Kwon-Chung, Y. Chang, K. S. Kim, K. Suzuki, and A. Y. Jong.** 2003. Cryptococcus neoformans induces alterations in the cytoskeleton of human brain microvascular endothelial cells. J Med Microbiol **52:**961-70.

8. **Darzynkiewicz, Z., F. Traganos, H. Zhao, H. D. Halicka, and J. Li.** 2011. Cytometry of DNA replication and RNA synthesis: Historical perspective and recent advances based on "click chemistry". Cytometry A **79:**328-37.

9. **Davies, L. C., M. Rosas, P. J. Smith, D. J. Fraser, S. A. Jones, and P. R. Taylor.** 2011. A quantifiable proliferative burst of tissue macrophages restores homeostatic macrophage populations after acute inflammation. Eur J Immunol **41:**2155-64.

10. **Feldmesser, M., Y. Kress, P. Novikoff, and A. Casadevall.** 2000. Cryptococcus neoformans is a facultative intracellular pathogen in murine pulmonary infection. Infect Immun **68:**4225-37.

11. **Henriksen, M., B. Miller, J. Newmark, Y. Al-Kofahi, and E. Holden.** 2011. Laser scanning cytometry and its applications: a pioneering technology in the field of quantitative imaging cytometry. Methods Cell Biol **102:**161-205.

12. **Hornby, S. B., and J. P. Kellington.** 1990. DNA synthesis in alveolar macrophages and other changes in lavaged cells following exposure of CBA/H mice to cigarette smoke. Environ Health Perspect **85:**107-12.

13. **Ieong, M. H., C. C. Reardon, S. M. Levitz, and H. Kornfeld.** 2000. Human immunodeficiency virus type 1 infection of alveolar macrophages impairs their innate fungicidal activity. Am J Respir Crit Care Med **162:**966-70.

14. **Janssen, W. J., L. Barthel, A. Muldrow, R. E. Oberley-Deegan, M. T. Kearns, C. Jakubzick, and P. M. Henson.** 2011. Fas Determines Differential Fates of Resident and Recruited Macrophages During Resolution of Acute Lung Injury. Am J Respir Crit Care Med.

15. **Jenkins, S. J., D. Ruckerl, P. C. Cook, L. H. Jones, F. D. Finkelman, N. van Rooijen, A. S. MacDonald, and J. E. Allen.** 2011. Local macrophage proliferation, rather than recruitment from the blood, is a signature of TH2 inflammation. Science **332:**1284-8.

16. **Kamentsky, L.** 2001. Laser scanning cytometry. Methods Cell Biol.

17. **Kechichian, T. B., J. Shea, and M. Del Poeta.** 2007. Depletion of alveolar macrophages decreases the dissemination of a glucosylceramide-deficient mutant of Cryptococcus neoformans in immunodeficient mice. Infect Immun **75:**4792-8.

18. **Luo, Y., and A. Casadevall.** 2010. Intracellular cryptococci suppress Fc-mediated cyclin D1 elevation. Commun Integr Biol **3:**390-1.

19. **Luo, Y., B. M. Isaac, A. Casadevall, and D. Cox.** 2009. Phagocytosis inhibits F-actin-enriched membrane protrusions stimulated by fractalkine (CX3CL1) and colony-stimulating factor 1. Infect Immun **77:**4487-95.

20. **Luo, Y., J. W. Pollard, and A. Casadevall.** 2010. Fcgamma receptor cross-linking stimulates cell proliferation of macrophages via the ERK pathway. J Biol Chem **285:**4232-42.

21. **Luo, Y., S. C. Tucker, and A. Casadevall.** 2005. Fc- and complement-receptor activation stimulates cell cycle progression of macrophage cells from G1 to S. J Immunol **174:**7226-33.

22. **Luther, E., and L. A. Kamentsky.** 1996. Resolution of mitotic cells using laser scanning cytometry. Cytometry **23:**272-8.

23. **Ma, H., J. E. Croudace, D. A. Lammas, and R. C. May.** 2006. Expulsion of live pathogenic yeast by macrophages. Curr Biol **16:**2156-60.

24. **Maus, U., S. Herold, H. Muth, R. Maus, L. Ermert, M. Ermert, N. Weissmann, S. Rosseau, W. Seeger, F. Grimminger, and J. Lohmeyer.** 2001. Monocytes recruited into the alveolar air space of mice show a monocytic phenotype but upregulate CD14. Am J Physiol Lung Cell Mol Physiol **280:**L58-68.

25. **Mosser, D. M., and J. P. Edwards.** 2008. Exploring the full spectrum of macrophage activation. Nat Rev Immunol **8:**958-69.

26. **Murphy, J., R. Summer, A. A. Wilson, D. N. Kotton, and A. Fine.** 2008. The prolonged life-span of alveolar macrophages. Am J Respir Cell Mol Biol **38:**380-5.

27. **Nougayrede, J. P., F. Taieb, J. De Rycke, and E. Oswald.** 2005. Cyclomodulins: bacterial effectors that modulate the eukaryotic cell cycle. Trends Microbiol **13:**103-10.

28. **Osterholzer, J. J., G. H. Chen, M. A. Olszewski, Y. M. Zhang, J. L. Curtis, G. B. Huffnagle, and G. B. Toews.** 2011. Chemokine receptor 2-mediated accumulation of fungicidal exudate macrophages in mice that clear cryptococcal lung infection. Am J Pathol **178:**198-211.

29. **Osterholzer, J. J., J. E. Milam, G. H. Chen, G. B. Toews, G. B. Huffnagle, and M. A. Olszewski.** 2009. Role of dendritic cells and alveolar macrophages in regulating early host defense against pulmonary infection with Cryptococcus neoformans. Infect Immun **77:**3749-58.

30. **Spector, W. G., and K. M. Wynne.** 1976. Proliferation of macrophages in inflammation. Agents Actions **6:**123-6.

31. **Spurzem, J. R., C. Saltini, W. Rom, R. J. Winchester, and R. G. Crystal.** 1987. Mechanisms of macrophage accumulation in the lungs of asbestos-exposed subjects. Am Rev Respir Dis **136:**276-80.

32. **Tarling, J. D., H. S. Lin, and S. Hsu.** 1987. Self-renewal of pulmonary alveolar macrophages: evidence from radiation chimera studies. J Leukoc Biol **42:**443-6.

33. **Telford, W. G., A. Komoriya, and B. Z. Packard.** 2002. Detection of localized caspase activity in early apoptotic cells by laser scanning cytometry. Cytometry **47:**81-8.

34. **Tucker, S. C., and A. Casadevall.** 2002. Replication of Cryptococcus neoformans in macrophages is accompanied by phagosomal permeabilization and accumulation of vesicles containing polysaccharide in the cytoplasm. Proc Natl Acad Sci U S A **99:**3165-70.

35. **Vadiveloo, P. K.** 1999. Macrophages--proliferation, activation, and cell cycle proteins. J Leukoc Biol **66:**579-82.

36. **Vadiveloo, P. K., E. Keramidaris, W. A. Morrison, and A. G. Stewart.** 2001. Lipopolysaccharide-induced cell cycle arrest in macrophages occurs independently of nitric oxide synthase II induction. Biochim Biophys Acta **1539:**140-6.

37. **Wojcik, E., S. Saraga, J. Jin, and J. Hendricks.** 2001. Application of laser scanning cytometry for evaluation of DNA ploidy in routine cytologic specimens. Diagn Cytopathol **24:**200-205.

38. **Xaus, J., M. Cardo, A. F. Valledor, C. Soler, J. Lloberas, and A. Celada.** 1999. Interferon gamma induces the expression of p21waf-1 and arrests macrophage cell cycle, preventing induction of apoptosis. Immunity **11:**103-13.

39. **Xaus, J., M. Comalada, M. Barrachina, C. Herrero, E. Gonalons, C. Soler, J. Lloberas, and A. Celada.** 2000. The expression of MHC class II genes in macrophages is cell cycle dependent. J Immunol **165:**6364-71.

40. **Xaus, J., M. Comalada, A. F. Valledor, J. Lloberas, F. Lopez-Soriano, J. M. Argiles, C. Bogdan, and A. Celada.** 2000. LPS induces apoptosis in macrophages mostly through the autocrine production of TNF-alpha. Blood **95:**3823-31.

41. **Zaragoza, O., M. Alvarez, A. Telzak, J. Rivera, and A. Casadevall.** 2007. The relative susceptibility of mouse strains to pulmonary Cryptococcus neoformans infection is associated with pleiotropic differences in the immune response. Infect Immun **75:**2729-39.

42. **Zbigniew Darzynkiewicz, E. H., Alberto Orfao, William G. Telford, and Donald Wlodkowic.** 2011. Recent Advances in Cytometry, Part A: Instrumentation, Methods, 5th ed, vol. 102. AP Publishers.Tables

Chapter 3

_____

The interaction of *Cryptococcus neoformans* with murine macrophages results in mitochondrial damage

Abstract

Cryptococcus neoformans (Cn) is a human fungal pathogen that is the causative agent of cryptococcosis. Human infection is acquired by inhalation of infectious particles, which deposits in host lungs. Thus, alveolar macrophages are likely to be the first line of immune defense and in fact, macrophages are crucial for the host immunity against cryptococcosis. However, macrophages display little ability to kill Cn *in vitro*. Moreover, ingestion of Cn leads to macrophage death in 24 to 48 h. Recently, we showed that infection with Cn induces early progression of the macrophage cell cycle that is subsequently followed by mitotic arrest. To understand the pathways of macrophage damage after Cn phagocytosis, we measured activation of death effector molecules. Both cell proliferation and death are tightly regulated cellular events that are often dependent on mitochondrial function, which has led us to evaluate the macrophage mitochondrial modulation during cryptococcal infection. The interaction of Cn with macrophages resulted in caspase activation, depolarization of mitochondria and a decrease in intracellular ATP. Macrophage Cn infection was associated with release of mitochondrial mediators of death. These results provide evidence that Cn intracellular residence interferes with host mitochondrial function. Macrophage mitochondrial damage could contribute to the pathogenesis of cryptococcal infection by undermining the health of this critical host defense cell.

Introduction

The outcome of the interaction of the human pathogenic fungus *Cryptococcus neoformans* (Cn) with macrophages is thought to be a critical event in the course of cryptococcal infection (1-8). Cn is a facultative intracellular pathogen and its interaction with macrophages can lead to intracellular replication and outcomes that range from host cell lysis to non-lytic exocytosis (9-11). Previous work has demonstrated that the yeast causes damage to cellular processes: lysosomes become permeable (1), cyclin D1 is inhibited (12), and non-lytic exocytosis is followed by the formation of large residual vacuoles (13). The capsule of Cn and its main components glucuronoxylomannan (GXM) and galactoxylomannan (GalXM) also mediate cell damage (14-17), causing LDH release in epithelial cells, cell death, with inhibition of caspase-3, in macrophages and activation of caspase-8 in T cells. In particular, GXM was reported to cause mitochondrial depolarization and apoptosis in peritoneal macrophages (14).

Cellular death can proceed either by Necrosis or Programmed Cell Death (PCD) (18). Necrosis is instantaneous and inflammatory, while PCD is tightly regulated. The first described PCD was apoptosis (19). Caspases are the effector molecules of apoptosis (20). Death receptor ligation activates initiator caspase-8 in the extrinsic apoptotic pathway. Cellular damage activates initiator caspase-9 for the intrinsic pathway of apoptosis. In some cells, death receptor activation of caspase-8, requires an extra step of mitochondrial outer membrane permeability, which is sensed as intracellular damage and results in the activation of caspase-9 (21). However, they all converge into activation of effector caspase-3. Extensive crosstalk exists between both pathways of apoptosis. Other types of PCD have been recently described. These share morphological characteristics of necrosis and apoptosis. As such, their classification relies on identification of the effector molecule (18). Cells are believed to die by necroptosis when there is: 1) not enough ATP for apoptosis; 2) impairment of caspase activation; and 3) an overall need to release inflammatory signals (22). For example, inhibition of caspases after ligation of death receptors, results in necroptosis through Receptor Interacting Kinases (RIP) - necroptosis (18). RIP-Necroptosis is activated by the same factors as extrinsic apoptosis: TNF, FasL and their adaptor molecules (23). RIP mediates dissipation of mitochondrial potential, leading to mitochondrial failure and cell death. A distinct pathway is activated in response to DNA damage. Activation of Poly(ADP)ribose-polymerase (PARP), causes leakage of mitochondrial Apoptosis Inducing Factor (AIF) to the cytosol and has been called parthanatos. AIF translocates to the nucleus where it mediates DNA fragmentation (21, 22, 24). The exact mechanism of AIF leakage into the cytosol is under discussion (24). Of special interest to immunity is pyroptosis, whose hallmark is activation of caspase-1, which in turn activates several cytokines: Il-1β, Il-18 and to a smaller extent IFN-γ and TNF-α (25-27), and culminates in a cell death where cellular permeability occurs at a very early stage. One of the major activators of caspase-1 is the inflammasome (26). To date the mechanisms of host cell death in cryptococcal infection have not been investigated in detail.

Most of pathways described here have one mitochondrial step. In fact, mitochondria occupy a central role in the molecular pathways of death and are an integration center for cell death or survival decisions. In immunity, they can be producers of reactive oxygen species (28) and major activators of the inflammasome (29, 30). Viral, bacterial and protozoan pathogens have a myriad of factors that manipulate host cell mitochondria (31, 32) but no comparable information is available for fungal pathogens.

Recently, we established that phagocytosis of Cn by murine macrophages leads macrophages into cell cycle progression, but ultimately the process results in cell cycle arrest for the majority of cells (33). The mechanism for cell cycle arrest has not been characterized in detail but may involve aneuploidy (34). Different mechanisms of death can influence the immunological outcome (35) and pathogens have multiple strategies to manipulate host cell death (36). In this work, we have investigated the mechanism of macrophage injury after Cn infection.

Our results indicate Cn phagocytosis is accompanied by mitochondrial modulation that could promote or accompany host cell damage.

Materials and Methods

Fungal strains.

C. neoformans var. *grubii* strain H99 (serotype A), Superoxide dismutase (SOD) mutant (ΔSOD1) and reconstituted strain (sod1rec) were a kind gift of Dr. John Perfect (Durham, NC). Acapsular mutant cap59 and original wild-type K99 were a kind gift of Joseph Heitman (Durham, NC). Yeast cells for infection were grown for 2 d in Sabouraud dextrose broth (Difco, Carlsbad, California) at 37°C.

Macrophage cells.

Three types of macrophages were used in parallel for most experiments: the macrophage-like murine cell line J774.16, Bone Marrow Derived Macrophages (BMDM) and peritoneal macrophages.

J774.16 were kept in media consisting of Dulbecco's minimal essential medium (DMEM) (CellGro, Mediatech, Manassas, Virginia, USA), 10% NCTC-109 Gibco medium (LifeTechnologies, Grand Island, NY), 10% heat-inactivated FCS (Atlanta Biologicals, Lawrenceville, Georgia, USA), and 1% non-essential amino acids (CellGro, Mediatech, Manassas, Virginia, USA).

BMDM were obtained by extracting bone marrow from hind leg bones of 6-8 weeks BALB/C female mice (National Cancer Institute, Bethesda, Maryland, USA) and maturing them in vitro for 6-8 d. Briefly, mice were killed by CO_2 asphyxiation and bone marrow cells were harvested. The harvested cells were cultured at 37°C with 5% CO_2 in DMEM media with 20% L-929 cell conditioned media, 10% fetal bovine serum, 2 mM L-glutamine (CellGro, Mediatech, Manassas, Virginia, USA), 1% non-essential amino acids (CellGro, Mediatech, Manassas, Virginia, USA), 1% HEPES buffer (CellGro, Mediatech, Manassas, Virginia, USA) and β-mercaptoethanol (Gibco, Carlsbad, California, USA).

Peritoneal macrophages were extracted by injecting 10 mL of ice-cold PBS into mice peritoneal cavity, with gentle massage. Cells were seeded and cultured overnight in the same media as J774.16 macrophages.

All animal experiments were conducted according to ethical guidelines, with the approval of the Institutional Animal Care and Use Committee (IACUC) of Albert Einstein College of Medicine.

In vitro phagocytosis, killing and caspase activation assays

Laser Scanning Cytometry experiments were performed as described previously (33). Macrophages were plated to achieve a density of 1 x10^5 /mL at time of infection, in all assays. Cn were added at a Multiplicity of Infection (MOI) of 1:2 (unless otherwise noted) along with capsular monoclonal antibody (mAb) 18B7 (37) at 10 μg/mL as an opsonin. For some experiments Cn was heat-killed (HK Cn) by incubating at 60°C for 60 min. Phagocytosis was allowed to proceed for the indicated time at 37°C under 5% CO_2 atmosphere. For fungal killing assays cells were detached by vigorous pipetting and diluted in sterile PBS onto Saboraud plates. Colony Forming Units (CFU) were counted after 2 d at 30°C. Specific caspase activity was detected using a Fluorochrome Inhibitor of Caspases (FLICA) (Immunochemistry Technologies, LLC, Bloomington, MN, USA) assay, by following manufacturer's instructions. Carboxyfluorescein-labeled inhibitor peptide was added 1 h before the termination of phagocytosis. At the termination of phagocytosis, cells were washed twice with wash buffer and incubated for 5 min with 0.1 μg/mL of Hoechst and 12.5 μg/mL of Propidium Iodide for detection of necrotic/ late apoptotic cells. Cells were then fixed with the provided fixative and analyzed immediately. After analysis, cells were permeabilized with methanol and stained for analysis of phagocytosis. Briefly, macrophage

cytoplasm and nuclei was stained with Wheat Germ Agglutinin (WGA) conjugated to Alexa 633 (LifeTechnologies, Grand Island, NY) at 10 μg/mL and 5 μg/mL of Propidium Iodide and yeast cells were stained with 0.1 μg/mL of Uvitex 2B (Polysciences, Inc, Warrington, PA, USA). Images obtained with caspases inhibitors were merged to post fixation images to allow analysis of caspase activation and correlation with phagocytic events.

Caspase activation was measured by imaging 20-40 fields in each well with the 40x objective at 0.5 μm resolution, allowing a field size of 500 μm x 192 μm. Some fields were imaged with 60x objective at 0.15 μm resolution, for illustration purposes.

Images were obtained in the iCys® Research Imaging Cytometer (CompuCyte Corporation, Westwood, Massachusetts, USA). Instrument control, data acquisition and analysis were performed using the software the iCys Cytometric Analysis Software®.

ATP and Yeast Killing measurements

ATP contents and Lactate dehydrogenase (LDH) release can be used to estimate cell numbers, and cellular viability. Total cell ATP measurements were performed by adding equal volumes of cell ATP extraction reagent: Triton-X100 at 0.25% (Sigma-Aldrich, St. Louis, MO) and 2 mM EDTA (Sigma-Aldrich, St. Louis, MO) to the wells containing cells. Next, 25 μl of this extract was incubated with Enliten ATP assay system (Promega, Madison, WI) and counts per second (CPS) measured in a standard luminometer. In parallel, macrophages were disrupted by vigorous pipetting and supernatants were diluted to count Colony Forming Units (CFU).

Reactive Oxygen Species (ROS), mitochondrial potential and mitochondrial mass measurements

ROS were measured by incubating macrophage cells with CellROX® Deep Red Reagent (LifeTechnologies, Grand Island, NY) for 30 min at 5 μM concentration. Jc-1 was added 5 min before termination of assay, according to manufacturer instructions. TMRE and Mitotracker green were added to the cells for 45 min before termination of the experiment at concentrations of 200 and 25nM, respectively. As controls, mitochondrial toxins rotenone (5 μM) and carbonyl cyanide m-chlorophenyl hydrazone (CCCP-1 at 10 μM) were included in most experiments. Peritoneal macrophage population was confirmed selecting for CD11c + cells and their scatter characteristics. Fluorescent signal from viable cells, as measured by DAPI exclusion, was detected in a Becton Dickinson LSRII instrument (BD Biosciences, Franklin Lakes, NJ).

Mitochondrial morphology

Cells were also plated in optical quality dishes (Maktek Corporation, Ashland, MA) and their mitochondrial morphology observed after stained with Mitotracker Green or a Alexa 488 conjugated-cytochrome c antibody, clone 6H2.B4 (BDPharmingen, San Jose, CA). Images were acquired with 0.2 μm steps with Inverted Olympus IX71 coupled to a Photometrics CoolSnap HQ CCD camera and analyzed using Volocity 3D (Perkin Elmer, Waltham, MA).

Transmission Electron Microscopy (TEM)

Macrophages were infected with Cn for 24 hours and fixed with 2% glutaraldehyde, 4% paraformaldehyde in 0.1 M cacodylate at room temperature for 2 h, followed by overnight incubation in 4% formaldehyde, 1% glutaraldehyde in PBS. The samples were subjected to postfixation for 90 min in 2% osmium, serially dehydrated in ethanol, and embedded in Spurrs epoxy resin. Sections (70-80 nm thick) were cut on a Reichart Ultracut UCT and stained with 0.5% uranyl acetate and 0.5% lead citrate. Samples were viewed in a JEOL 1200EX transmission electron microscope at 80 kV.

Immunoblot analysis

Cytosolic protein extracts were obtained by re-suspending the cell pellet in (Sigma-Aldrich, St. Louis, MO), supplemented with cOmplete Mini Protease Inhibitor Cocktail (Roche Applied Science, Indianapolis, IN), followed by 20 strokes with a Dounce homogenizer and centrifugation at 3000 rpm for 10 min to separate cell debris and organelles. Total cell protein extracts were obtained as previously described (38). Briefly, cells re-suspended in RIPA buffer supplemented with protease inhibitors cocktail, followed by 20 strokes with a Dounce homogenizer. Approximately 200 μl of RIPA buffer per 5 x 10^6 macrophages was used. After 1 h on ice, cells were spun at 13000 g for 40 min and supernatants collected. Protein samples were stored at -80°C until further analysis. Western blot was performed in a NuPAGE SDS-PAGE (LifeTechnologies, Grand Island, NY) system and blotted into an Immobilon-P membranes (Millipore, Bedford, MA), as per manufacturer instructions. We used the following primary antibodies: rabbit anti-AIF and mouse anti-RIP (1:2000 to 1:200, from BD Biosciences, San Jose, CA) and mouse anti- cytochrome c (1:200) (clone xx) (Abcam, Cambridge, MA). Protein signal was detected after incubation with anti-mouse or anti-rabbit secondary antibodies coupled to peroxidase (Southern Biotech Associated, Birmingham, Al) and developed by using Supersignal West Pico enhanced chemiluminescence (Thermo Scientific, Hudson, NH). Beta-actin antibody coupled to peroxidase (1:5000, Sta. Cruz Technologies, Sta. Cruz, CA) was used as a loading control.

Statistical analysis and plotting

Graphs, statistical analysis and figures were assembled in Prism version 6.00 for Mac OS X, GraphPad Software, San Diego, California, USA.

Results:

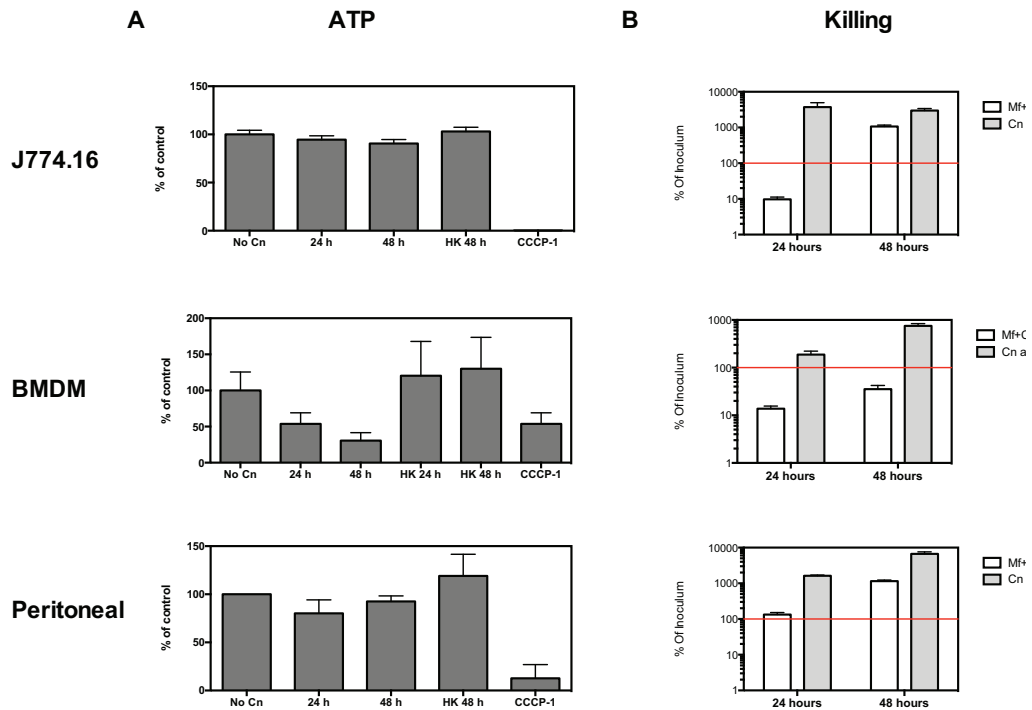**A**   **ATP**   **B**   **Killing**

Fig. 1. Murine macrophages restrict Cn growth with minimal cell death *in vitro*.

A) Cn growth after infection of murine macrophages. B) Total ATP levels in co-cultures of macrophages and Cn. Murine macrophages were infected with opsonized Cn for the indicated time points. Colony Forming Units (CFU) and ATP levels were measured the total contents of co-infection. CCCP-1 causes rapid depolarization of mitochondria, by uncoupling the proton gradient and causes cell death at 24 h. Experiments were repeated 2-3 times for J774.16 macrophages, BMDM and peritoneal macrophages. Triplicates wells for CFU and quintuplicates wells for ATP were performed. Shown is mean and SD of representative experiments.

Macrophage death upon Cn infection

We aimed to investigate how ingestion of the fungal pathogen Cn could affect murine macrophages. Previously we have reported a diminute increase in DNA fragmentation and cell permeability (33), arguing that Cn infection does not result in substantial macrophage killing after 24 hours of infection. Live cell microscopy (Carlos de Leon-Rodriguez, manuscript under preparation) has shown that during the first 24 hours of infection, Cn and the macrophage can coexist *in vitro,* with very little death for each side. We attempted to quantify macrophage death using alternative methods, but our infection model consists of two eukaryotic cell types and thus most methods were not able to discriminate between cells. Measurement of LDH release showed that prolonging the infection up to 48 h also did not result in measurable macrophage death (data not shown). Based on selective extraction of ATP from eukaryotic and yeast cells, we could use total ATP level as a measure of macrophage number (reflecting the number of cells and metabolic status). In murine macrophages infected
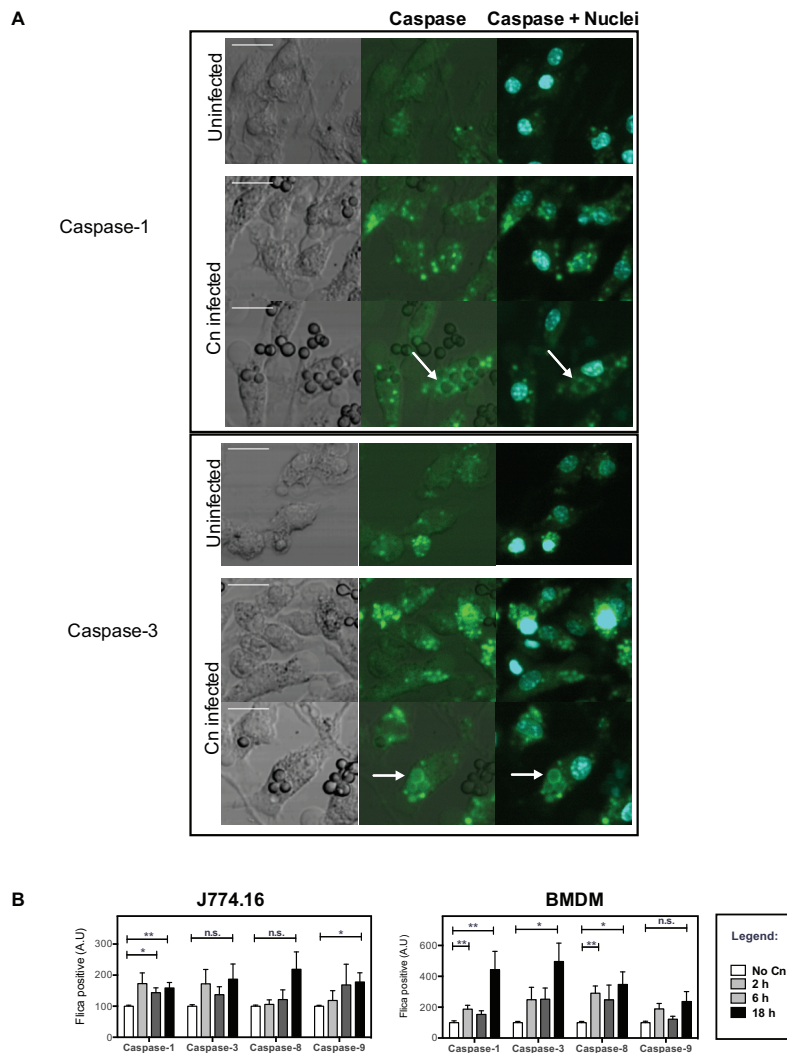
98

A

Caspase Caspase + Nuclei

Caspase-1

Caspase-3

B

J774.16

BMDM

Legend:
No Cn
2 h
6 h
18 h

Fig. 2. Caspases are activated in response to Cn infection.

A) Morphology of BMDM showing caspase activation after 2 h infection with Cn. Caspase shows a punctuate pattern that is characteristic of activation, and sometimes localizes around the Cn (arrows), suggesting trafficking to the lyssossome. Greyscale: brightfield images; Green: caspase-specific FLICA; Cyan: Hoechst. Images were obtained by LSC at original magnification of 60x at a resolution of 0.15 μm.   Scale bars represent 20 μm. Quantification of caspase activation after infection Cn infection of B) BMDM and C) J774.16 macrophages. Caspases-1, -3 and -8 are activated in response to infection and J774.16 activate caspase-1 and caspase-9. Experiments were repeated 3-5 times for J774.16 macrophages and BMDM.   Shown is mean and SEM of all experiments.

with Cn, there was a tendency to decrease ATP levels starting at 24 h of infection, which was worsened at 48 h (Fig. 1A). All macrophages were capable of restricting Cn growth and even some degree of Cn killing at 24 h, but this effect was lost at 48 h. Thus we chose to study the infection in its first 24 h of infection, to investigate what is modified in macrophages before significant damage is established.

Pathways of death activated upon Cn infection

We investigated caspase activation in macrophages after ingestion of Cn. FLICA assays for caspase-1, -3, -8 and -9 were performed at 2, 6 and 18 h after Cn infection. BMDM activate caspase-1 and caspase-3 at 2 h of infection (Fig. 2A). Moreover, both caspases showed a punctuate pattern when Cn is present, which is indicative of activation (39). In some cases, both caspases appeared to localize around internalized Cn cells suggesting that caspases trafficked to the phagosome at some point (arrows). BMDM, at later times of infection, activated caspase-1, -8 and -3. J774.16 macrophages manifested a different pattern of caspase activation. These cells showed active caspase-1 throughout infection but at later time of infection we could only detect caspase-9 (Fig. 2B). To investigate whether caspase activity affected the outcome of infection, we measured intracellular ATP levels and killing of Cn cells by macrophages after treating with pan-caspase inhibitor z-VAD-FMK (Supplemental Figure 1). Addition of z-VAD-FMK did not alter the outcome of infection, as measured by these assays.

To further investigate the possible involvement of mitochondria in Cn infection, we investigated expression of mitochondrial molecules, which have been involved in pathways of death and inflammation (illustrated in Figure 4). Two of the most widely studied are RIPK1 and AIF. We measured totals levels of RIP and AIF release into the cytosol. We found that J774.16 cells had increased RIP expression, but AIF levels were not changed upon infection (Fig. 3A). On the other hand, BMDM increased expression of AIF levels in the cytoplasm (Fig. 3B).

Mitochondrial potential modulated upon Cn infection

The observed decrease in ATP levels reflects a degree of alteration of macrophage number upon ingestion of Cn. However, it is known that upon activation by TLR agonists, immune cells, such as dendritic cells, will switch to a glycolytic state (40), which might affect ATP content. Furthermore, mitochondria play an active role in most death pathways and, recently were also involved in immune effector functions (30). Consequently, we measured mitochondrial potential by measuring the red/green fluorescence signal of the Jc-1 dye or the accumulation of TMRE dye (41). All macrophage types showed some
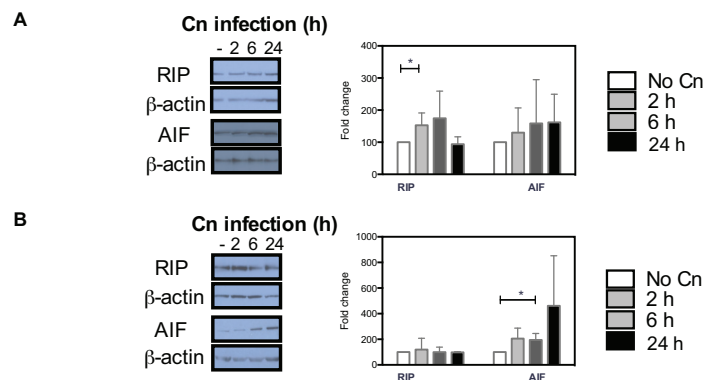
Figure 3. Activation of mitochondrial death pathways upon Cn infection.

A) J774.16 and B) BMDM immunoblot of total RIP and cytoplasmatic AIF after infection with Cn. Representative immunoblot (left) and quantification protein expression (right). Protein quantification was normalized to β-actin and to fold change over uninfected cells. Experiments were repeated 2-3 times for each cell type. Shown is mean and SD of all experiments.
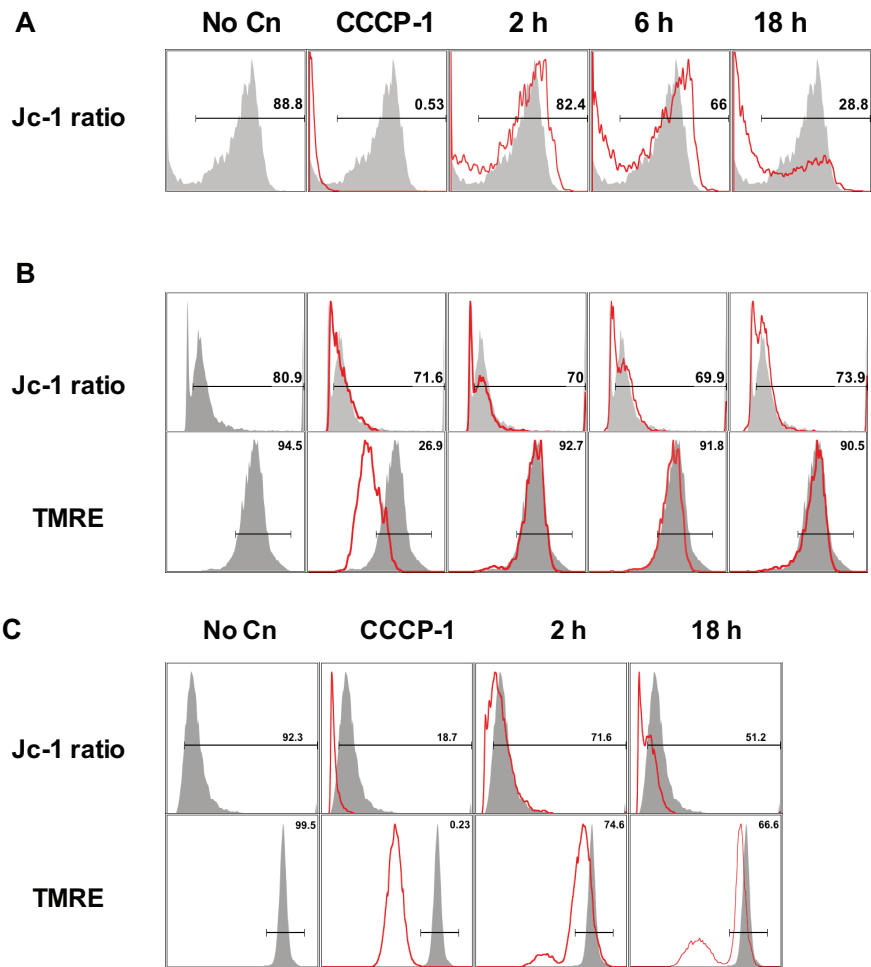
Figure 4. Murine macrophages depolarize mitochondria after infection with Cn.

A) J774.16; B) BMDM and C) Peritoneal macrophages were infected with Cn for the indicated time points and mitochondrial potential was measured by flow cytometry analysis of Jc-1 ratio or TMRE accumulation. Ratio of red/green fluorescent signal reflects mitochondrial polarization. CCCP-1 causes rapid depolarization of mitochondria, by uncoupling the proton gradient. Shaded grey is non infected macrophages compared to experimental condition in red outline. Numbers represent % of cells with hyperpolarized healthy mitochondria. Experiments were repeated 2-3 times for each macrophage cell type.

hyperpolarized of their mitochondria upon initiation of phagocytosis, by a slight increase in mean fluorescence intensity at 2 h of infection. Overall, most macrophages depolarized their mitochondria after 2 h of Cn infection (Fig. 4). We note that in primary cells BMDM the mitochondrial potential was decreased to a much lower extent (Fig. 4B). These cells were resistant to CCCP-1 mitochondrial depolarization. We suggest that phagocytosis of a fungal cell triggers alterations in macrophages which include mitochondria depolarization. Mitochondrial ultrastructure was not altered, as observed by TEM (Fig.5).
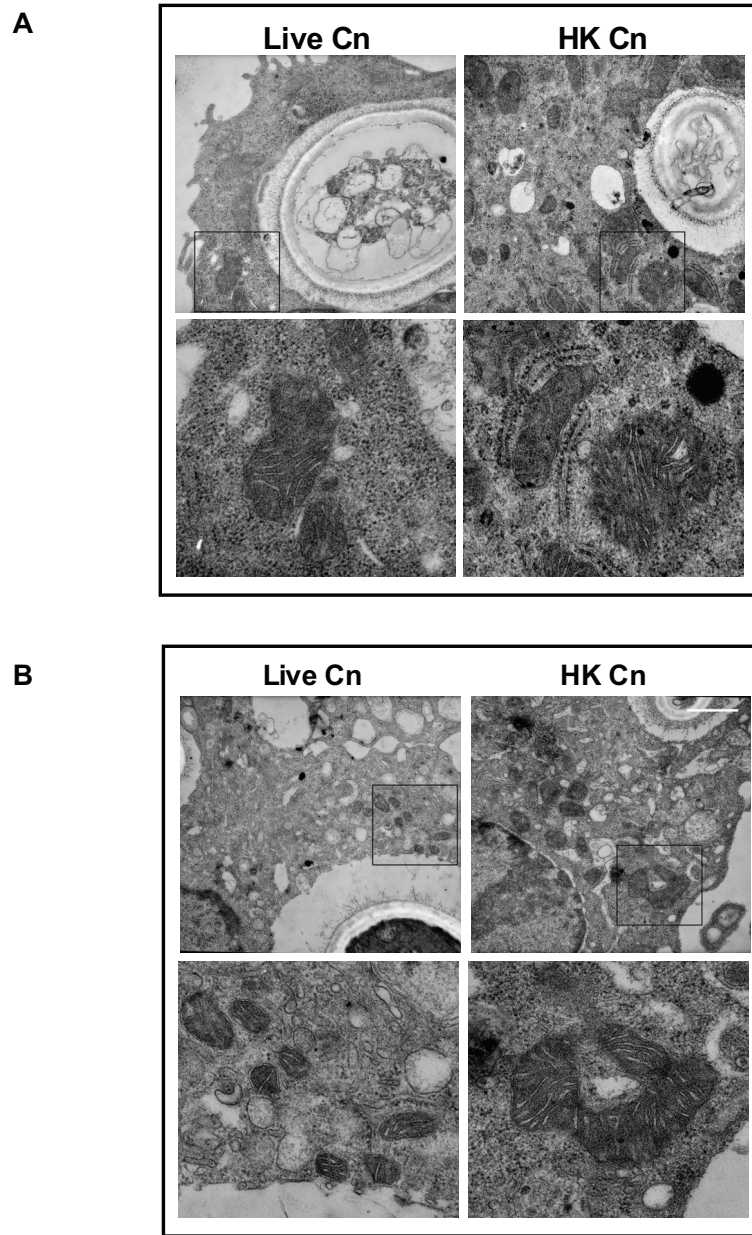
Figure 5. Ultrastructure of mitochondria is not altered upon Cn infection.

A) J774.16 and B) BMDM were infected with live Cn or Heat-killed Cn (HK Cn) for 24h and electron micrograph is shown in top row. Bottom row is magnification of insets. When macrophages are infected with Cn, mitochondria localize close or in aposition with the phagosomal membrane (arrow). However no alteration of mitochondria morphology -- non existent or swollen cristae -- could be detected. Original magnification 15000x. Scale bar is 1 μm. Experiments were repeated twice and one representative experiment is shown.
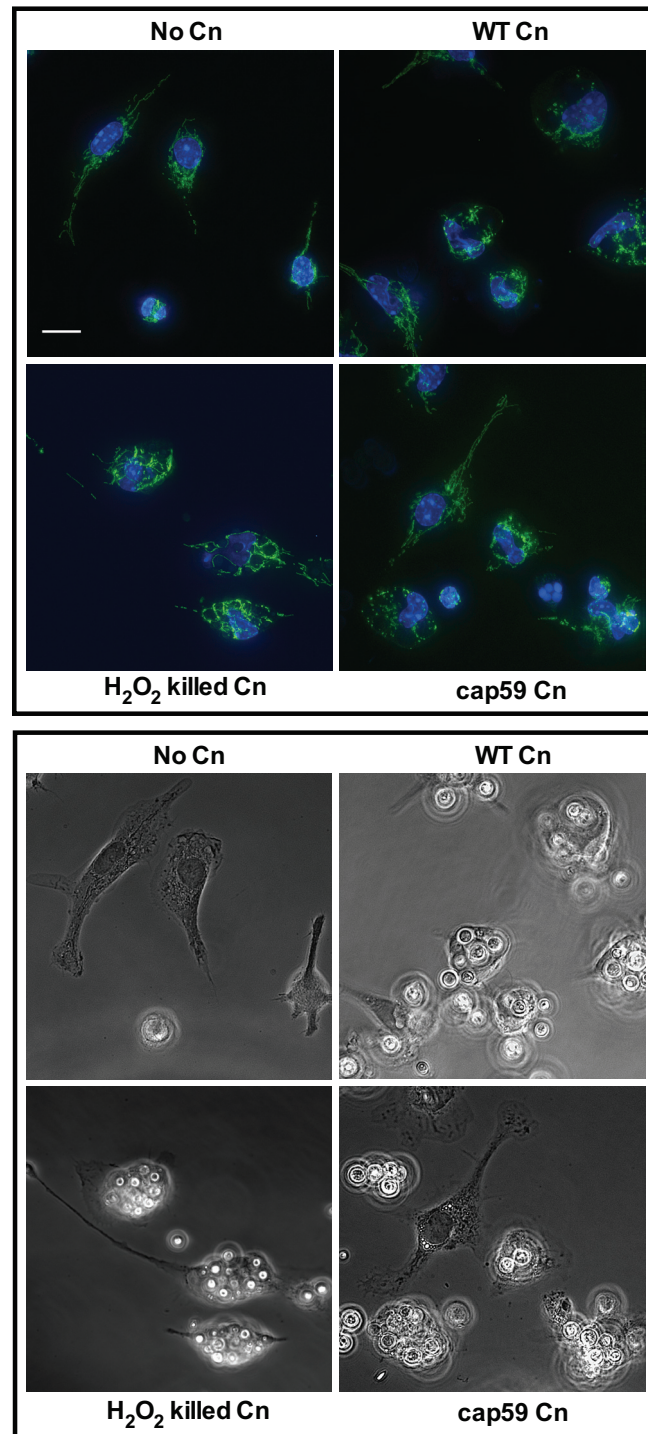
Figure 6. Peritoneal macrophages infected with Cn show fragmented mitochondrial network. A) Immunofluorescence microscopy of peritoneal macrophages infected with either wild-type H99 Cn, H_2O_2 killed Cn or cap59 acapsular Cn. Mitochondrial network, as infered by cytochrome c immunostaining (green), was altered by the presence of Cn. Images were countersained with Hoechst nuclear dye (blue). B)Corresponding brightfield image. Scale bar 50 μm. Original magnification 63x. Experiments were repeated three times and representative images are shown.
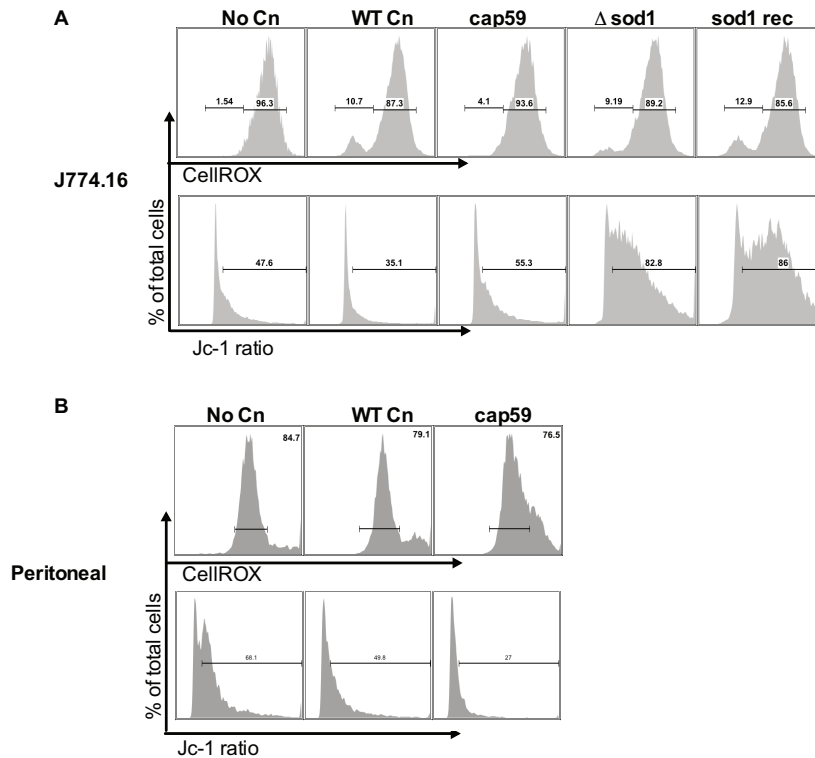
Figure 7. Mitochondrial potential depolarization or ROS production, are not altered for a capsular mutant. No ROS is produced in J774.16 macrophages or BMDM (not shown). Mitochondrial depolarization happens only for H99 strain and for the SOD mutant, but is very discrete or non existent for acapsular strain cap59. Only peritoneal macrophages produced ROS after infection of Cn. In peritoneal macrophages cap59 strain could trigger depolarization of macrophages. A) J774.16 and B) peritoneal macrophages were infected for 2 hours with an acapsular strain (cap59), SOD1-deficient Cn strain (Δsod1) and its reconstituted strain (sodrec). Total ROS were measured by CellROX® Deep Red Reagent and mitochondrial potential was measured by ratio of Jc-1 red/green fluorescence, using flow cytometry. Numbers represent % of cells within each region. Experiments were repeated at least twice for all macrophage types. Shown are plots of a representative experiment.

There was no release of cytochrome c into the cytoplasm in any of the macrophage cell types (data not shown), which together with the morphological data support that no substantial mitochondrial damage occurs in the system. There was however alterations in the mitochondrial network, where infected macrophages displayed fragmented networks (punctae) (Fig. 6).

Production of Reactive Oxygen Species

One of the most common responses to infection is the release of ROS, which in addition to antimicrobial defense, serve as a signaling molecule for inflammation. It has been suggested that ROS are in   in tight connection with mitochondrial function for their immune functions (30). We decided to measure ROS and mitochondrial depolarization in macrophages using wild-type Cn and strains deficient for antioxidant defenses: a SOD1 mutant (42) and an acapsular mutant (cap59) (43). We found that both J774.16 and BDMD produced
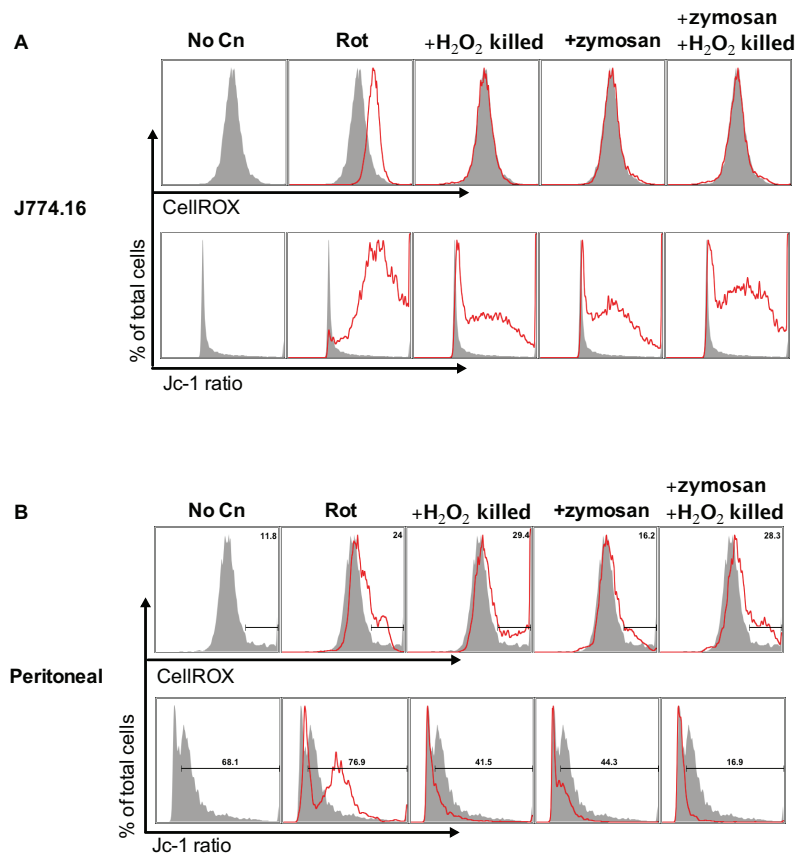
Figure 8. Mitochondrial polarization or depolarization does not correlate with presence of ROS. Given the absence of measurable ROS, we infected macrophages with H_2O_2 killed Cn and zymosan, which would quench all anti-oxidative defenses. Both particles resulted in mitochondrial hyperpolarization, but no ROS production in J774.16 macrophages. In peritoneal macrophages, mitochondria were still depolaryzed in response to inert particle phagocytosis and production of ROS was abundant. Rotenone blocks mitochondrial respiratory chain, resulting in accumulation of electrons, hyperpolarization and increase in cellular ROS. Total ROS were measured by CellROX® Deep Red Reagent and mitochondrial potential was measured by ratio of Jc-1 red/green fluorescence, using flow cytometry. Numbers represent % of cells within each region. Experiments were repeated twice for both J774.16 and peritoneal macrophages. Shown are plots of a representative experiment.

little if any ROS after phagocytosis of Cn (Fig. 7A). However, peritoneal macrophages produced abundant ROS upon phagocytosis of both wild-type and cap59 strains. The Cn strain deficient in SOD and its reconstituted pair both hyperpolarized mitochondria in J774.16 macrophages and depolarized mitochondria in BMDM (data not shown). We found no explanation for this result and thus did not study these strains further.

To demonstrate the absence of link between ROS production and mitochondria, we decided to quench every ROS defense of Cn by incubating Cn with a lethal concentration of H_2O_2. Rotenone triggered hyperpolarization coupled to ROS production in both macrophage types, but for unknown reasons mitochondrial hyperpolarization does not result in ROS production in J774.16 cells (Fig. 8A). In peritoneal macrophages the opposite was true, abundant ROS production was seen but the mitochondria still depolarized (Fig. 8B). These data argue that mitochondrial modulation is disconnected from ROS production in our model. These conclusions are supported by investigation of interference of antioxidants in the fungicidal potential of

macrophages. We investigated if killing of yeast cells could be altered by addition of antioxidants to this cell interaction. We found that neither β-mercaptoethanol (BME) in physiological concentrations (44) nor N-acetyl cysteine (NAC) resulted in increased killing of yeasts cells or influenced ATP contents of the cell for J774.16 or for BMDM (Supplemental Figure 2).

A

B
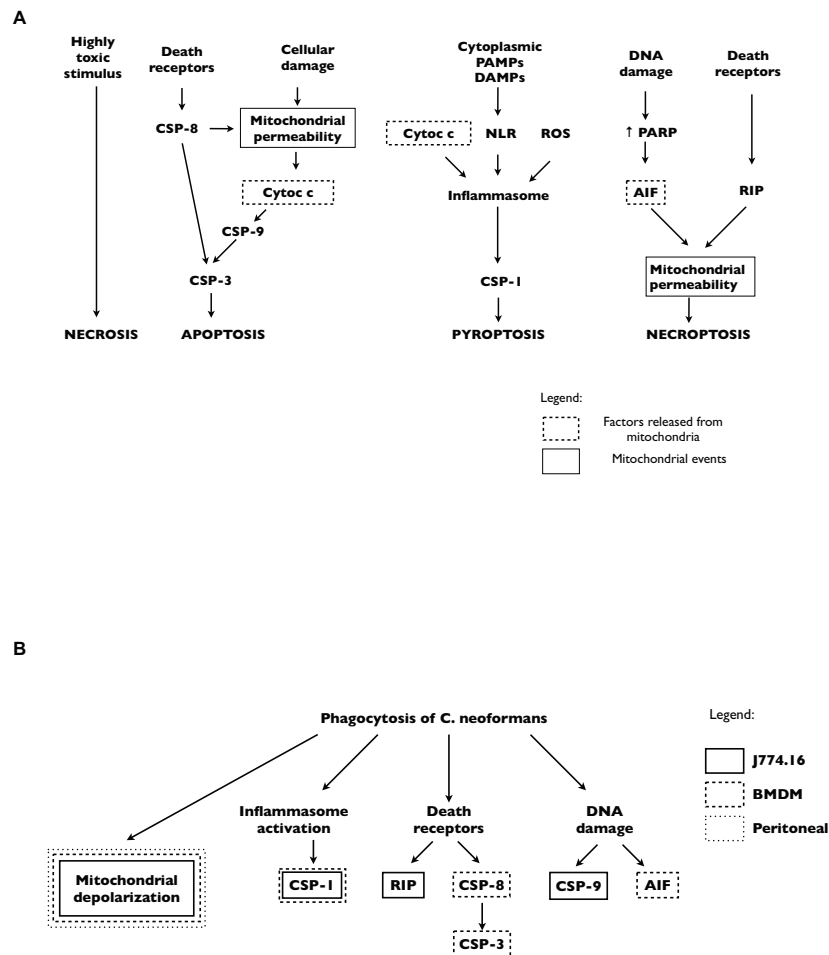
Fig. 9. Schematic of death pathways studied in this work.

A)Most cellular death pathways require mitochondrial components to be released from the mitochondria (dashed boxes) or whole mitochondrial permeability (solid boxes). Necrosis is accidental cell death. Apoptosis can proceed through the extrinsic pathway that is dependent on death receptor stimulation or through the intrinsic pathway. Type II cells require the extrinsic pathway and the intrinsic pathway to communicate through mitochondrial permeability. Pyroptosis is the result of stimulation of DAMP's or PAMP's in the cytoplasm. Based on references (18, 54) B) Summary of findings of this study, the cellular stress pathways activated upon ingestion of Cn in murine macrophages.

Discussion:

There is now considerable evidence that the interaction of Cn with macrophages leads to host cell damage, even before there are obvious signs of cytotoxicity or significant cell death. The type of damage includes phagosomal leakage (1), giant vacuole formation (13) and cell cycle arrest (33). Such damage can progress to trigger cellular death in the form of cell lysis and, less frequently, apoptosis (18, 39). Our goal was to investigate the mechanisms of macrophage cell damage after Cn phagocytosis. Specifically, we sought to understand how both cells could coexist and identify host cell components that were affected by presence of ingested Cn.

Our initial studies focused on the expression of caspases after the interaction of macrophages with Cn. Prior studies had provided evidence that some fungal pathogens activated host cell caspases. Analysis of macrophages infected with *Paracaccidioides brasiliensis* (45) found up-regulation of caspase-2, caspase-8 and caspase-3 using gene arrays. Similarly *Histoplasma capsulatum* was found to activate caspase-1 and -3 in macrophages (46). In BMDM, we noted that, upon phagocytosis, active caspase-1 and caspase-3 appeared to localize in the Cn-containing phagosome. This was a surprising observation, since caspases are cytoplasmatic factors and we have found no reports of trafficking for the phagosome. Caspase-1 activation is a hallmark of pyroptosis. In previous work, we found rare instances of cellular permeability (33). Our results with Cn indicate caspase-1 activation upon infection of macrophages. The activation of caspase-1 results in inflammasome activation but does not result in extensive pyroptosis. The finding that *P. brasiliensis*, *H. capsulatum* and Cn each triggered caspase-1 activation in macrophages strongly suggests that activation of caspase-1 activation is a conserved response in fungal infection.

Distinct cell death pathways were activated by J774.16 cells and BMDM in response to Cn infection (Fig. 10). In BMDM, caspase-3 activation with subsequent apoptosis were triggered by the extrinsic pathway of apoptosis. There was concomitant release of AIF into the cytoplasm, a mediator of DNA damage induced necroptosis. Isolated capsular component GXM is enough to cause AIF release in rat peritoneal macrophages (14), suggesting that AIF release is capsule dependent. From these results, we conclude that infection of BMDM results in a small degree of apoptosis and AIF-mediated necroptosis. In J774.16 macrophage-like cells, the intrinsic pathway of apoptosis was activated, but effector caspase-3 was not active, implicating the absence of apoptosis. We found RIP protein was highly expressed in infected J774.16 cells. RIP is activated upon TNF-α binding, and its activation does not necessarily reflects necroptosis (23), but can occur when caspase-8 is inhibited or not activated (23). We detected characteristics of pyroptosis, apoptosis and necroptosis that occur in a low level in macrophage cells, highlighting the complexity of host response to a fungal pathogen. Our results emphasize how the death pathways are interconnected and can coexist with complex systems.

Despite considerable crosstalk and overlap between death pathways, different death pathways result in different immune outcomes (35, 47). Activation of macrophages, infected with *Yersinia,* is enough to direct macrophage death from apoptosis to pyroptosis, with beneficial effects in pathogen control (48). One possible mechanism for augmented pathogen control was elucidated in *Mycobacterium tuberculosis* (35)*.* Instances of necrosis will allow the bacterial proteins to interact with a new host cell and thus immune recognition, while apoptotic death will contain bacterial proteins within host membranes and prevents the interaction of the pathogen with a new host cell. However we found that the fungal damage to murine macrophages is discrete, with a minor number of macrophages dying with our experimental conditions. Our data supports that the most common outcome of infection of macrophages *in vivo* is a latent state of infection with survival of both host and pathogen (3).

Mitochondria are key organelles for the integration of cell death and survival signaling (30). They have also been proposed to be the integrating center for immune signaling (49). One type of primary macrophages was less sensitive to the Cn-mediated depolarization but also to the CCCP-1 mitochondrial uncoupler, implying different susceptibility to mitochondrial modulation of this cell type. Nevertheless Cn infection caused a decrease in mitochondrial potential in all macrophage types tested. Other examples of mitochondrial modulation by pathogens can be found in the bacterial field. Macrophages infected with *Shigella flexneri* decreased their mitochondrial potential and ATP levels (50). Moreover, upon phagocytosis of apoptotic cells (51), macrophages increase their mitochondrial potential and pharmacological modulation of mitochondrial potential affects phagocytic capacity. In their model, ingestion of inert particles lead to no alteration of mitochondrial potential, while ingestion of apoptotic cells lead to hyperpolarization. These results were confirmed in our model where inert particles such as zymosan and H_2O_2 killed Cn hyperpolarized mitochondria in immortalized macrophages, but not peritoneal macrophages. Ingestion of live yeasts always lead to depolarization. These authors also observed that chemical decoupling of mitochondria increased phagocytic potential of macrophages, an effect that we have not tested but is likely conserved in our model. Thus, modulation of mitochondrial function is a frequent event in phagocytic processing and constitutes an additional argument for mitochondria's central role in immunity.

One of the possible roles of mitochondria in immunity is production of mitochondrial ROS are microbicidal and can contribute to inflammasome activation (52), but the relationship of Cn with ROS has eluded clarification. Herein and in other studies, there is evidence of concomitant caspase-1 activation and Il-18 and Il-1β release (manuscript in preparation). These molecules activate the inflammasome when danger molecules are present. These danger molecules are either microbial molecules, on one side and, in the host side ROS, lysosomal damage and K^+ ion flux. ROS can usually produced by the NADPH oxidase, but hypoxic environments such as infections can impair ROS production by NADPH oxidase (28). In these cases, mitochondria can become the source ROS through mitochondrial hyperpolarization and leakage of electrons (53). However we found that ROS are only produced by one of the cell types investigated. We hypothesized that Cn antioxidative defenses could quench ROS production to such an extent that would explain the absence of measurable ROS. However, infection of macrophages with Cn defective in antioxidant defenses had no effect on measurable ROS. Because we also found no increased fungicidal activity after addition of antioxidants, we conclude that ROS is not a fungicidal mechanism for J774.16 and BMDM. Furthermore, our data support the notion that ROS that are produced in infection are not mitochondrial derived, since the pattern of ROS liberation is opposite to the pattern of mitochondrial hyperpolarization. Wiese and colleagues found that killing of *Staphylococcus aureus* is mitochondria dependent, but ROS independent, which led them to hypothesize that the mechanism of mitochondria killing is a novel, oxygen independent, mechanism (28). Thus, a novel mitochondrial antimicrobial mechanisms could explain our results.

The implications of mitochondrial modulation in the immune cells are not fully understood yet. The observed impairment of the mitochondrial chain is a reflexion of a metabolic switch to glycolysis. This switch has been described for T-cells and is now believed that proper immune activation requires a switch to glycolytic metabolism.

In summary, our results establish that several pathways of acellular damage are activated upon Cn ingestion. Moreover, mitochondrial function is modulated by the interaction of Cn with macrophages. Our results also indicate a correlation between presence of capsule and mitochondrial modulation in the host. These results provide additional evidence for a cytopathic effect of Cn on macrophages and suggest the need for additional investigations to understand how toxicity to macrophages contributes to the pathogenesis of cryptococcal infection.

Acknowledgments:

References:

1. **Tucker SC**, **Casadevall A**. 2002. Replication of Cryptococcus neoformans in macrophages is accompanied by phagosomal permeabilization and accumulation of vesicles containing polysaccharide in the cytoplasm. Proc Natl Acad Sci USA **99**:3165–3170.

2. **Osterholzer JJ**, **Milam JE**, **Chen G-H**, **Toews GB**, **Huffnagle GB**, **Olszewski MA**. 2009. Role of dendritic cells and alveolar macrophages in regulating early host defense against pulmonary infection with Cryptococcus neoformans. Infect Immunit **77**:3749–3758.

3. **Feldmesser M**, **Kress Y**, **Novikoff P**, **Casadevall A**. 2000. Cryptococcus neoformans is a facultative intracellular pathogen in murine pulmonary infection. Infect Immunit **68**:4225–4237.

4. **Qin Q-M**, **Luo J**, **Lin X**, **Pei J**, **Li L**, **Ficht TA**, **de Figueiredo P**. 2011. Functional Analysis of Host Factors that Mediate the Intracellular Lifestyle of Cryptococcus neoformans. PLoS Pathog **7**:e1002078.

5. **Gordon SB**, **Read RC**. 2002. Macrophage defences against respiratory tract infections. Br. Med. Bull. **61**:45–61.

6. **Brown GD**. 2011. Innate antifungal immunity: the key role of phagocytes. Annu Rev Immunol **29**:1–21.

7. **Shao X**, **Mednick A**, **Alvarez M**, **van Rooijen N**, **Casadevall A**, **Goldman DL**. 2005. An innate immune system cell is a major determinant of species-related susceptibility differences to fungal pneumonia. J Immunol **175**:3244–3251.

8. **Goldman DL**, **Lee SC**, **Mednick AJ**, **Montella L**, **Casadevall A**. 2000. Persistent Cryptococcus neoformans pulmonary infection in the rat is associated with intracellular parasitism, decreased inducible nitric oxide synthase expression, and altered antibody responsiveness to cryptococcal polysaccharide. Infect Immunit **68**:832–838.

9. **Alvarez M**, **Casadevall A**. 2006. Phagosome extrusion and host-cell survival after Cryptococcus neoformans phagocytosis by macrophages. Curr Biol **16**:2161–2165.

10. **Ma H**, **Croudace JE**, **Lammas DA**, **May RC**. 2006. Expulsion of live pathogenic yeast by macrophages. Curr Biol **16**:2156–2160.

11. **Alvarez M**, **Burn T**, **Luo Y**, **Pirofski L-A**, **Casadevall A**. 2009. The outcome of Cryptococcus neoformans intracellular pathogenesis in human monocytes. BMC Microbiol. **9**:51.

12. **Luo Y**, **Casadevall A**. 2010. Intracellular cryptococci suppress Fc-mediated cyclin D1 elevation. Commun Integr Biol **3**:390–391.

13. **Alvarez M**, **Casadevall A**. 2007. Cell-to-cell spread and massive vacuole formation after Cryptococcus neoformans infection of murine macrophages. BMC Immunol. **8**:16.

14. **Chiapello LS**, **Baronetti JL**, **Garro AP**, **Spesso MF**, **Masih DT**. 2008. Cryptococcus neoformans glucuronoxylomannan induces macrophage apoptosis mediated by nitric oxide in a caspase-independent pathway. Int Immunol **20**:1527–1541.

15. **Barbosa FM**, **Fonseca FL**, **Holandino C**, **Alviano CS**, **Nimrichter L**, **Rodrigues ML**. 2006. Glucuronoxylomannan-mediated interaction of Cryptococcus neoformans with human alveolar cells results in fungal internalization and host cell damage. Microbes Infect **8**:493–502.

16. **Pericolini E**, **Cenci E**, **Monari C**, **De Jesus M**, **Bistoni F**, **Casadevall A**, **Vecchiarelli A**. 2006. Cryptococcus neoformans capsular polysaccharide component galactoxylomannan induces apoptosis of human T-cells through activation of caspase-8. Cell Microbiol **8**:267–275.

17. **Villena SN**, **Pinheiro RO**, **Pinheiro CS**, **Nunes MP**, **Takiya CM**, **DosReis GA**, **Previato JO**, **Mendonça-Previato L**, **Freire-de-Lima CG**. 2008. Capsular polysaccharides galactoxylomannan and glucuronoxylomannan from Cryptococcus neoformans induce macrophage apoptosis mediated by Fas ligand. Cell Microbiol **10**:1274–1285.

18. **Galluzzi L**, **Vitale I**, **Abrams JM**, **Alnemri ES**, **Baehrecke EH**, **Blagosklonny MV**, **Dawson TM**, **Dawson VL**, **El-Deiry WS**, **Fulda S**, **Gottlieb E**, **Green DR**, **Hengartner MO**, **Kepp O**, **Knight RA**, **Kumar S**, **Lipton SA**, **Lu X**, **Madeo F**, **Malorni W**, **Mehlen P**, **Nuñez G**, **Peter ME**, **Piacentini M**, **Rubinsztein DC**, **Shi Y**, **Simon H-U**, **Vandenabeele P**, **White E**, **Yuan J**, **Zhivotovsky B**, **Melino G**, **Kroemer G**. 2012. Molecular definitions of cell death subroutines: recommendations of the Nomenclature Committee on Cell Death 2012. Cell Death Differ. **19**:107–120.

19. **Kerr JF**, **Wyllie AH**, **Currie AR**. 1972. Apoptosis: a basic biological phenomenon with wide-ranging implications in tissue kinetics. Br. J. Cancer **26**:239–257.

20. **Siegel RM**. 2006. Caspases at the crossroads of immune-cell life and death. Nat Rev Immunol **6**:308–317.

21. **Kroemer G**, **Galluzzi L**, **Brenner C**. 2007. Mitochondrial membrane permeabilization in cell death. Physiol. Rev. **87**:99–163.

22. **Boujrad H**, **Gubkina O**, **Robert N**, **Krantic S**, **Susin SA**. 2007. AIF-mediated programmed necrosis: a highly regulated way to die. Cell Cycle **6**:2612–2619.

23. **Declercq W**, **Vanden Berghe T**, **Vandenabeele P**. 2009. RIP kinases at the crossroads of cell death and survival. Cell **138**:229–232.

24. **Sevrioukova IF**. 2011. Apoptosis-inducing factor: structure, function, and redox regulation. Antioxid. Redox Signal. **14**:2545–2579.

25. **Miao EA**, **Rajan JV**, **Aderem A**. 2011. Caspase-1-induced pyroptotic cell death. Immunol Rev **243**:206–214.

26. **Brodsky IE**, **Medzhitov R**. 2011. Pyroptosis: macrophage suicide exposes hidden invaders. Curr Biol **21**:R72–5.

27. **Miao EA**, **Leaf IA**, **Treuting PM**, **Mao DP**, **Dors M**, **Sarkar A**, **Warren SE**, **Wewers MD**, **Aderem A**. 2010. Caspase-1-induced pyroptosis is an innate immune effector mechanism against intracellular bacteria. Nat Immunol **11**:1136–1142.

28. **Wiese M**, **Gerlach RG**, **Popp I**, **Matuszak J**, **Mahapatro M**, **Castiglione K**, **Chakravortty D**, **Willam C**, **Hensel M**, **Bogdan C**, **Jantsch J**. 2012. Hypoxia-mediated impairment of the mitochondrial respiratory chain inhibits the bactericidal activity of macrophages. Infect Immunit **80**:1455–1466.

29. **Zhou R**, **Yazdi AS**, **Menu P**, **Tschopp J**. 2011. A role for mitochondria in NLRP3 inflammasome activation. Nature **469**:221–225.

30. **Tschopp J**. 2011. Mitochondria: Sovereign of inflammation? Eur J Immunol **41**:1196–1202.

31. **Rudel T**, **Kepp O**, **Kozjak-Pavlovic V**. 2010. Interactions between bacterial pathogens and mitochondrial cell death pathways. Nat Rev Microbiol **8**:693–705.

32. **Hwang I-Y**, **Quan JH**, **Ahn M-H**, **Ahmed HAH**, **Cha G-H**, **Shin D-W**, **Lee Y-H**. 2010. Toxoplasma gondii infection inhibits the mitochondrial apoptosis through induction of Bcl-2 and HSP70. Parasitol. Res. **107**:1313–1321.

33. **Coelho C**, **Tesfa L**, **Zhang J**, **Rivera J**, **Gonçalves T**, **Casadevall A**. 2012. Analysis of cell cycle and replication of mouse macrophages after in vivo and in vitro Cryptococcus neoformans infection using laser scanning cytometry. Infect Immunit **80**:1467–1478.

34. **Ben-Abdallah M**, **Sturny-Leclère A**, **Avé P**, **Louise A**, **Moyrand F**, **Weih F**, **Janbon G**, **Mémet S**. 2012. Fungal-induced cell cycle impairment, chromosome instability and apoptosis via differential activation of NF-κB. PLoS Pathog **8**:e1002555.

35. **Briken V**. 2012. "With a Little Help from My Friends": Efferocytosis as an Antimicrobial Mechanism. Cell Host Microbe **12**:261–263.

36. **Ashida H**, **Mimuro H**, **Ogawa M**, **Kobayashi T**, **Sanada T**, **Kim M**, **Sasakawa C**. 2011. Cell death and infection: a double-edged sword for host and pathogen survival. J Cell Biol **195**:931–942.

37. **Casadevall A**, **Cleare W**, **Feldmesser M**, **Glatman-Freedman A**, **Goldman DL**, **Kozel TR**, **Lendvai N**, **Mukherjee J**, **Pirofski LA**, **Rivera J**, **Rosas AL**, **Scharff MD**, **Valadon P**, **Westin K**, **Zhong Z**. 1998. Characterization of a murine monoclonal antibody to Cryptococcus neoformans polysaccharide that is a candidate for human therapeutic studies. Antimicrob Agents Chemother **42**:1437–1446.

38. **Klockenbusch C**, **Kast J**. 2010. Optimization of formaldehyde cross-linking for protein interaction analysis of non-tagged integrin beta1. J Biomed Biotechnol **2010**:927585.

39. **Bergsbaken T**, **Fink SL**, **Cookson BT**. 2009. Pyroptosis: host cell death and inflammation. Nat Rev Microbiol **7**:99–109.

40. **Everts B**, **Amiel E**, **van der Windt GJW**, **Freitas TC**, **Chott R**, **Yarasheski KE**, **Pearce EL**, **Pearce EJ**. 2012. Commitment to glycolysis sustains survival of NO-producing inflammatory dendritic cells. Blood **120**:1422–1431.

41. **Perry SW**, **Norman JP**, **Barbieri J**, **Brown EB**, **Gelbard HA**. 2011. Mitochondrial membrane potential probes and the proton gradient: a practical usage guide. BioTechniques **50**:98–115.

42. **Cox GM**, **Harrison TS**, **McDade HC**, **Taborda CP**, **Heinrich G**, **Casadevall A**, **Perfect JR**. 2003. Superoxide dismutase influences the virulence of Cryptococcus neoformans by affecting growth within macrophages. Infect Immunit **71**:173–180.

43. **Chang YC**, **Kwon-Chung KJ**. 1994. Complementation of a capsule-deficient mutation of Cryptococcus neoformans restores its virulence. Mol Cell Biol **14**:4912–4919.

44. **Chang MP**, **Strehler BL**, **Makinodan T**. 1982. Requirement of 2-mercaptoethanol for in vitro growth factor production by T cells and vulnerability of the response to age. Mech. Ageing Dev. **20**:65–73.

45. **Silva SS**, **Tavares AHFP**, **Passos-Silva DG**, **Fachin AL**, **Teixeira SMR**, **Soares CMA**, **Carvalho MJA**, **Bocca AL**, **Silva-Pereira I**, **Passos GAS**, **Felipe MSS**. 2008. Transcriptional response of murine macrophages upon infection with opsonized Paracoccidioides brasiliensis yeast cells. Microbes Infect **10**:12–20.

46. **Deepe GS**, **Buesing WR**. 2011. Deciphering the Pathways of Death of Histoplasma capsulatum-Infected Macrophages: Implications for the Immunopathogenesis of Early Infection. J Immunol.

47. **Duprez L**, **Wirawan E**, **Vanden Berghe T**, **Vandenabeele P**. 2009. Major cell death pathways at a glance. Microbes Infect **11**:1050–1062.

48. **Bergsbaken T**, **Cookson BT**. 2007. Macrophage activation redirects yersinia-infected host cell death from apoptosis to caspase-1-dependent pyroptosis. PLoS Pathog **3**:e161.

49. **West AP**, **Shadel GS**, **Ghosh S**. 2011. Mitochondria in innate immune responses. Nat Rev Immunol **11**:389–402.

50. **Koterski JF**, **Nahvi M**, **Venkatesan MM**, **Haimovich B**. 2005. Virulent Shigella flexneri causes damage to mitochondria and triggers necrosis in infected human monocyte-derived macrophages. Infect Immunit **73**:504–513.

51. **Park D**, **Han CZ**, **Elliott MR**, **Kinchen JM**, **Trampont PC**, **Das S**, **Collins S**, **Lysiak JJ**, **Hoehn KL**, **Ravichandran KS**. 2011. Continued clearance of apoptotic cells critically depends on the phagocyte Ucp2 protein. Nature **477**:220–224.

52. **Tschopp J**, **Schroder K**. 2010. NLRP3 inflammasome activation: the convergence of multiple signalling pathways on ROS production? Nat Rev Immunol **10**:210–215.

53. **Novo E**, **Parola M**. 2008. Redox mechanisms in hepatic chronic wound healing and fibrogenesis. Fibrogenesis Tiss Repair **1**:5.

54. **Antico Arciuch VG**, **Elguero ME**, **Poderoso JJ**, **Carreras MC**. 2012. Mitochondrial regulation of cell cycle and proliferation. Antioxid. Redox Signal. **16**:1150–1180.

Supplemental Figures

A

ATP

J774.16

B

BMDM

C

Killing

D
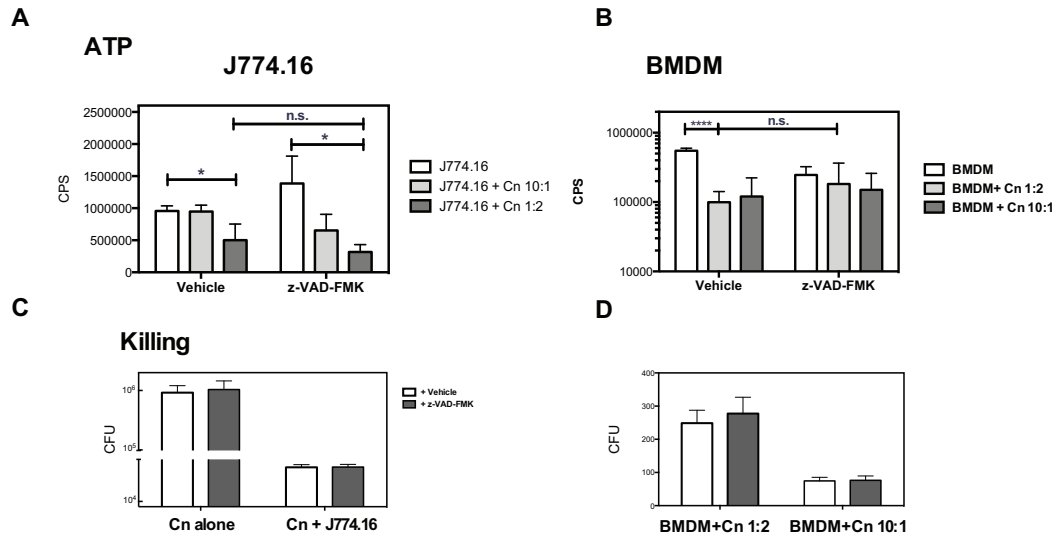
Supplemental Fig. 1. **Outcome of Cn-macrophage interaction *in vitro* is not affected by the pan-inhibition of caspases .**

ATP levels or killing of Cn was not affected by addition of z-VAD-FMK, a pan-caspase inhibitor. A) ATP quantification for Cn infected J774.16, at 18 h infection. B) Killing of Cn by J774.16 macrophages after 18 h of infection. Cn was plated and Colony Forming Units (CFU) counted. C) ATP quantification and D) Killing experiments were repeated for BMDM. Experiments were repeated twice, in triplicates or quintuplicates, for J774.16 and BMDM macrophages. Shown is mean and SD of one representative experiment.
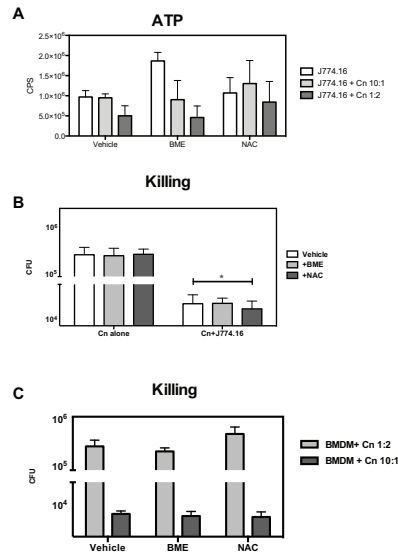
Supplemental Fig. 2. Outcome of Cn-macrophage interaction *in vitro* is not affected by the presence of antioxidants.

A) ATP quantification for Cn infected J774.16, at 18 h infection. ATP decrease was not prevented by addition of n-acetyl-cysteine (NAC) or addition of β-mercaptoethanol (BME). B) Killing of Cn by J774.16 macrophages after 18 h of infection. Cn was plated and Colony Forming Units (CFU) counted. C) Kiling experiments were repeated for BMDM. Experiments were repeated twice, in triplicates or quintuplicates, for J774.16 and BMDM macrophages. Shown is mean and SD of one representative experiment.

Chapter 4

_____

Discussion and

Future Directions

The interaction of Cn with host macrophages is critical for the outcome of infection (1-3). *In vivo*, survival against Cn challenge is associated with a Th1-type activation of macrophages and restriction of Cn growth (1, 4-6). Eradication of Cn infection is not a certain and it often originates a latent infection (7, 8), possibly due to intracellular residency of Cn within host macrophages (9). *In vitro*, phagocytosis of Cn results in macrophage death, starting at 24 hours post infection. However, very little is known about the events that determine death of either cell, or the establishment of intracellular residency. A deeper understanding of the intracellular residency of Cn and of the mutual influence between host and pathogen will provide insights into Cn pathogenesis. As such, the aim of this thesis was to investigate how murine macrophages are affected by Cn phagocytosis. Specifically, we developed an LSC-based high content microscopy protocol to aid our studies. Then, we described cell cycle alterations, activation of death pathways and mitochondrial modulation in macrophages upon Cn infection.

The protocol we developed for LSC allowed us to associate phagocytosis with measurements of macrophage cellular functions. LSC was crucial for the findings here described, particularly the coupling of the macrophage ingestion of Cn to alterations in macrophage division and caspase activation. One of the major advantages of the developed protocol is its wide applicability, this protocol can be used to perform high throughput screening studies across a wide range of disciplines with only minor adaptations.

Upon infection with Cn, we detected an increase in cell cycle progression of macrophage. Previous work had found that phagocytosis of Cn cells, latex beads or frustrated phagocytosis leads to cell cycle progression (10). This evidence strongly supports that phagocytosis-induced cell cycle progression is a conserved mechanism in macrophages. To the best of our knowledge, an increase in macrophage proliferation has not been described for phagocytosis of bacteria. To explain this difference we hypothesized that cell cycle progression was triggered only by particles of a certain size. Bacteria are of a significantly smaller size, than the particles used by Luo et al (10). Both Cn and latex beads were of at least 3 μm diameter, while frustrated phagocytosis is a frustrated ingestion of the surface the macrophage is attached to, determining an infinite size. However, we cannot provide evidence to support this hypothesis given the scarcity of studies on this subject.

The ultimate purpose of macrophage replication is undoubtedly to generate new cells to fight pathogens. Alternatively it is possible that phagocytosis-triggered macrophage division could be a step in formation of granulomas or giant cells. Multinucleated macrophage cells are required for granuloma formation, and granulomas have with strong degradative capacities in comparison with isolated macrophages (11). Both granulomas and giant multinucleated cells could be formed by endoreplication and/or fusion of daughter cells, providing an alternative function for macrophage replication.

Previous studies have characterized the molecular pathways linking frustrated phagocytosis to cell cycle proliferation (12). It is likely that our model shares the same pathways. However, we focused on a more functional side. We established that cell cycle progression required the presence of macrophage growth factors, such as M-CSF originating from L929 cell conditioned media. We also established that phagocytosis of yeast overcomes the previously described LPS and IFN-γ cell cycle arrest (13). These findings highlight how distinct is stimulation of a macrophage cell with an isolated cytokine or with a microbial cell, with its diversity of PAMPs (14). Proliferation of macrophages is a conserved response to phagocytosis, and Cn infection could be a useful model to study it.

As infection progressed, we observed that macrophages were less capable of completing mitosis. To measure this, we combined pulse-chase of a labeled nucleotide with DNA content quantification. We observed that although more macrophage cells entered S phase, macrophages became arrested at G2/M phase. Cn could cause cell cycle arrest because the macrophage been damage to such an extent that it cannot divide or alternatively, by direct interference with the cell cycle molecules. In fact, such factors have been described in bacteria. Cyclomodulins are bacterial proteins which cause alterations in cell cycle and cytoskeleton in host cells (15), mediating mitotic defects and endoreplication. Either damage of macrophages or direct modulation of host cell cycle, requires that activation of cell cycle checkpoints is altered. In concordance with this, inhibition of cyclin D1, a G1-S checkpoint, was reported 4 hours after Cn phagocytosis (16). Another laboratory has described aneuploidy in macrophages that are co-cultured with, but have not ingested, Cn (17). We showed that most macrophages were not undergoing a late stage of the death program at time of infection. However, this does not exclude that macrophage might have already sustained enough damage to prevent cell

cycle progression. Therefore, our results do not elucidate if cell cycle arrest is triggered by damage or by direct interference with cell cycle regulation.

In an attempt to extend *in vitro* results to an *in vivo* setting, we quantified newly synthesized DNA, a hallmark of proliferation, in alveolar macrophages. We showed that alveolar macrophage proliferated in naive conditions and upon Cn infection. This has been reported, very recently, in macrophages from other tissues (18-20). Our results expand the findings into a new tissue and a new inflammation model. Macrophage proliferation in tissue has been proven relevant for an effective immune response and its resolution (20, 21). In fact, modulation of macrophage proliferation can have therapeutic value, for example in a model of brain ischemia (22). We were unable to investigate increased rate of replication or cell cycle alterations in alveolar macrophages, given the scarcity of these cells. However, it is likely that lung macrophage proliferation affects lung immune response to Cn.

Death of the macrophage is caused by Cn-induced macrophage damage. Macrophage death, in turn, influences immune outcome. We discovered that distinct cell death pathways were activated by J774.16 cells and BMDM upon Cn phagocytosis. In BMDM, we detected apoptosis and DNA damage induced necroptosis. Caspase activation is a hallmark of apoptosis and causes DNA fragmentation (23). In turn, DNA damage triggers AIF mediated necroptosis (24). Any of these phenomena is consistent with the previously observed cell cycle arrest. Nevertheless, it remains to be determined which factor is responsible for the cell cycle arrest. Part of damage might be attributed to the Cn capsule. Isolated GXM is capable of causing AIF release *in vitro* (25). Similarly, induction of apoptosis was dependent on capsule, in macrophages co cultured with Cn (17). These findings suggest a new virulence mechanism for the capsule: the ability to cause DNA damage in the host cell, and possibly cell cycle arrest. In J774.16 macrophage-like cells, we noticed absence of apoptosis and we showed evidence of RIP mediated necroptosis. Activation of the different death pathways in macrophages of different origins could be due to differences intrinsic to the macrophages. However, despite distinct pathways activation in distinct cell types, the stimuli that caused this activation is common to both. Cn phagocytosis triggers death receptor mediated death and DNA damage stress pathways.

Decisions of cellular life or death are frequently integrated by the mitochondria (26), as well as cell cycle and proliferation (27). In addition, mitochondrial signaling plays an effector role in antibacterial and antiviral immunity, but has not been investigated in response to fungal infections (28, 29). Modulation of mitochondria most basic function, oxidative phosphorylation, reflects a change in cellular energy demands (27), immune signaling (28, 29) or mitochondrial damage and death signaling (26). This prompted us to investigate if a mitochondrial function could be modulated upon Cn intracellular residency.

We found evidence that mitochondria were modulated at Cn infection, with a decrease in ATP and a decrease in mitochondrial potential. Further proof to support that mitochondrial activity is affected by pathogen sensing is that mitochondrial potential is increased in response to plasma membrane TLRs, but not endosomal TLRs (30). On the other hand, upon phagocytosis of apoptotic cells the mitochondrial potential increases and inert bead phagocytosis leads to no changes in mitochondrial potential (31). These results tie mitochondrial to a finely tuned recognition of phagocytic targets. We have extended these observations to the fungal field and found that mitochondrial function is downmodulated upon Cn infection. This is not the first report of mitochondrial potential being modulated upon infection. Phagocytosis of *Shigella flexneri* (32) lead to a rapid decrease in mitochondria potential, followed by cell death. Phagocytosis of *Listeria monocytogenes* (33) lead to a decrease in mitochondrial potential and mitochondrial fragmentation. Interestingly the decrease in mitochondrial potential was dependent on the bacterial virulence factor listeriolysin O (33). In a manner analogous to bacterial pathogens, we attempted to identify if a sole Cn virulence factor was responsible for the downregulation of the mitochondrial potential, in a manner analogous to the bacterial pathogens (33). Studies with Cn mutants susceptible to oxidative stress failed to identify a Cn virulence factor responsible for the mitochondrial potential decrease. Cn pathogenesis is caused by a synergy of virulence factors (34) and thus it could be difficult to isolate a single virulence factor that affects host mitochondria. However it highly likely that mitochondrial depolarization is a host mediated event and most likely caused by activation of Pattern Recognition Receptors upon Cn phagocytosis.

Blockage of the respiratory chain increases the mitochondrial potential and results in a burst of ROS production, whereas uncoupling of electron transfer chain (28) is usually a reflection of increased glycolysis and diversion of metabolism. Mitochondrial ROS have been suggested to possess signaling functions in immunity,

besides their well described antimicrobial activity (35). We have not found a correlation between production of ROS and mitochondrial modulation, discarding the hypothesis that mitochondrial ROS are a mitochondrial signaling molecule in response to Cn infection. In fact, the role of cellular ROS is unknown, since ROS deficient mice are less susceptible to Cn infection (36) and sustain a stronger Th1 response. It appears that production of ROS during Cn infection is more detrimental to the host than to Cn and that the yeast possesses redundant mechanisms for antioxidant defense.

A switch to glycolytic metabolism occurs as a result of immune cell activation. The metabolic switch is hypothesized to render cells more resistant to hypoxia that occurs at inflamed sites (38). Thus cells can no longer rely on reduction of oxygen for ATP production and instead must rely on glycolysis derived-ATP. The observed mitochondrial depolarization upon phagocytosis of Cn could reflect a metabolic adaptation that results of macrophage activation and that aims to facilitate survival in the hypoxic environment created upon infection. In LPS-stimulated dendritic cells, metabolic switch to glycolysis has been shown to depend on NO-mediated signaling (37). Some authors argue that mitochondrial depolarization can be a result of a mitochondrial microbicidal mechanism. This mechanism is not dependent of mitochondrial ROS production (39), but clues to its identity are non-existent at present. Our attempts to identify if selective blockage of components of the electron respiration chain could facilitate Cn killing were unsuccessful due to fungal toxicity. Thus the ultimate goal of mitochondrial depolarization upon Cn infection of macrophages remains an enigma.

It is remarkable that *in vivo* macrophages and Cn can coexist for years. Taken together, our results ultimately suggest that Cn ingestion triggers modifications in macrophage metabolism that facilitate pathogen survival. In fact, our data gathers evidence that macrophage death is not a fast, overwhelming process but that macrophages are indeed under stress responses. It is likely that the stress response impairs macrophage activation and response to pathogen. Ultimately we could hypothesize that Cn ingestion causes macrophage anergy that facilitates the establishment of a latent infection.

In summary, our results establish that cell cycle arrest and decrease in mitochondrial function occur after interaction of Cn with macrophages. It is both possible that mitochondrial modulation is an essential step in the cell cycle arrest and macrophage demise observed *in vitro* or that it is a reflexion of immune cell activation upon

122

ingestion of a pathogen. We have here described several novel cytopathic effects of fungal infection in murine

macrophages. This description of these effects will impact the understanding of the Cn-macrophage interaction.

References:

1. **Shao X**, **Mednick A**, **Alvarez M**, **van Rooijen N**, **Casadevall A**, **Goldman DL**. 2005. An innate immune system cell is a major determinant of species-related susceptibility differences to fungal pneumonia. J Immunol **175**:3244–3251.

2. **Monga DP**. 1981. Role of macrophages in resistance of mice to experimental cryptococcosis. Infect Immunit **32**:975–978.

3. **Osterholzer JJ**, **Milam JE**, **Chen G-H**, **Toews GB**, **Huffnagle GB**, **Olszewski MA**. 2009. Role of dendritic cells and alveolar macrophages in regulating early host defense against pulmonary infection with Cryptococcus neoformans. Infect Immunit **77**:3749–3758.

4. **Hardison SE**, **Herrera G**, **Young ML**, **Hole CR**, **Wozniak KL**, **Wormley FL**. 2012. Protective Immunity against Pulmonary Cryptococcosis Is Associated with STAT1-Mediated Classical Macrophage Activation. J Immunol **189**:4060–4068.

5. **Wozniak KL**, **Young ML**, **Wormley FL**. 2011. Protective immunity against experimental pulmonary cryptococcosis in T cell-depleted mice. CVI **18**:717–723.

6. **Hardison SE**, **Ravi S**, **Wozniak KL**, **Young ML**, **Olszewski MA**, **Wormley FL**. 2010. Pulmonary infection with an interferon-gamma-producing Cryptococcus neoformans strain results in classical macrophage activation and protection. Am J Pathol **176**:774–785.

7. **Goldman DL**, **Khine H**, **Abadi J**, **Lindenberg DJ**, **Pirofski La**, **Niang R**, **Casadevall A**. 2001. Serologic evidence for Cryptococcus neoformans infection in early childhood. Pediatrics **107**:E66.

8. **Dromer F**, **Mathoulin-Pélissier S**, **Fontanet A**, **Ronin O**, **Dupont B**, **Lortholary O**, **French Cryptococcosis Study Group**. 2004. Epidemiology of HIV-associated cryptococcosis in France (1985-2001): comparison of the pre- and post-HAART eras. AIDS **18**:555–562.

9. **Feldmesser M**, **Kress Y**, **Novikoff P**, **Casadevall A**. 2000. Cryptococcus neoformans is a facultative intracellular pathogen in murine pulmonary infection. Infect Immunit **68**:4225–4237.

10. **Luo Y**, **Tucker SC**, **Casadevall A**. 2005. Fc- and complement-receptor activation stimulates cell cycle progression of macrophage cells from G1 to S. J Immunol **174**:7226–7233.

11. **Vignery A**. 2008. Macrophage fusion: molecular mechanisms. Methods Mol Biol **475**:149–161.

12. **Luo Y**, **Pollard JW**, **Casadevall A**. 2010. Fcgamma receptor cross-linking stimulates cell proliferation of macrophages via the ERK pathway. J Biol Chem **285**:4232–4242.

13. **Xaus J**, **Cardó M**, **Valledor AF**, **Soler C**, **Lloberas J**, **Celada A**. 1999. Interferon gamma induces the expression of p21waf-1 and arrests macrophage cell cycle, preventing induction of apoptosis. Immunity **11**:103–113.

14. **Underhill DM**, **Goodridge HS**. 2012. Information processing during phagocytosis. Nat Rev Immunol **12**:492–502.

15. **Nougayrède J-P**, **Taïeb F**, **Rycke JD**, **Oswald E**. 2005. Cyclomodulins: bacterial effectors that modulate the eukaryotic cell cycle. Trends Microbiol **13**:103–110.

16. **Luo Y**, **Casadevall A**. 2010. Intracellular cryptococci suppress Fc-mediated cyclin D1 elevation. Commun Integr Biol **3**:390–391.

17. **Ben-Abdallah M**, **Sturny-Leclère A**, **Avé P**, **Louise A**, **Moyrand F**, **Weih F**, **Janbon G**, **Mémet S**. 2012. Fungal-induced cell cycle impairment, chromosome instability and apoptosis via differential activation of NF-ϰB. PLoS Pathog **8**:e1002555.

18. **Jenkins SJ**, **Ruckerl D**, **Cook PC**, **Jones LH**, **Finkelman FD**, **van Rooijen N**, **MacDonald AS**, **Allen JE**. 2011. Local macrophage proliferation, rather than recruitment from the blood, is a signature of TH2 inflammation. Science **332**:1284–1288.

19. **Janssen WJ**, **Barthel L**, **Muldrow A**, **Oberley-Deegan RE**, **Kearns MT**, **Jakubzick C**, **Henson PM**. 2011. Fas determines differential fates of resident and recruited macrophages during resolution of acute lung injury. Am J Respir Crit Care Med **184**:547–560.

20. **Ajami B**, **Bennett JL**, **Krieger C**, **McNagny KM**, **Rossi FMV**. 2011. Infiltrating monocytes trigger EAE progression, but do not contribute to the resident microglia pool. Nat Neurosci **14**:1142–1149.

21. **Davies LC**, **Rosas M**, **Smith PJ**, **Fraser DJ**, **Jones SA**, **Taylor PR**. 2011. A quantifiable proliferative burst of tissue macrophages restores homeostatic macrophage populations after acute inflammation. Eur J Immunol **41**:2155–2164.

22. **Zhang Q**, **Chen C**, **Lü J**, **Xie M**, **Pan D**, **Luo X**, **Yu Z**, **Dong Q**, **Wang W**. 2009. Cell cycle inhibition attenuates microglial proliferation and production of IL-1beta, MIP-1alpha, and NO after focal cerebral ischemia in the rat. Glia **57**:908–920.

23. **Siegel RM**. 2006. Caspases at the crossroads of immune-cell life and death. Nat Rev Immunol **6**:308–317.

24. **Boujrad H**, **Gubkina O**, **Robert N**, **Krantic S**, **Susin SA**. 2007. AIF-mediated programmed necrosis: a highly regulated way to die. Cell Cycle **6**:2612–2619.

25. **Chiapello LS**, **Baronetti JL**, **Garro AP**, **Spesso MF**, **Masih DT**. 2008. Cryptococcus neoformans glucuronoxylomannan induces macrophage apoptosis mediated by nitric oxide in a caspase-independent pathway. Int Immunol **20**:1527–1541.

26. **Kroemer G**, **Galluzzi L**, **Brenner C**. 2007. Mitochondrial membrane permeabilization in cell death. Physiol. Rev. **87**:99–163.

27. **Antico Arciuch VG**, **Elguero ME**, **Poderoso JJ**, **Carreras MC**. 2012. Mitochondrial regulation of cell cycle and proliferation. Antioxid. Redox Signal. **16**:1150–1180.

28. **West AP**, **Shadel GS**, **Ghosh S**. 2011. Mitochondria in innate immune responses. Nat Rev Immunol **11**:389–402.

29. **Tschopp J**. 2011. Mitochondria: Sovereign of inflammation? Eur J Immunol **41**:1196–1202.

30. **Krawczyk CM**, **Holowka T**, **Sun J**, **Blagih J**, **Amiel E**, **DeBerardinis RJ**, **Cross JR**, **Jung E**, **Thompson CB**, **Jones RG**, **Pearce EJ**. 2010. Toll-like receptor-induced changes in glycolytic metabolism regulate dendritic cell activation. Blood **115**:4742–4749.

31. **Park D**, **Han CZ**, **Elliott MR**, **Kinchen JM**, **Trampont PC**, **Das S**, **Collins S**, **Lysiak JJ**, **Hoehn KL**, **Ravichandran KS**. 2011. Continued clearance of apoptotic cells critically depends on the phagocyte Ucp2 protein. Nature **477**:220–224.

32. **Koterski JF**, **Nahvi M**, **Venkatesan MM**, **Haimovich B**. 2005. Virulent Shigella flexneri causes damage to mitochondria and triggers necrosis in infected human monocyte-derived macrophages. Infect Immunit **73**:504–513.

33. **Stavru F**, **Bouillaud F**, **Sartori A**, **Ricquier D**, **Cossart P**. 2011. Listeria monocytogenes transiently alters mitochondrial dynamics during infection. Proc Natl Acad Sci USA **108**:3612–3617.

34. **Garcia-Solache MA**, **Izquierdo-Garcia D**, **Smith C**, **Bergman A**, **Casadevall A**. 2013. Fungal Virulence in a Lepidopteran Model Is an Emergent Property with Deterministic Features **4**:e00100–13–e00100–13.

35. **Zhou R**, **Yazdi AS**, **Menu P**, **Tschopp J**. 2011. A role for mitochondria in NLRP3 inflammasome activation. Nature **469**:221–225.

36. **Snelgrove RJ**, **Edwards L**, **Williams AE**, **Rae AJ**, **Hussell T**. 2006. In the absence of reactive oxygen species, T cells default to a Th1 phenotype and mediate protection against pulmonary Cryptococcus neoformans infection. J Immunol **177**:5509–5516.

37. **Everts B**, **Amiel E**, **van der Windt GJW**, **Freitas TC**, **Chott R**, **Yarasheski KE**, **Pearce EL**, **Pearce EJ**. 2012. Commitment to glycolysis sustains survival of NO-producing inflammatory dendritic cells. Blood **120**:1422–1431.

38. **Riboldi E**, **Porta C**, **Morlacchi S**, **Viola A**, **Mantovani A**, **Sica A**. 2013. Hypoxia-mediated regulation of macrophage functions in pathophysiology. Int Immunol **25**:67–75.

39. **Wiese M**, **Gerlach RG**, **Popp I**, **Matuszak J**, **Mahapatro M**, **Castiglione K**, **Chakravortty D**, **Willam C**, **Hensel M**, **Bogdan C**, **Jantsch J**. 2012. Hypoxia-mediated impairment of the mitochondrial respiratory chain inhibits the bactericidal activity of macrophages. Infect Immunit **80**:1455–1466.